AD NUMBER

AD-513 619

CLASSIFICATION CHANGES

TO **UNCLASSIFIED**

FROM **CONFIDENTIAL**

AUTHORITY

OCA; JUL 31, 1982

AD NUMBER

AD-513 619

NEW LIMITATION CHANGE

TO **DISTRIBUTION STATEMENT - A**
Approved for public release;
distribution is unlimited

LIMITATION CODE: 1

FROM **NO PRIOR DISTR SCTY CNTRL ST'MT ASSIGNED**

AUTHORITY

AFRPL; FEB 5, 1986

SECURITY MARKING

The classified or limited status of this report applies to each page, unless otherwise marked.
Separate page printouts MUST be marked accordingly.

THIS DOCUMENT CONTAINS INFORMATION AFFECTING THE NATIONAL DEFENSE OF THE UNITED STATES WITHIN THE MEANING OF THE ESPIONAGE LAWS, TITLE 18, U.S.C., SECTIONS 793 AND 794. THE TRANSMISSION OR THE REVELATION OF ITS CONTENTS IN ANY MANNER TO AN UNAUTHORIZED PERSON IS PROHIBITED BY LAW.

NOTICE: When government or other drawings, specifications or other data are used for any purpose other than in connection with a definitely related government procurement operation, the U.S. Government thereby incurs no responsibility, nor any obligation whatsoever; and the fact that the Government may have formulated, furnished, or in any way supplied the said drawings, specifications, or other data is not to be regarded by implication or otherwise as in any manner licensing the holder or any other person or corporation, or conveying any rights or permission to manufacture, use or sell any patented invention that may in any way be related thereto.

CONFIDENTIAL

AFRPL-TR-70-86 VOLUME II

INJECTOR/CHAMBER SCALING FEASIBILITY PROGRAM (U)

ABLATIVE CHAMBER DESIGN AND LONG DURATION TESTING VOLUME II

G.A.VOORHEES,JR
B. G. MORTON

TRW SYSTEMS GROUP
ONE SPACE PARK • REDONDO BEACH • CALIFORNIA

TECHNICAL REPORT AFRPL-TR-70-86 VOLUME II

JULY 1970

SEE INSIDE FRONT COVER FOR PATENT SECRECY ORDER NOTICE

[redacted]

AIR FORCE ROCKET PROPULSION LABORATORY
AIR FORCE SYSTEMS COMMAND
UNITED STATES AIR FORCE
EDWARDS, CALIFORNIA

CONFIDENTIAL

NOTICE

(U) When U.S. Government drawings, specifications; or other data are used for any purpose other than a definitely related Government procurement operation, the Government thereby, incurs no responsibility nor any obligation whatsoever and the fact that the Government may have formulated, furnished, or in any way supplied the said drawings, specifications, or other data, is not to be regarded by implication or otherwise, or in any manner licensing the holder or any other person or corporation, or conveying any rights or permission to manufacture, use, or sell any patented invention that may in any way be related thereto.

PATENT SECRECY ORDER

(U) The subject matter in this document contains information which is the subject matter of patent applications on which the United States Patent Office has issued secrecy orders. These secrecy orders are superimposed on the usual secrecy regulations which are in force with respect to military contractors' activities. Information under patent secrecy orders must not be disclosed to unauthorized persons.

(U) By statute, violation of a Secrecy Order is punishable by a fine not to exceed $10,000 and/or imprisonment for not more than two years.

FOREWORD

(U) This final technical report (Volume II) covers all work performed in Task II of Contract F04611-68-C-0085, "Injector/Chamber Scaling Feasibility Program." The Task II phase of the program covered the period from 11 December 1968 to 5 February 1970. The report was prepared by G. A. Voorhees, Jr., Program Manager, Applied Technology Department of the Technology Laboratory. The subscale Materials Evaluation Program section (Appendix B) was prepared by B. G. Morton; Lowell Smith was responsible for the thermal analysis and liner sizing. Richard Williams was responsible for the data reduction. This program was carried out under the direction of Dr. Harland L. Burge, Department Manager, Applied Technology Department.

(U) Air Force technical direction was provided by M. F. Powell.

(U) This technical report has been reviewed and is approved.

Roy A. Silver
Project Engineer
Air Force Rocket Propulsion Laboratory

ABSTRACT

(U) The results of the Task II phase of an injector/chamber scaling feasibility program are presented. During the fourteen month program covering the period from 11 December 1968 to 5 February 1970 three ablative thrust chambers were designed, fabricated and test fired. Low-cost liner materials were used in three chamber designs; the material selection was based upon subscale test data generated by both AFRPL and TRW Systems. Low-cost fabrication techniques were employed throughout, ablative components were fabricated by tape-wrapping, hand lay-up, high pressure molding and casting. Several fabrication problems with the low-cost materials were delineated. Four ablative materials were evaluated in the test program. Two of the materials evaluated (MX-2600 silica-phenolic and Dow-Corning 93-104 filled silicone rubber) had acceptable performance for use in low-cost engines of this type and for use in multi-million pound thrust booster engines.

CONTENTS

LIST OF FIGURES

LIST OF FIGURES (Con't)

LIST OF TABLES

NOMENCLATURE

F	thrust, lbf
P	pressure, psia
ε	aren ratio
O	oxidizer
F	fuel
I_{sp}	specific impulse, lbf/lbm-sec
η	efficiency
C*	characteristic velocity, ft/sec
γ	specific heat ratio
K	conductance, defined in text
KLJCF	fuel injector conductance
PIF	fuel injection pressure
KLJCO	oxidizer injector conductance
ΔP	pressure difference, psi
ΔPr	pressure difference ratio, ΔPio/ΔPif
μ	mixture ratio, $\dot{w}o/\dot{w}f$
$\dot{W}$	flowrate, lb/sec
dr/dt=R	erosion rate, (mils/sec)

Subscripts

e	exit
c	chamber
o	nozzle stagnation, or oxidizer
r	ratio
i	injection
f	fuel

SECTION 1
INTRODUCTION AND SUMMARY

1.1 INTRODUCTION

(U) This report is Volume II of a two volume final report on the Injector/Chamber Scaling Feasibility Program, Contract F04611-68-C-0085. Under the requirements of this contract TRW Systems designed and fabricated low-cost injector/chamber hardware for test and evaluation at the AFRPL. The program consisted of two tasks: (1) Task I - 250,000 lb_f thrust Injector/Chamber Development; and (2) Task II - 250,000 lb_f thrust long Duration Ablative Chamber Evaluation.

(U) The objectives of the program were to demonstrate performance, stability and injector/ablative liner compatibility and to verify scaling techniques for rocket engines over a range of thrust levels of 100,000 lb_f to 5,000,000 lb_f. The Task I effort is summarized in Volume I of this final report.

(U) Volume II describes the Task II effort during the period from 11 December 1968 to 5 February 1970 and covers the design, fabrication and test of three low-cost ablative thrust chambers.

1.2 SUMMARY

(U) Following is a summary of the significant subtasks performed in support of the Task II program objectives.

1.2.1 Design and Fabrication - Ablative Thrust Chamber Assemblies

(U) The material selections for the three ablative chambers were based upon results of subscale test programs conducted at both the AFRPL and TRW Systems. Cost-effectiveness studies were made of chamber liners using the most promising materials. Final material selections were based on the cost-effectiveness studies, fabrication processes adaptable to larger size ablative liners, and new material technology. Cost-effectiveness ($/sq. foot installed) findings for the four materials used in the chamber liners are summarized as follows:

Material	Fabrication Method	Liner Component		
		Chamber	Throat	Exit Cone
MXA-150	Layed-up	114	-	-
MXA-150	Molded	-	-	120
MX-2600	Layed-up	-	-	115
MX-2600	Tape-wrapped	-	434	-
DC-93-104	Cast	145	294	142
DP-5-161	Cast	144	-	-

(U) Three thrust chamber assemblies were designed and fabricated. The pressure shells to contain the ablative liners were designed and fabricated of United States Steel (USS) T-1 steel alloy. Table 1-1 summarizes the three long duration engine assemblies.

(U) Table 1-1. 250,000 Lbf Thrust Low-Cost Ablative Engines

Engine Assembly	X405090-1	X405090-2	X405090-3
Injector (S/N)	003	002	001
Thrust Chamber	X404361-1	X404362-1	X404363-1
Materials			
Injector	LCS*	LCS	LCS
T/C Shell	USS T-1	USS T-1	USS T-1
Ablative Liner			
Chamber Section	MXA-150	DC-93-104	DP5-161
Throat	MX-2600	DC-93-104	MX-2600
Exit Cone	MX-2600	DC-93-104	MXA-150
Weight (Lbs)			
Injector Assy.	1500	1500	1500
Pressure Shell	2850	2850	2850
Ablative Liner	1010	680	1130
Dimensions (Inches)			
Throat Diameter	26.10	26.10	26.10
Contraction Ratio	1.80	2.07	1.80
Chamber Length	54.0	54.0	54.0
Chamber Length Dia.	1.54	1.44	1.54
Characteristic Length,L*	89	104	89
Expansion Ratio	4.0	4.0	4.0

* Low Carbon Steel

(U) The configuration 1 ablative liner consisted of a tape-wrapped MX-2600 (silica-phenolic) throat insert, an MX-2600 (silica-phenolic) exit cone liner layed up in a rosette pattern, and an MXA-150 (asbestos-phenolic) chamber liner which was layed-up parallel-to-surface. The exit cone and chamber sections were cured in place at 100 psi while the throat insert was cured in an autoclave at 100 psi, machined and secondarily bonded into the pressure shell using an epoxy adhesive. The chamber internal configuration consists of an 89 inch L*, a 1.54 chamber length to diameter ratio, and a 1.80 contraction ratio.

(U) The configuration 2 ablative liner consisted of a cast Dow-Corning 93-104 filled-silicone rubber throughout the chamber. The liner was cast in three sections; the throat-exit cone, the dome section, and the cylindrical chamber section using internal plaster molds and sheet metal/plywood mandrels. The cast chamber was cured at room temperature. This chamber internal configuration consists of a 104 inch L*, a 1.44 chamber length to diameter ratio, and a 2.07 contraction ratio.

(U) The configuration 3 ablative liner consisted of a tape-wrapped MX-2600 (silica-phenolic) throat insert, an MXA-150 (asbestos-phenolic) exit cone liner and a cast Ironsides Resin DP5-161 chamber liner. The exit cone was fabricated from compression molded MXA-150 segments which were secondarily bonded into the pressure shell. The DP5-161 chamber section was cast in

two sections, the dome and cylindrical chamber section, using internal plaster molds and sheet metal/plywood mandrels. The cast chamber section was cured at room temperature. This chamber internal configuration consists of an 89 inch L*, a 1.54 chamber length to diameter ratio, and a 1.80 contraction ratio.

1.2.2 Test Results

1.2.2.1 Demonstration and Development Injector Firings

(U) Four checkout firings of the S/N 003 demonstration injector were made prior to start of the ablative liner firings. The data from these four firings were in substantial agreement with those data obtained with the S/N 001 and S/N 002 injectors. The S/N 003 demonstration injector was then used with the configuration 1 ablative liner (X404361-1).

1.2.2.2 Ablative Liner Configuration 1

(C) The X404361-1 ablative liner assembly was fired on 4 December 1969 for 66 seconds. The erosion rate of the silica-phenolic throat insert was about 6 mils/second which was slightly lower than the predicted value. The average erosion rate of the silica-phenolic exit cone was essentially as predicted, although there were several localized regions which indicated higher erosion rates than normal. Erosion of the MXA-150 asbestos-phenolic material in the dome-chamber section was approximately twice that predicted by the AFRPL material screening program for MXA-150. In addition, the erosion rate was nearly twice that predicted for the only asbestos-phenolic material tested in the TRW Systems subscale test program.

1.2.2.3 Ablative Liner Configuration 2

(C) The X404362-1 ablative liner assembly was fired on 7 January 1970 for 98 seconds. The erosion rate of the DC-93-104 material in the throat was about 3.0 mils/sec which was slightly lower than the predicted value. There was essentially no erosion in the exit cone. The char layer was estimated at approximately 0.4 inches thick at the exit plane with 0.2 inches of virgin material remaining. Erosion of the silicone rubber in the chamber-dome section was essentially zero. Most of the char layer was lost during the shutdown and purging period but the char layer that remained was estimated at 0.4 inches with approximately 0.4 inches of virgin material remaining.

1.2.2.4 Ablative Liner Configuration 3

(C) The X404363-1 ablative liner assembly was fired on 12 December 1969 for 83 seconds. The erosion rate of the silica-phenolic throat insert was about 3 mils/second which was considerably lower than the predicted values. Erosion of the DP5-161 silica-phenolic material in the chamber section was also lower than the predicted value determined in the AFRPL material screening program. The chamber liner was subjected to considerable cracking and portions of the dome and chamber liner were ejected on shutdown.

1.2.3 Program Evaluation

(C) The measured specific impulse of the three ablative engines was 88 percent ± 0.5 percent of the theoretical value at the nominal design mixture ratio of 2.60. The maximum performance measured was 89 percent at a mixture ratio of 2.50. The average weight of the three long duration ablative engines is estimated to be 5290 pounds. The injector assembly weighs 1500 pounds, the thrust chamber pressure vessel weighs 2850 pounds and the ablative liners weigh from 680 to 1130 pounds with the configuration 2 ablative liner being the lightest weight design.

(U) The inherent dynamic combustion stability of the three injectors was demonstrated during the checkout firings and three long duration firings in this phase of the program.

(U) Acceptable ablative performance was achieved with the Fiberite MX-2600 (silica-phenolic tape or broadgoods) used as a liner for two of the three throat inserts and in one exit-cone. Acceptable ablative performance also was achieved with the Dow-Corning DC-93-104 silicone rubber used throughout the configuration 2 liner.

(U) A number of low-cost fabrication techniques were evaluated. Tape wrapping over a male mandrel, and hand lay-up of standard ablative materials in conjunction with a low-pressure cure cycle appear applicable for fabricating large ablative components but would require expensive tooling. Casting of room temperature curing ablators is a feasible technique for producing large ablative components without the use of expensive tooling. The high pressure molding of interlocking panels appears to be a practical technqiue. The joint design and secondary bonding of the molded panels to the shell become the critical and expensive part of the ablative component.

SECTION 2

ENGINE DESIGN AND FABRICATION

2.1 GENERAL

(U) The TRW low-cost, pressure-fed engine design consisted of two major assemblies - a centrally located, coaxial injector and an ablatively cooled thrust chamber. The engine used low-cost storable propellants (N_2O_4/UDMH) which are compatible with conventional materials of construction. The engine was designed with a minimum of "precision" tolerances such that industrial fabrication techniques could be used to fabricate both the injector and thrust chamber shell. Low-cost ablative-type thrust chamber liners, capable of being fabricated by low-cost techniques, were used to protect the chamber shell during the long duration engine firings.

(U) The Task II Design and Fabrication effort consisted of the design and fabrication of three long duration thrust chamber assemblies (TCA's) comprised of an ablative liner and pressure shell. The selected ablative materials for these TCA's were based upon subscale test results and material studies conducted at both TRW Systems and the AFRPL. The demonstration injectors to be fired with the three TCA's were fabricated during Task I of the program. These injectors were based upon the test results achieved with the development injector configurations. The average assembly weight of the three ablative engines is estimated to be 5290 pounds with the lighest engine being the configuration 2 (5030 pounds) design. The injector assembly weighs 1500 pounds, the thrust chamber pressure vessel weighs 2850 pounds, and the ablative liners weigh from 680 pounds to 1130 pounds.

2.2 250,000 LBF THRUST DEMONSTRATION ENGINE DESIGN

(U) The 250,000 lbf thrust (vacuum) demonstration engine design (X405090) is shown in Figure 2-1. This engine is comprised of two major assemblies, the centrally located, coaxial demonstration injector and the ablative lined thrust chamber. The design is based on achieving the parameters shown in Table 2-1. The design test duration was 120 seconds. The two primary objectives of the test firings were the determination of injector/chamber compatibility and the evaluation of low-cost ablative materials.

(C) Table 2-1 Static Test Engine Design Parameters (U)

F(vac), lbf	250,000
P, psia	300
ϵ_e, Ae/At	4.0
ϵ_c, Ac/At	2.0 (Nominal)
O/F	2.60 (Nominal)
I_{sp} (vac), lbf-sec/lbm	283.3 (Theoretical Shifting Equil.@O/F=2.60)
η_{Isp}	0.90
C*, ft/sec	5596 (Theoretical Shifting Equil.@O/F=2.60)
η_{C*}	0.9375

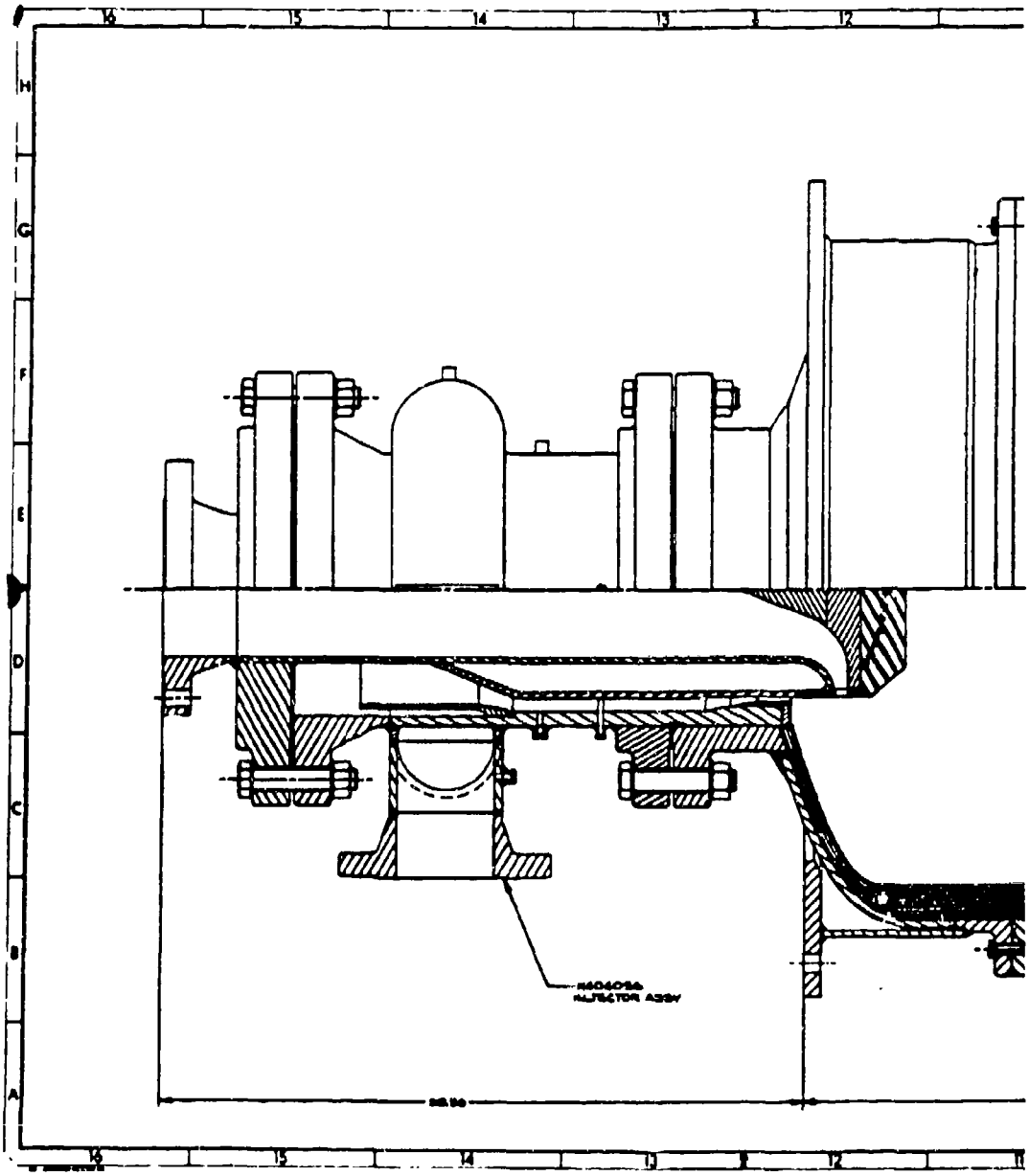

Figure 2-1. X405090 Engine Ass'y
250K Demonstration,
Static Test (U)

(This page is unclassified.)

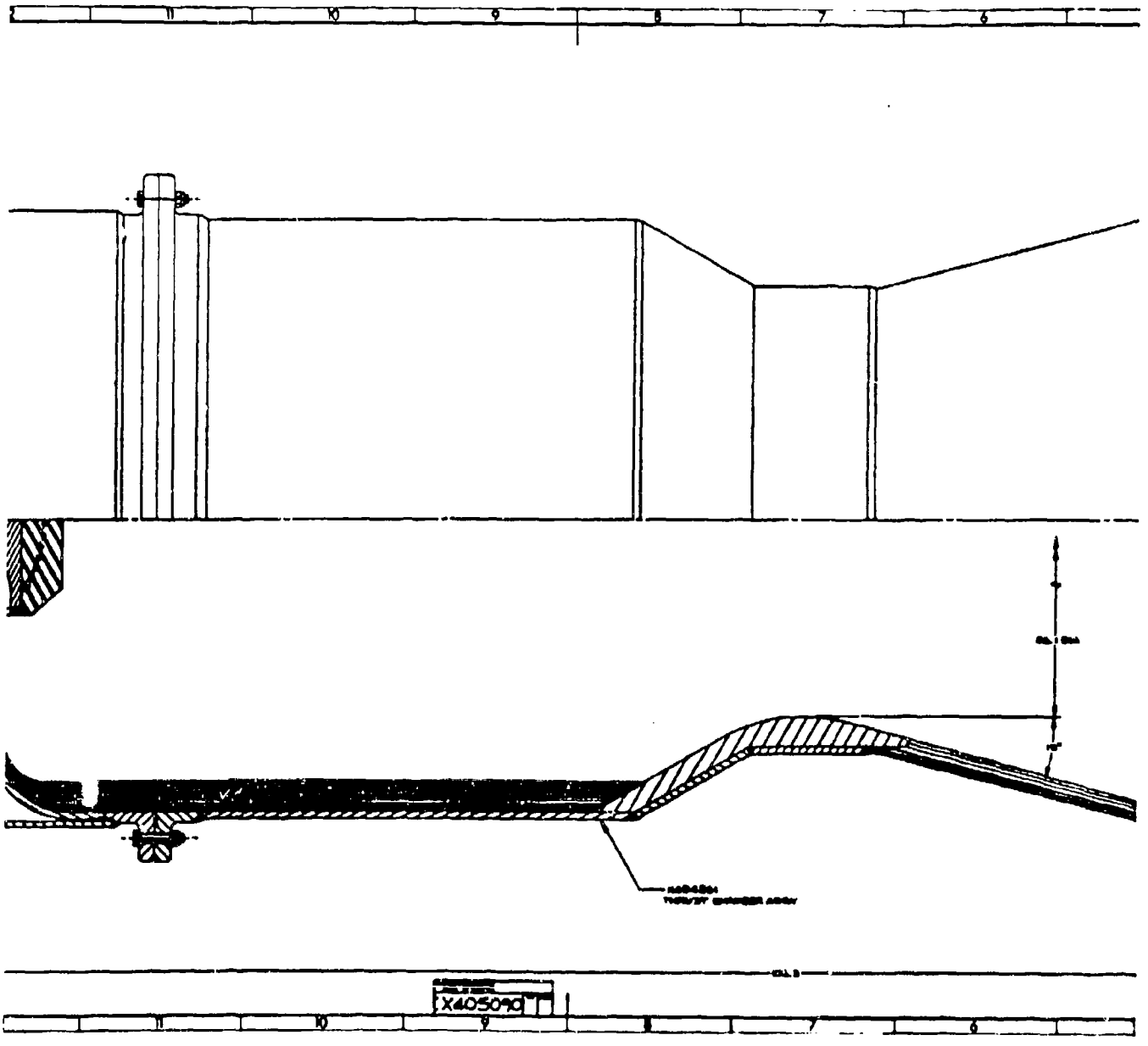
X405090

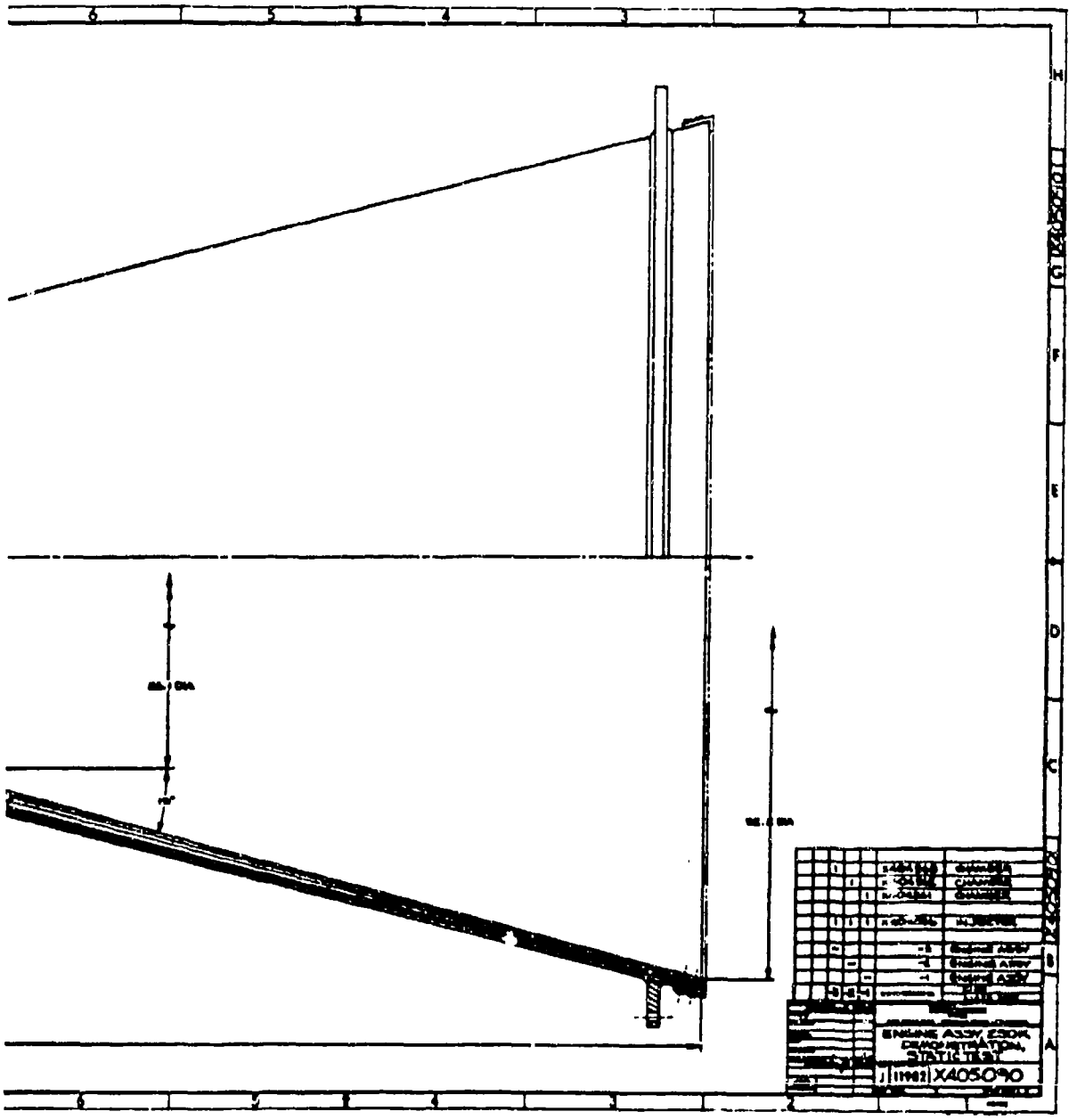
ENGINE ASSY ESOK
DEMONSTRATOR
STATIC TEST
X405090

(U) The design criteria, including propellant flows, calculated pressure drops, and predicted stress levels used in the development hardware design have been detailed in Volume I. The demonstration injectors used in Task II are essentially identical to the development injector except for method of attachment of the oxidizer orifice ring. The pressure shell used with the ablative liners is fabricated from USS T-1 steel alloy in all areas except the long weld neck flange which is ASTM A-181 carbon steel. The stress analysis for the pressure shell used with the ablative liners is presented in Appendix A. The stress analysis was based on a steady-state pressure of 600 psi in the injector and chamber.

(U) The selection of materials to be used in the ablative liners were based upon test results obtained in the AFRPL "in-house" material screening program and the TRW Systems sub-scale Materials Evaluation Program (Appendix B). The thicknesses of the various materials were determined using the procedure given in Appendix C.

(U) The unit costs for quantities of 1, 3 and 10 pressure shells and ablative liner assemblies are given in Appendix D.

2.2.1 Engine Operation

(U) Combustion was initiated by opening an 8-inch facility oxidizer valve (propellant valves were not supplied with the engine) so as to provide a definite oxidizer lead. Oxidizer entered the injector through an 8-inch, 300 lb ASA welding neck flange located on the injector centerline and flowed through the oxidizer tube. The oxidizer was turned 90° by the contoured pintle tip and was injected radially through multiple orifices. Fuel entered the fuel manifold through a 6-inch, 300 lb ASA welding neck flange and then was injected as a hollow cylindrical sheet.

(U) The fuel sheet impinged with the radial oxidizer streams approximately 2.5 inches from the fuel orifice. Since the propellants were hypergolic, combustion took place upon contact of the fuel with the oxidizer. After 120 seconds of operation both facility propellant valves were to be sequenced closed. Gaseous nitrogen was used to purge the residual propellants from the manifold.

2.3 THRUST CHAMBER DESIGN AND FABRICATION

2.3.1 Pressure Shell

2.3.1.1 Design

(U) The pressure shell design for the ablative liners was similar to the X403646-1 heat-sink combustion chamber design which was used in the Task I program. Two major changes were made in the design of the pressure shell; (1) the body was split into two sections with flanges to allow insertion of the tape-wrapped throat insert and (2) the thickness of the exit cone shell was decreased from 0.5 inches to 0.25 inches.

(U) The X404342 pressure shell (Figure 2-2) was designed using USS T-1 steel in all areas except the long weld neck flange (X404342-14) which was ASTM A-181, Grade II, carbon steel. The head (X404342-13) was a 2:1 ASME Code elliptical head of USS T-1 steel, 39.0 inch I.D. by 0.5 inch wall thickness. The plate sections of the chamber sections were 0.50 inch thickness while the exit cone plate thickness was 0.25 inches. The closure flanges (X404342-9, 10) were machined from USS T-1 forgings.

(U) The thrust mount consisted of a 1/2 in. thick support ring (X404342-11) fabricated from USS T-1 steel plate 8.7 inch wide by 130.0 inch long. The support ring was welded to the cylindrical chamber section downstream of the weld which connected the semi-elliptical head (X404342-13) to the fore flange (X404342-10). Shims were used to space the -11 support ring so that a minimum 0.040 inch clearance was maintained between the support ring and semi-elliptical head. The thrust mount ring was fabricated from 1.00 inch thick USS T-1 steel plate which was welded to the support skirt. The mounting hole pattern was 20, 1-1/8 inch diameter holes, on a 44.0 inch diameter bolt circle. This thrust mount configuration was used on both heat-sink combustion chambers which were fabricated during Task I.

(U) The pressure shell design incorporates twenty-two 1/4-18 NPT ports for the purpose of thermocouple installation and pressure measurement. The two pressure taps were located in the 16-inch 300 psi ASA long welding neck flange. This allowed for a head-end pressure measurement in the annulus between injector and flange. Twenty of the ports were located at five axial positions to measure the ablative liner backwall temperature.

(U) The major differences in the design of the three pressure shells were in the exit cone area. The X404342-2 exit cone section was designed to a 53.60 inch exit plane ID to accommodate the 0.7 inch thick ablative liner while both the X404342-1 and X404342-21 were fabricated to a 53.20 inch exit plane ID for the 0.5 inch thick ablative liners. Identical stiffener rings were added to the -1 and -2 pressure shell configurations. The stiffener ring on the X404342-21 pressure shell assembly was designed with 48, 21/32 inch holes to match the end closure tooling which was used for curing the MX-2600/MXA-150 in place.

2.3.1.2 Fabrication

(U) Three pressure shells were fabricated from the basic design. The X404342-1 pressure shell configuration was used for the X404362-1 ablative-lined long-duration thrust chamber assembly; the X404342-2 pressure shell configuration was used for the X404363-1 thrust chamber assembly, and the X404342-21 pressure shell shown in Figure 2-3 was used for the X404361-1 thrust chamber assembly.

(U) All pressure shells, were fabricated using rolled and welded USS T-1 steel sections as shown in Figure 2-4. The two conical sections, -3 and -7, and the three cylindrical sections, -5, -8 and -11 were rolled from single pieces of steel plate and had only one longitudinal weld. The 2:1 elliptical head was a commercial head fabricated from a single piece blank. The X404342-14 long weld-neck flange was a commercial 16 inch 300 ASA flange.

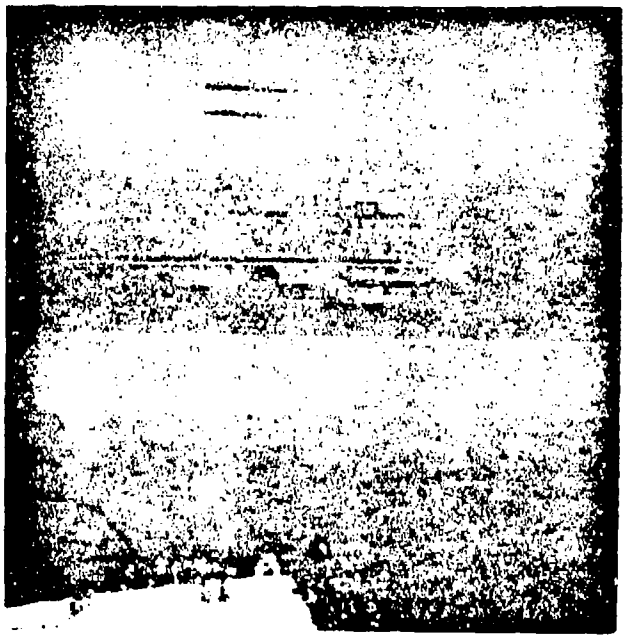

Figure 2-3. X404342-21 Pressure Shell(U) (65542-69-10)

(U) All circumferential welds used to join the various sections were made using automatic, submerged-arc welding techniques. Multiple passes were used on all weld joints. A 100 percent X-ray requirement was imposed on all butt welds and dye penetrant inspection was used on all fillet welds. All welds were certified in accordance with applicable ASME boiler and pressure vessel codes.

(U) Two lifting eyes were added to the chamber shell, as shown in TRW drawing X404342, to facilitate handling.

2.3.2 Ablative Liner No. 1

2.3.2.1 Design

(U) The original design of the X404361-1 ablative liner was based on the use of MX-2600 (Fiberite) silica-phenolic material throughout. The material thicknesses were based upon the test results obtained with the DC-93-104 material during the TRW Systems sub-scale Materials Evaluation Program (Reference 8). MX-2600 had not been tested in the sub-scale program but subsequent testing at the 1500 lbf level confirmed that the design was conservative.

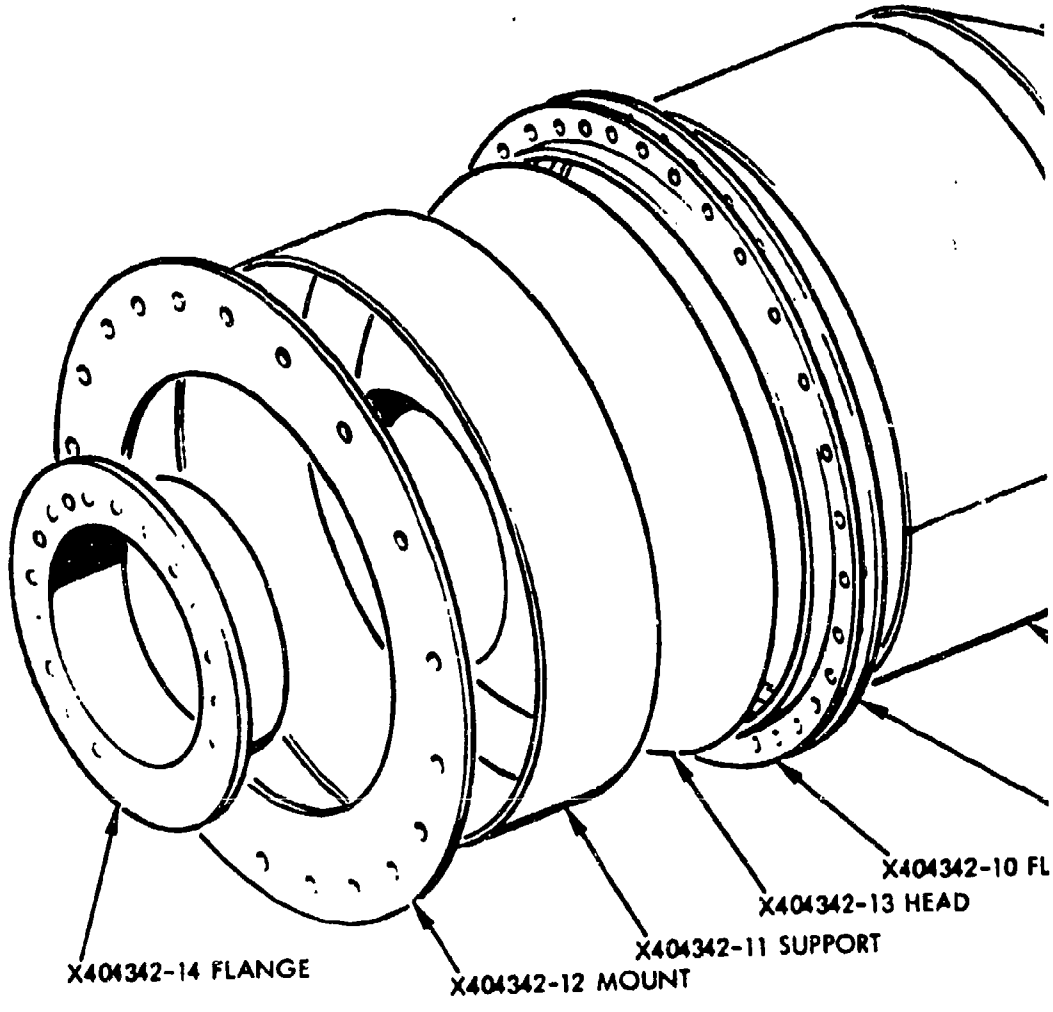
X404342-14 FLANGE
X404342-12 MOUNT
X404342-11 SUPPORT
X404342-13 HEAD
X404342-10 FL

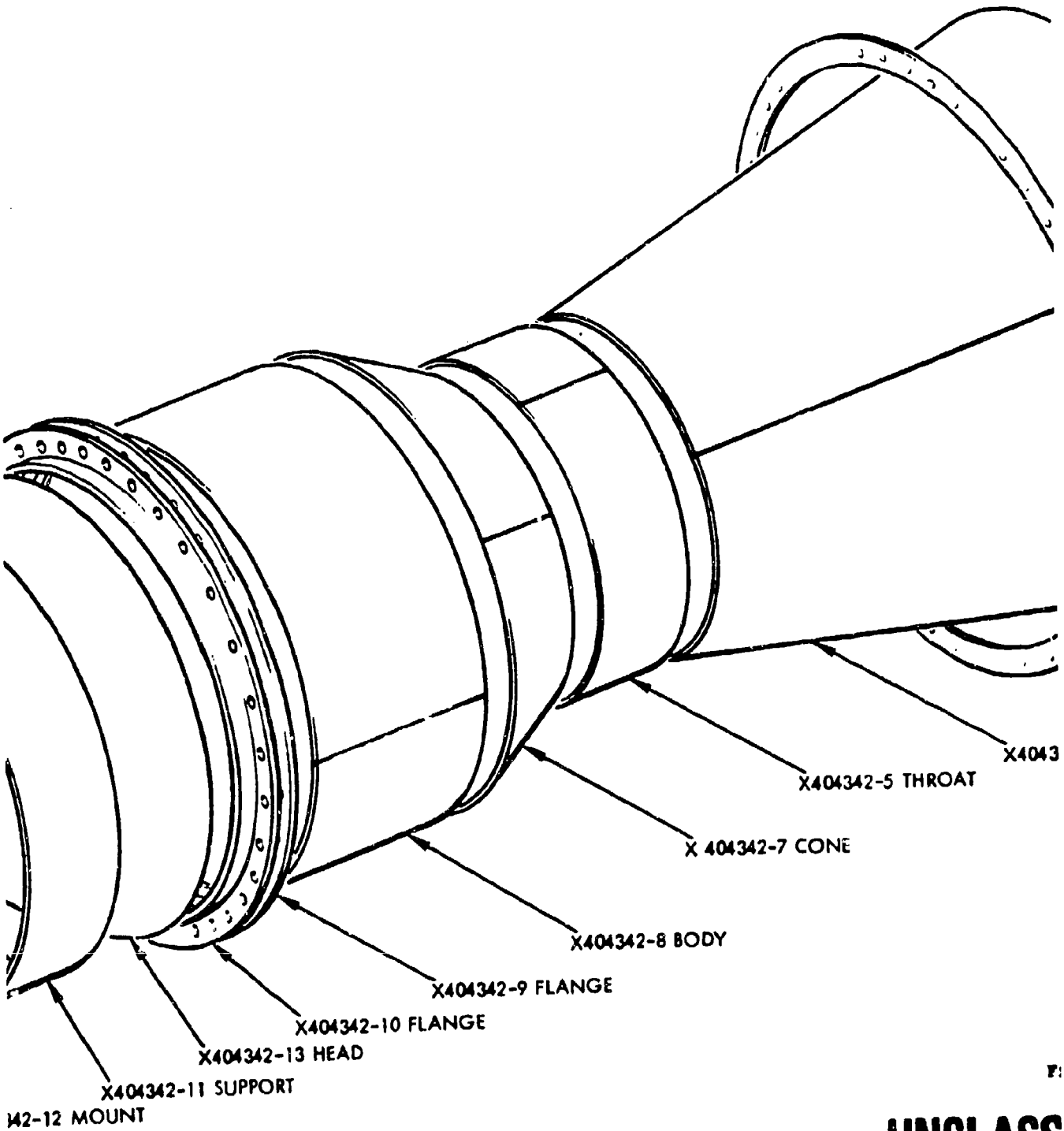
X4043
X404342-5 THROAT
X 404342-7 CONE
X404342-8 BODY
X404342-9 FLANGE
X404342-10 FLANGE
X404342-13 HEAD
X404342-11 SUPPORT
142-12 MOUNT

F

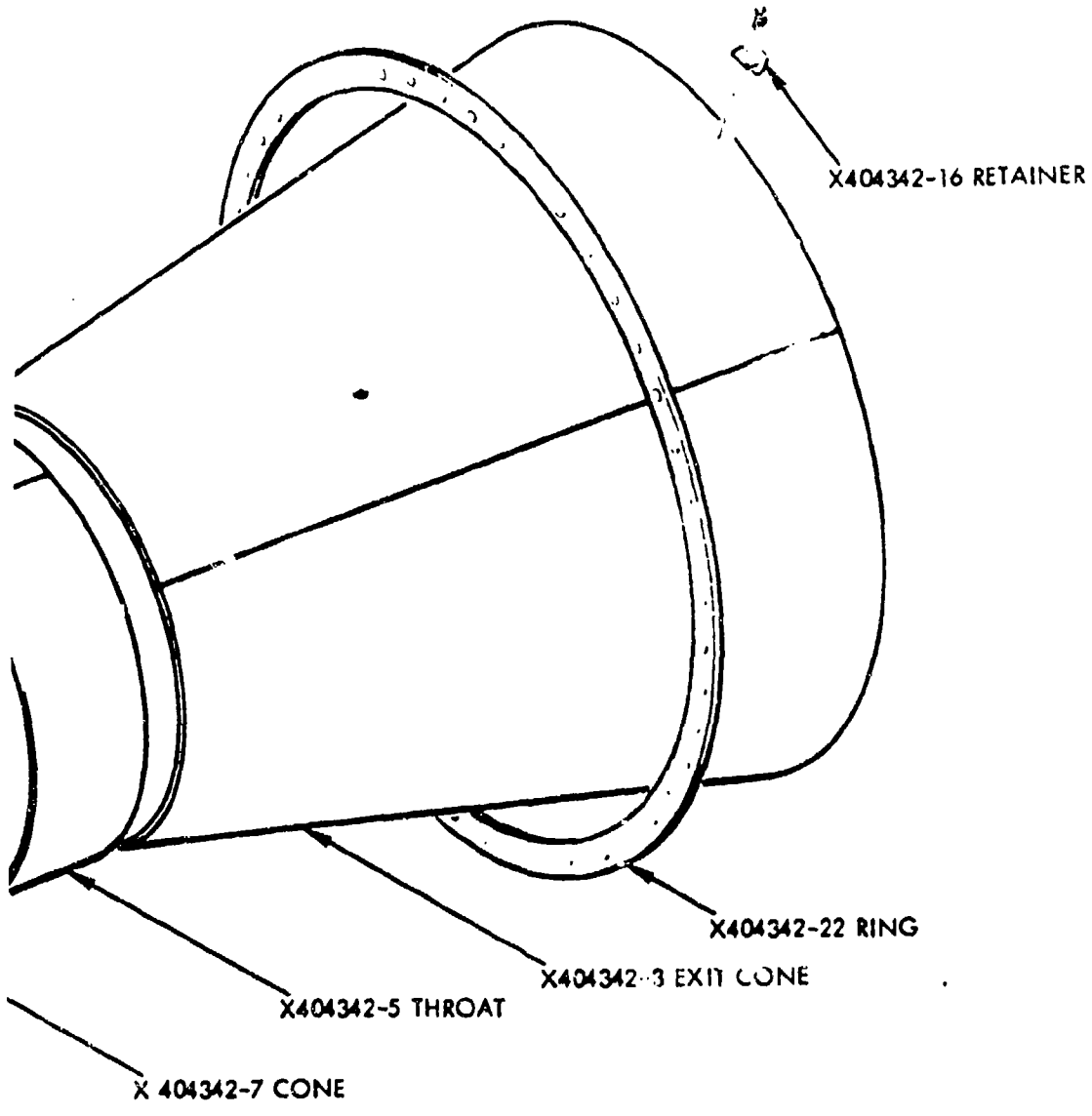

404342-8 BODY

GE

Figure 2-4. X404342-21 Thrust Chamber Shell Assembly (U)

(U) The TRW Systems Charring and Ablation Computer Program (AH054A), employing the erosion model of Munson and Spindler were used to size the ablative material thicknesses (Appendix C). The input data to these programs consisted of the erosion data, surface temperature, and effective heat of ablation obtained during the subscale test program of the various materials. The criterion used in the liner sizing was based on a 4850° throat recovery temperature and a maximum backwall temperature of 600°F after 120 seconds of firing.

(U) The required thicknesses are shown in Figure 2-5 for four candidate liner materials. The AFRPL approved design, which is shown in Figure 2-6, consisted of an MX-2600 silica-phenolic throat insert, an MX-2600 silica-phenolic exit-cone liner and an MXA-150 asbestos-phenolic chamber-dome liner. The MXA-150 asbestos phenolic material was not tested in the TRW Systems sub-scale program but data furnished by the AFRPL on the erosion-char rate of the MXA-150 (0.98 inches/60 seconds) indicated that the material was at least comparable to the Haveg-41 asbestos-phenolic material tested in both the TRW Systems sub-scale program (1.00 inches/60 seconds) and the AFRPL material screening program (1.04 inches/60 seconds). The material thickness of the MXA-150 was increased to 2.0 inches from the indicated 1.60 inches for the Haveg-41 at a 35.0 inch chamber I.D.

(U) Tape wrapping at 60° to centerline was chosen for fabricating the throat insert. This method and laminate orientation provided maximum erosion resistance in an area where both heat-flux and shear-stress are maximum. A rosette lay-up was selected for the exit cone. This method of fabrication is used on LMDE exit cones. The chamber-dome section was designed as a parallel-to-surface lay-up of material; a reduction in material thickness was made in going from the cylindrical section to the dome section.

2.3.2.2 Fabrication

(U) The materials employed in the X404361-2 liner assembly were MX-2600 silica-phenolic and MXA-150 asbestos-phenolic manufactured by the Fiberite Corporation. The MX-2600 used for the throat section X404361-4 was furnished as bias tape while MX-2600 broadgoods was used for the exit cone. The MXA-150 asbestos-phenolic material used in the chamber-dome section was furnished as a broadgoods. Typical properties of the three materials are given in Table 2-2.

(U) The X404361-4 throat section was tape-wrapped on a net, male mandrel at 60° to centerline. Tape width was chosen to provide the proper component thickness when oriented at the desired angle to the flow, with allowances for wrapping guidance accuracy and trim, pull-down of bias material in wrapping operations and loss of material in debulk during cure.

(U) The wrapping operation shown in progress in Figure 2-7 shows the mandrel set-up in a lathe with a pressure roller being used to compress the tape as it is wrapped. The as wrapped density is approximately 95 percent of the cured part density. Heat-guns were used to heat the tape and previously wrapped material during the wrapping operation. There was no tendency for wrinkling of the inner portions of the ply during the wrapping operation even though ply widths as large as 4 inches were employed. Figure 2-8 shows the throat section near completion of wrapping.

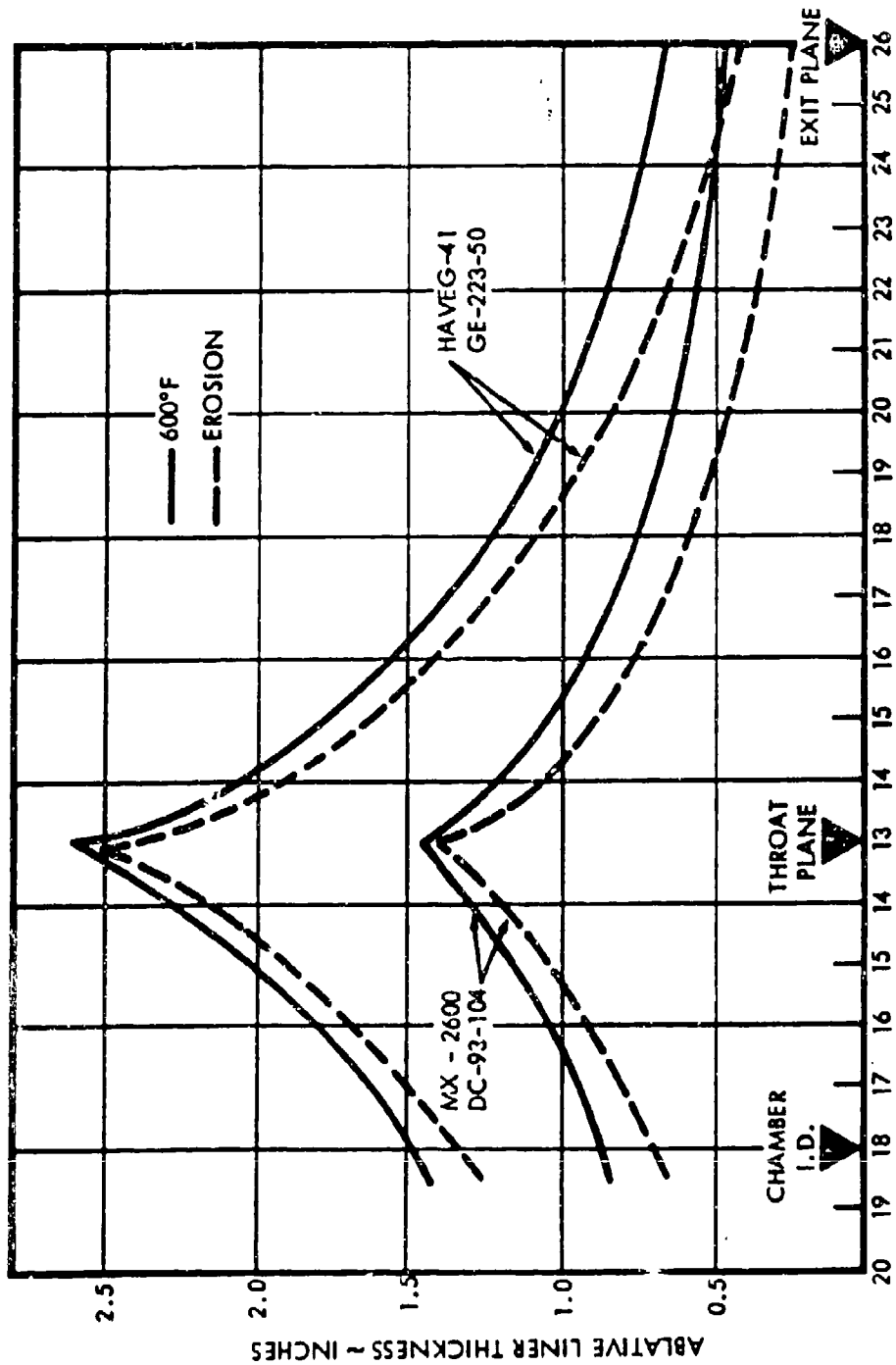

Figure 2-5. 250,000 lbf Long-Duration Thrust Chamber Ablative Liner Thickness for Single 120-second Continuous Burn (Gas Recovery Temperature = 4850°F) (U)

Table 2-2

Properties of Materials Used in X404361-2 Liner Assembly (U)

	MX-2600	MX-2600	MXA-150
Form	Tape	Broadgoods	Broadgoods
Lot No.	H-355	H-387	H-375
Resin	MIL-R-9299(II)	MIL-R-9299(II)	MIL-R-9299(II)
Filler (Silica), %	7.8	N/A*	5.0
Fabric reinforcement, % min.	96.0	96.0	N/A
Resin solids, %	31.0	31.4	48.5
Volatile Content, %	7.0	7.5	12.5
Specific Gravity	1.71	N/A	1.56

* Not Available

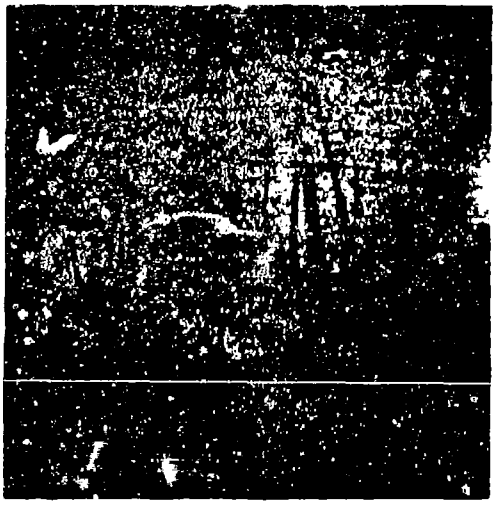

Figure 2-7. X404361-4 Tape wrapping operation(U)
(65542-69-3)

Figure 2-8. X404361-4 Throat section near completion (U)
(65542-69-4)

(U) Following completion of wrapping the part was prepared for curing. Nylon shrink tape was wrapped over the MX-2600 bias tape. A bleeder cloth and "monkey-fur" material were then applied to the part. Finally a Mylar vacuum bag was applied to the wrapped part. The vacuum bagged part was cured in an autoclave at 100 psi and 290-310°F for five hours. The temperature in the autoclave was increased from ambient temperature to 300°F in approximately 4 hours. The cure process is visualized as occurring from the inside of the mandrel outward through the layed-up part. The outer surface is protected by the insulative properties of the bleeder cloth, separation sheets and mylar vacuum bag. In this manner, volatiles are always removed through uncured material and into the bleeder cloth, and a uniformly cured part results. Figure 2-9 shows the part as removed from the autoclave with part of the vacuum bag and bleeder cloth removed.

(U) The machining of the cured ablative throat did not present any particular problems. Only the O.D. surface of the throat was machined to mate with the I.D. of the pressure shell. The part was machined to allow for a glue line thickness of approximately 0.060 inches. The part was machined on the mandrel which was used for the wrapping operation as shown in Figure 2-10. The finished part prior to assembly into the X404361-2 liner assembly is shown in Figure 2-11, with the forward part of the split mandrel in the background.

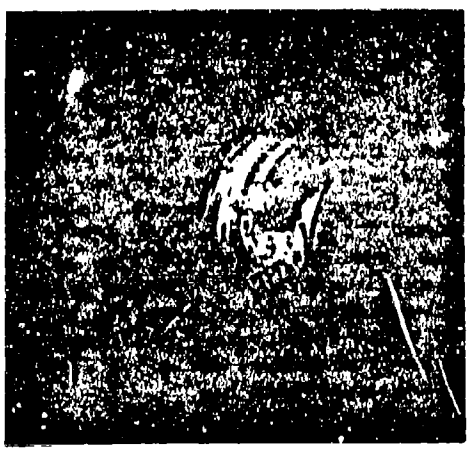

Figure 2-9. X404361-4 Throat Section After Cure (U)

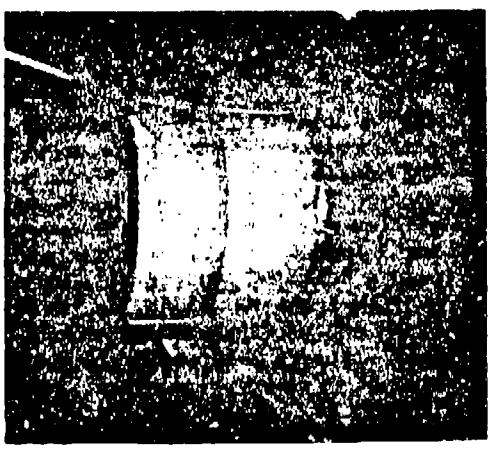

Figure 2-10. X404361-4 Throat Section After Machining (U)

Figure 2-11. X404361-4 Finished Throat Section (U)
(65543-69)

(U) Prior to start of layup of the MX-2600 broadgoods in the exit cone section of the pressure shell the inside surface was sandblasted and then cleaned using methylethylketone (MEK). The cleaned surfaces were then primed using Monsanto SC 1008 phenolic resin.

(U) The X404361-5 exit cone liner was layed-up in a rosette pattern using the steel shell as a female mandrel. Trapezoidal plies 6 in. wide x 4 in. wide x 50 in. long were cut from the MX-2600 broadgoods and layed in place in the pressure shell as shown in Figure 2-12. The lead on the forward end was approximately 0.110 inches while the lead on the aft end was approximately 0.190 inches. This resulted in a 21 ply thickness at the aft end (exit plane) and a 55 ply thickness at the forward end (throat extension plane). The plies were held in place by vacuum bagging while the shell was being rotated. Figure 2-13 shows the completed layup prior to curing. Approximately 830 plies were used in exit cone layup.

(U) A separation sheet, bleeder cloth and Mylar vacuum bag were put in place over the layup. The steel pressure shell served as the autoclave. The ends of the pressure shell were sealed-off; a flatplate closure was used on the 16 in. flange end while an elliptical dome was used to close off the exit end. The exit cone was cured at 100 psia and 290-310°F for 5 hours. The temperature was raised from ambient to 300°F in approximately 4 hours. Heat applied from the metal (shell) side causes volatiles to flow from the shell side through uncured material and into the bleeder cloth and out through the vacuum system which results in a uniformly cured part. Figure 2-14 shows the part with the end closure off after cure and removal of separation sheet, bleeder cloth and vacuum bag.

(U) The part was setup for machining of the recess in the exit cone liner as shown in Figures 2-15 and 2-16. The X404361-5 exit cone liner was machined to allow for a glue line thickness of approximately 0.060 inches. Following machining of the exit cone the throat was bonded to the shell and exit cone using Epon 901/B3 adhesive. Figure 2-17 shows the throat with adhesive being lowered into the pressure shell. The adhesive was allowed to setup for 24 hours prior to start of the MXA-150 layup.

Figure 2-12. X404361-5 Exit Cone Lay-up (U)

(65907-69-8)

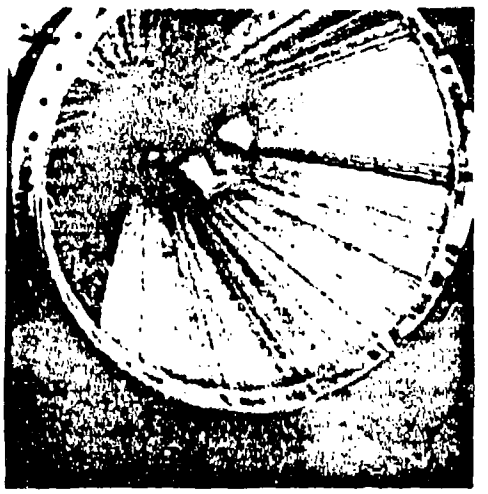

Figure 2-13. X404361-5 Completed Exit Cone Lay-up (U)

(65908-69-1)

Figure 2-14. X404361-5 Cured Exit Cone (U)

(67990-69-9)

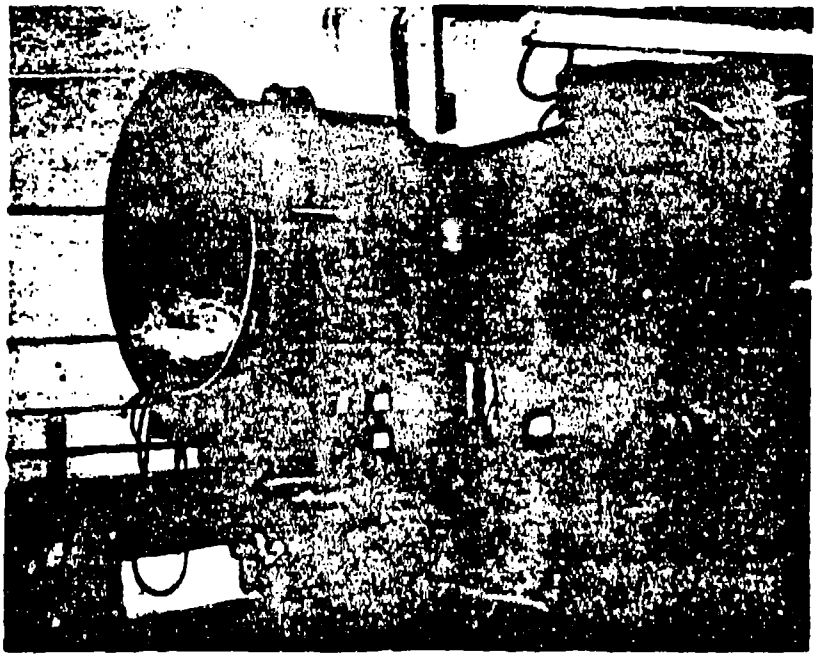

Figure 2-15. X404361-5 Installed in Pressure Shell Set-Up for Machining (U) (66777-69-1)

Figure 2-16. X404361-5 Exit Cone Being Machined (U) (66777-69-2)

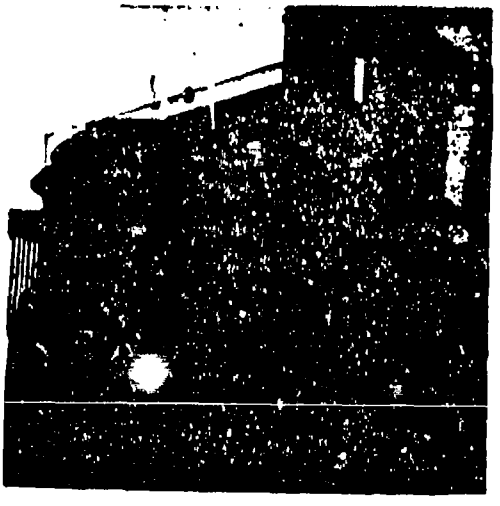

Figure 2-17. X404361-4 Throat Section Being Lowered Into Chamber (U) (65543-69-10)

(U) The X404361-3 chamber liner was layed up using "orange-peel" sections of MXA-150 asbestos-phenolic from the forward opening (16 inch flange) to the throat liner. Plies were layed up parallel to centerline in the chamber section. The 2.0 inch thickness required approximately 55 plies. The length of the plies was increased as the thickness was tapered to 0.8 inches at the forward opening. Approximately 23 plies were used to achieve the 0.8 inch thickness. The plies were layed up in the chamber section with a maximum overlap of the longitudinal joint of one-half inch. The adjacent plies did not have any coincident joints. The layup was accomplished in three steps; the initial 16 plies were vacuum bagged and debulked at 100 psi and 180°F. The layup was also subjected to the same debulking cycle after 36 plies had been layed-up. Following layup of the last 23 plies the part was covered with a separation sheet, bleeder cloth and Mylar vacuum bag. The final cure was affected in the same manner as that used for the X404361-5 exit cone liner. Closures were used on both ends of the pressure shell. The part was cured for four hours at 100 psi and 290-310°F. Approximately 4 hours were required to reach 300°F.

(U) Shrinkage of the MXA-150 asbestos-phenolic material was expected and shrinkage of about 0.030 inch on a side did occur. The dome section of the pressure shell was removed and Epon 934 adhesive was applied to the asbestos-phenolic part and the head was rebonded to the X404361-5 chamber liner. Shrinkage in the cylindrical chamber section was not as uniform. The void between liner and shell was back-filled with a 1:1 mixture of Versamide 115-Epon 828 adhesive. Figure 2-18 shows the adhesive on the dome section prior to reinstallation of the dome portion of the pressure shell.

(U) Measurements were taken of the exit plane diameter, throat diameter, chamber diameter and location of the throat plane prior to shipment. The throat diameter was 26 1/8 inches $\pm$ 1/16 inch while the exit plane diameter was 52 1/8 inches $\pm$ 1/8 inch. The chamber diameter was 35 inches $\pm$ 1/16 inch. The thickness at the exit plane varied from 0.56 inch to 0.62 inch around the circumference. The thickness at the forward end was a nominal 0.80 inch plus 0.060 inch bond line thickness.

(U) Material samples were taken from each end of the MX-2600 throat, the aft end of the MX-2600 exit cone and the forward end of the MXA-150 chamber liner. Specific gravity samples of the throat indicate a Sp. Gr. of 1.73 for both samples. The throat was also weighed (180 + lbs); using the calculated volume results in an apparent bulk density of 1.74. Samples from the aft end of the exit cone indicated a Sp. Gr. of 1.66 while the Sp. Gr. of the MXA-150 component was 1.50.

(U) The joint at the throat/exit interface was ground smooth as were the ends at both the forward flange section and exit plane. The X404362-16 retainer clips were reinstalled and the number 1 long duration thrust chamber assembly (X404361-1) shown in Figures 2-19, 2-20, and 2-21 was made ready for shipment.

Figure 2-18. X404361-3 MXA-150 Chamber Section(U)
(66777-69-5)

Figure 2-19. X404361-2 Liner Assy. Showing Exit Cone, Throat and Chamber Sections (U)
(66777-69-9)

(66777-69-11)

Figure 2-20. X404361-1 Long Duration Thrust Chamber Ass'y. No. 1 (U)

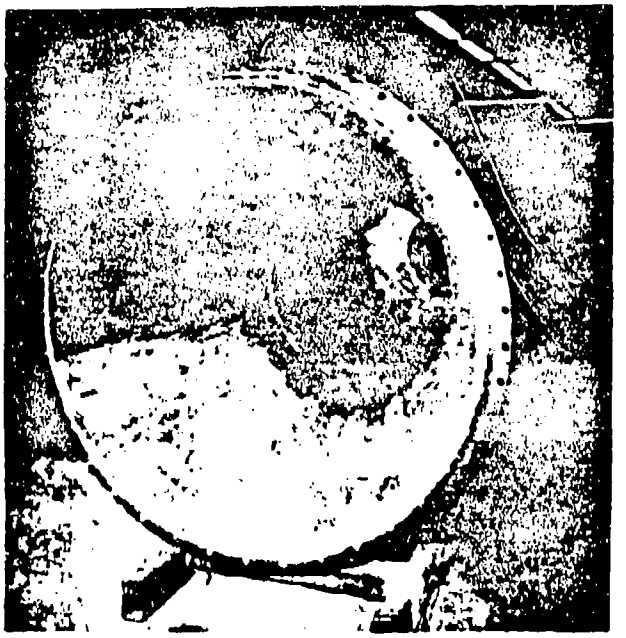

(66777-69-12)
Figure 2-21. X404361-1 Long Duration Thrust Chamber Ass'y. No. 1 (U)

2.3.3 Ablative Liner No. 2

2.3.3.1 Design

(U) The design of the X404362-1 ablative liner was based on the use of Dow Corning 93-104 (filled silicone rubber) material throughout. The material thicknesses were based upon test results obtained during the TRW Systems sub-scale Materials Evaluation Program (Appendix B).

(U) The erosion model of Spindler and Munson and the TRW Systems Charring and Ablation Computer Program (AH054A) were used to size the ablative material thicknesses (Appendix C). The input data to these programs consisted of the erosion data, surface temperature, and effective heat of ablation determined in the sub-scale program. The criterion used in the material sizing were based on a 4850°F throat recovery temperature and a maximum backwall temperature of 600°F after 120 seconds of firing.

(U) The required thicknesses for the X404362-1 liner are shown in Figure 2-5. These thicknesses were achieved by casting the material in the void created by the shell and the internal molds and mandrels. Cold joints were allowed in the cylindrical chamber section and the exit cone liner. The throat approach, throat and aft throat sections were cast as a single thick section. Elevated temperature cures were not specified for any sections. Figure 2-22 shows the AFRPL approved design.

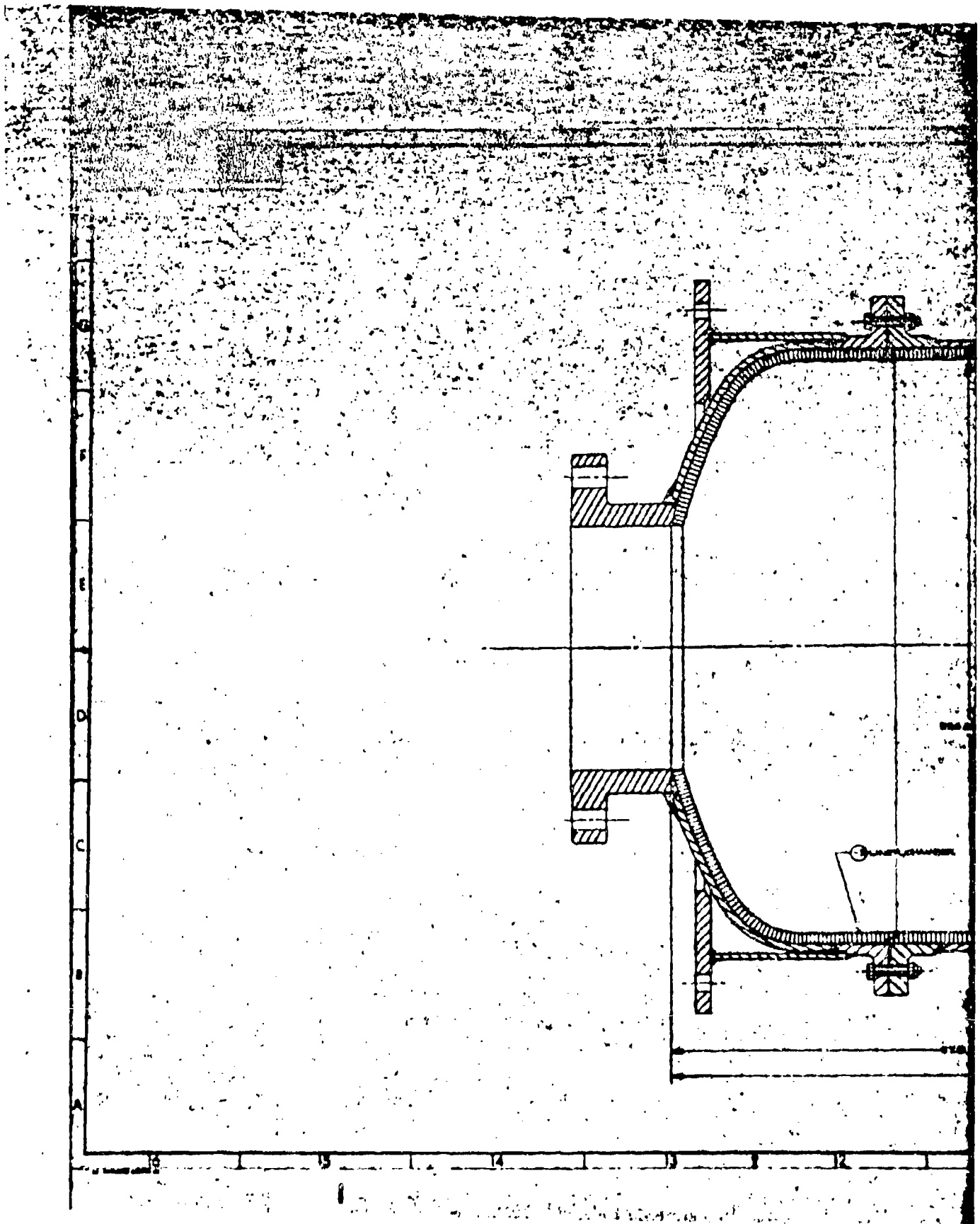

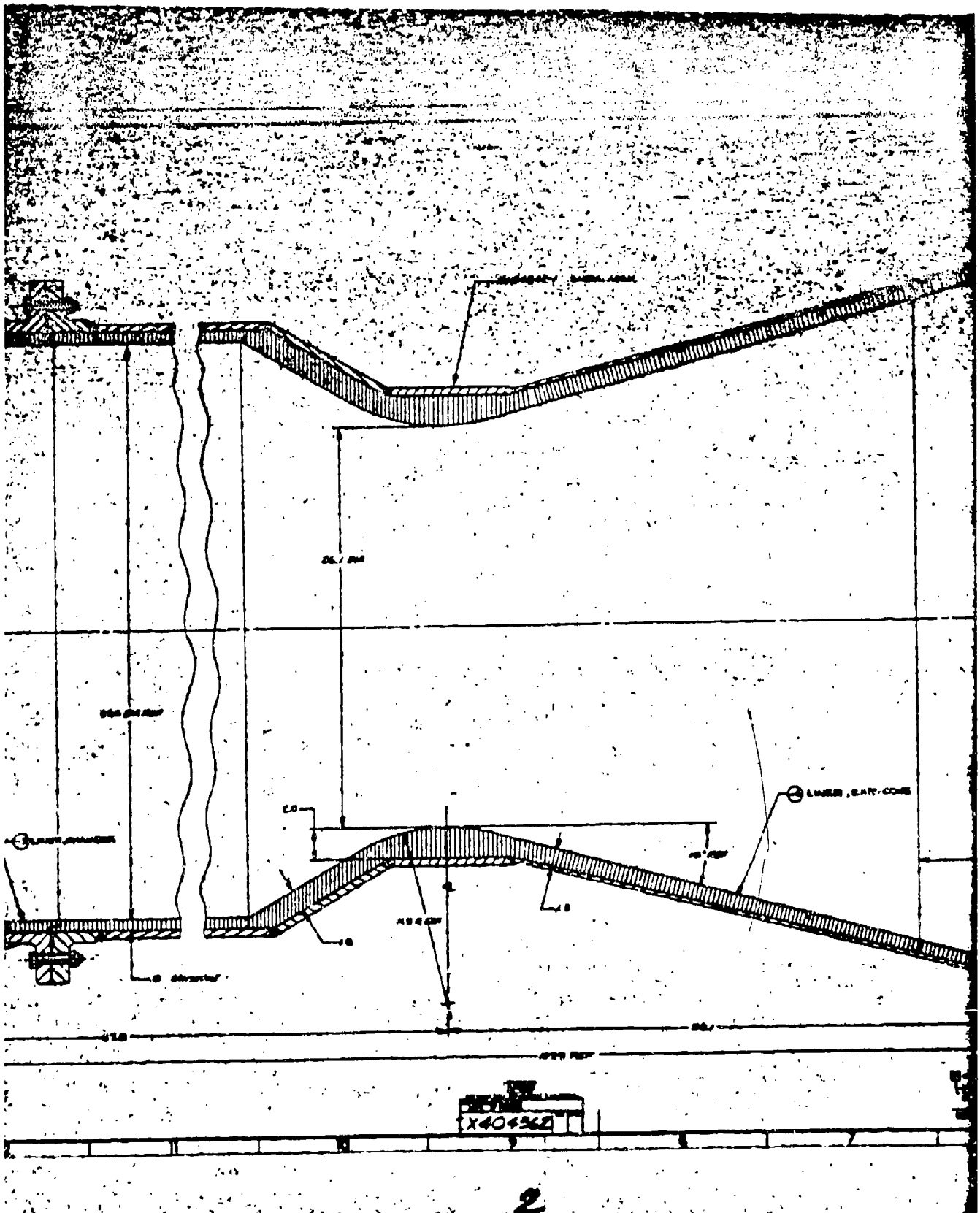

2

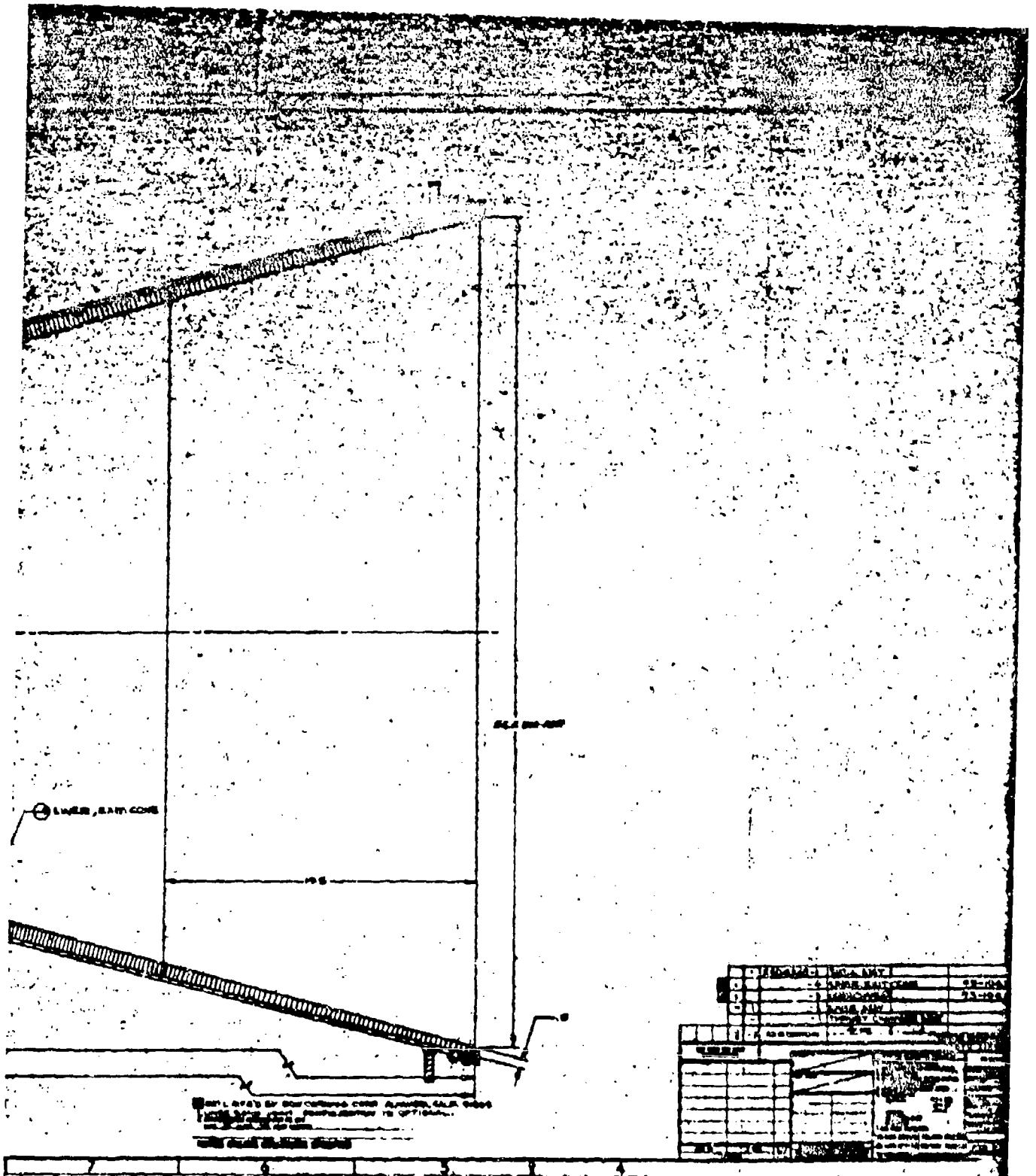

Figure 2-22.

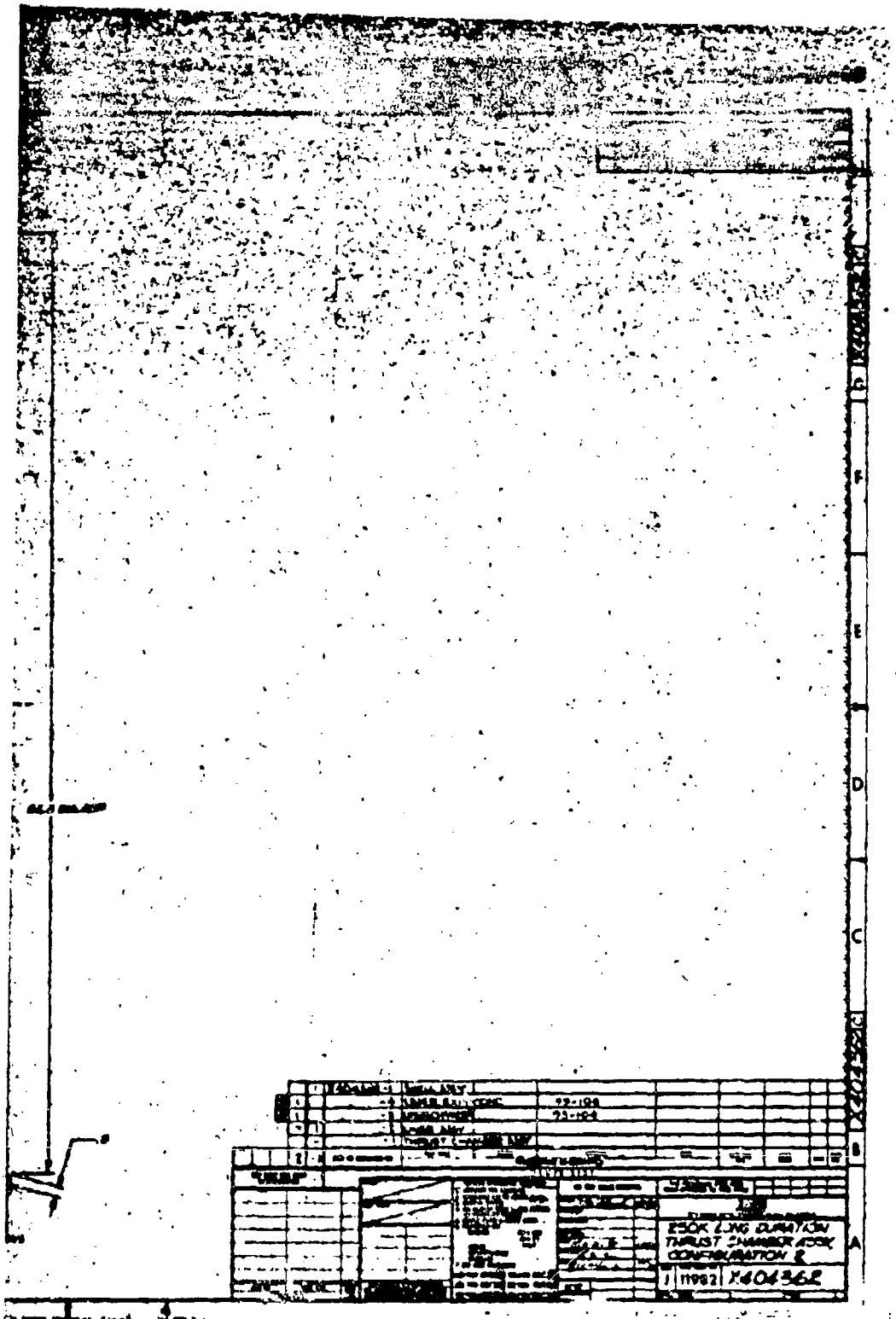

Figure 2-22. X604362 250K Long Duration Thrust Chamber Assy, Configuration 2 (U)

UNCLASSIFIED

2.3.3.2 Fabrication

(U) The X404362-2 liner assembly was cast from Dow-Corning 93-104 silicone rubber RTV using sheet metal-plywood mandrels and plaster molds to create the internal contour. Material from three lots were used to cast the entire chamber. Typical properties of the DC-93-104 material are given in Table 2-3.

Table 2-3

Properties of Materials Used in X404362-2 Liner Assembly (U)

Lot No.	203237	201319	301314
Amount	1 x 65 lbs	9 x 65 lbs	1 x 65 lbs
Viscosity, poises	2120	2160	2160
Working Time*	5 hrs	4 hrs-10 min	4 hrs-10 min
Sp. Gravity	1.47	1.45	1.45
Durometer, Shore	75	75	75
Tensile Strength, psi	260	242	242

*Time for material to reach a preliminary elastomeric state.

(U) The X404362-2 liner assembly was cast into the X404342-1 pressure shell assembly. The interior metal surfaces were sandblasted and degreased, then rinsed with methylethylketone (MEK) to prepare a scale-free, lint free substrate. Dow Corning 1200 primer was applied in a thin film by brushing and allowed to air dry prior to installation of the internal molds and mandrels.

(U) Casting of the DC-93-104 took place over a three day period. The throat approach, throat, throat extension and approximately 50 percent of the exit cone were cast during an 8 hour period; the balance of the exit cone and dome section were cast on the following day. The cylindrical chamber section was cast approximately one week later after receipt of additional material. The dome section was then bonded to the chamber section using DC-93-104 to seal the joint between the two components.

(U) DC-93-104 is a two component silicone material which is mixed in the ratio of 10 parts catalyst to 109 parts base material. The base material was not de-aired prior to mixing. Catalyst was added to the base material and mixed for approximately 5 minutes using a low speed mechanical mixer (Kol Inc., M-58). A sample from the initial batch was cured for 2 minutes at 300°F to check the mix and cure properties. Table 2-4 shows the weights

Table 2-4

DC-93-104 Batch Mixtures (U)

Batch No.	Base Weight, lbs	Catalyst Weight, lbs	Wt Cat/109 lbs Base
1	28.25	2.6	10.05
2	20.437	3.0	10.72
3	34.50	3.4	10.75
4	29.25	2.73	10.18
5	30.75	3.0	10.62
6	28.06	2.6	10.10
7	34.125	3.24	10.36
8	28.625	2.64	10.05
9	34.50	3.35	10.59
10	23.562	2.09	9.65
11	32.00	3.0	10.22
12	32.00	3.0	10.22
13	30.12	2.95	10.68
14	26.75	2.51	10.22
15	33.25	3.28	10.75
16	26.375	2.56	10.59
17	31.437	3.14	10.89
18	30.75	2.98	10.56
19	35.50	3.46	11.25
20	33.565	3.29	10.69
21	43.00	3.96	10.05
22	2.00	0.185	10.05
TOTALS	658.806	62.965	10.420 (Avg.)

TOTAL WEIGHT 721.77

(U) of base and catalyst for each of the mixtures cast into the liner assembly. As each batch was mixed it was drawn into a vacuum pot under 25 in.Hg vacuum and desired prior to injection. Samples of each mix were taken to check the working life of the material. Batches 1-4 were used to cast the throat approach and throat section; batches 4-7 were used to cast the throat extension section as shown in Figure 2-23. Batches 8-11 were used to cast the forward exit cone section, while batches 12-15 were used for the aft exit cone section. The dome section was cast using mix batches 15-17. The cylindrical chamber section was cast using batches 18-21 and batch 22 was used for the joint between the chamber and dome section and for repair of minor voids.

(U) The chamber was inverted and the plaster mold of the throat approach throat section positioned 50.1 inches from the exit plane and centrally located to provide a 2.1 $\pm$ .050 inch wall thickness at the throat. All surfaces of the plaster molds and sheet metal mandrels were wrapped with clear, 2-inch pressure sensitive polyethylene tape to act as a release film. The DC-93-104 was extruded from the deairating pot through tubing sub-surface into the space between the shell and plaster mold. Figure 2-24 shows the plaster mold located in position while Figure 2-25 shows the cast rubber nearly to the throat plane.

(U) The plaster mold for the throat extension section was then installed being keyed to the previous mold and the casting was continued using batches 4-7 for the throat extension. The forward exit cone mandrel was then installed and batches 8-11 cast. Difficulty with the extruding press and feed system for the catalyzed silicone rubber resulted in termination of the casting process following mix 11.

(U) The casting process was resumed the following morning and the balance of the exit cone was cast using batches 12-15. A central shaft was used to index the various sheet metal-plywood mandrels and plaster molds as shown in Figure 2-26. It is estimated that 440 lbs of material was used to cast the throat approach, throat, throat extension and exit cone section. This was approximately 10 percent greater than the calculated amount.

(U) A plaster mold was made for casting the dome section and is shown in Figure 2-27. This was positioned within the dome section as shown in Figure 2-23 and the rubber material was injected through 8 injection ports. The cast material and injection ports are shown in Figure 2-28. Batch mixes 15-17 were used for this section.

(U) The chamber-throat-exit cone was inverted following removal of the two plaster molds and two sheet metal-plywood exit cone mandrels and the chamber plaster mold shown in Figure 2-29 was installed. The cylindrical portion of the chamber was cast using batches 18-21. Following cure of the chamber section the plaster mold was removed and the chamber dome section was fitted to the cylindrical chamber section. A 1/2-inch x 3/8 inch step had previously been cast in each section. These two steps were joined using material from batch 22 as adhesive between the sections.

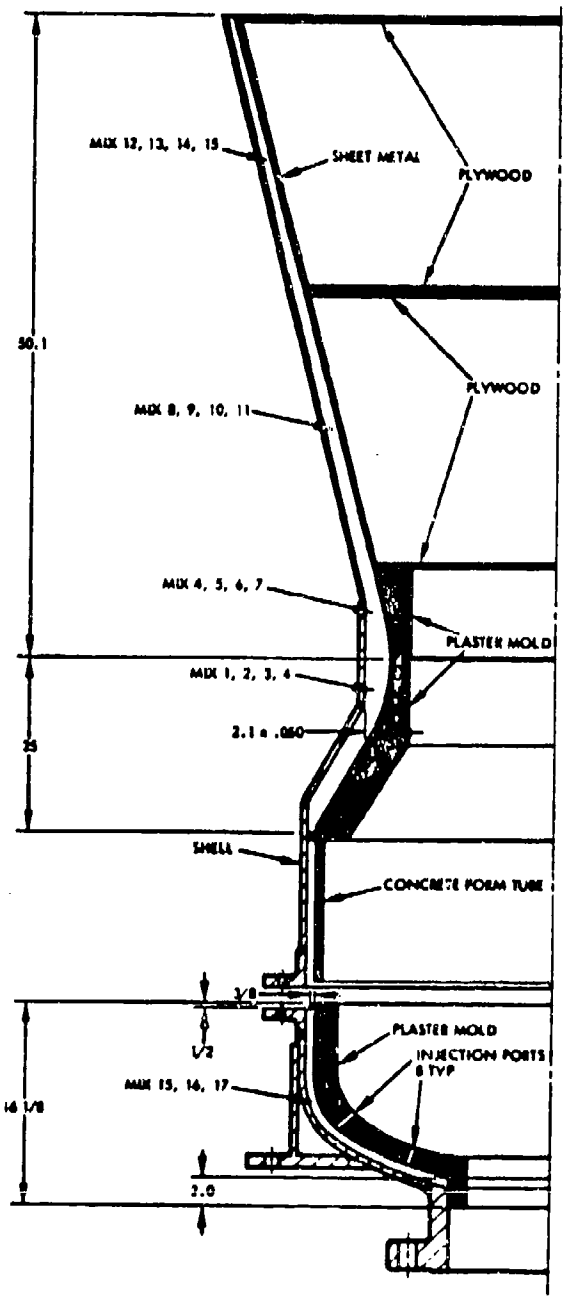

Figure 2-23. X404362 Chamber, DC-93-104 Casting Set-up (U)

Figure 2-24. X404362-1 DC-93-104 Chamber Throat Plaster in Place (U) (65907-69-1)

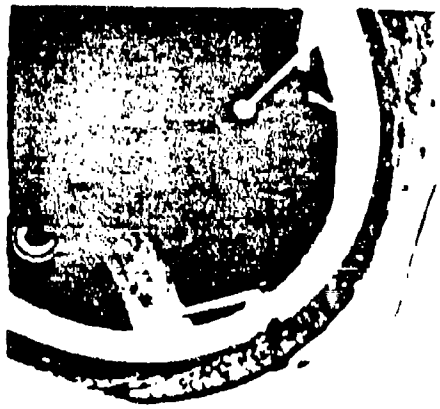

Figure 2-25. X404362-1 DC-93-104 Chamber Throat Casting (U) (65907-69-2)

Figure 2-26. X404362-1 DC-93-104 Chamber Exit Cone Mandrels and Casting (U) (65907-69-6)

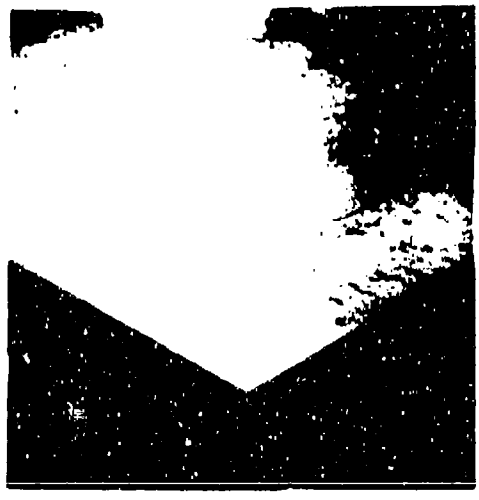

Figure 2-27. X404362-1 DC-93-104 Chamber Dome Section Plaster Mold (U) (65907-69-4)

Figure 2-28. X404362-1 DC-93-104 Chamber Cast Dome Section (U) (65907-69-7)

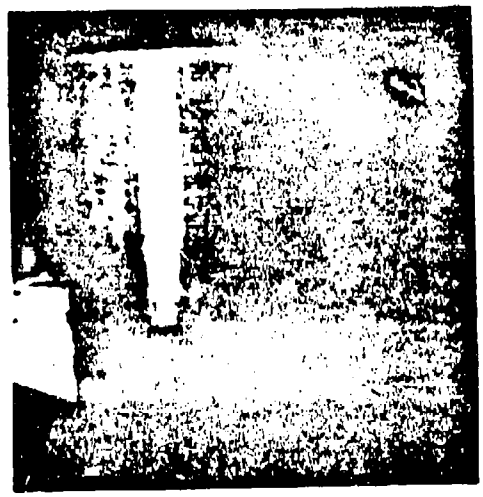

Figure 2-29. X404362-1 DC-93-104 Chamber Mandrel (U) (65907-69-5)

(U) Measurements were taken of the exit plane diameter, throat diameter and location of the throat plane following assembly. The throat diameter was 26.05 inches ±.050 inch while the exit cone diameter was 52.12 inches. The thickness at the exit plane varied from 0.56 inch to 0.62 inch around the circumference compared with the design value of 0.50 ±0.10 inch. The thickness at the forward end was a nominal 0.75 inch compared to the design value of 0.80 ±0.10 inch. The nominal ID was 37.5 inches.

(U) A specific gravity measurement taken on a sample from batch 7 indicated a specific gravity of 1.45 by the immersion method. Examination of the surface of the exit cone showed only very minute pin holes where air had been trapped between the material and polyethylene release tape. Obvious air bubbles were cleaned out and patched. The joint between cured material and uncured material (start of converging section) was thoroughly examined. There was no indication of any poor bonding condition.

(U) Figure 2-30 shows the finished liner assembly looking forward from the throat section. The marks left by the polyethylene tape and one of the injector ports are clearly visible. Figure 2-31 shows the finished assembly looking aft from the chamber side. The dark spots are places where voids have been repaired. Figure 2-32 shows the exit cone and throat section looking forward. The light coloration is where material has been trimmed from the cast part at the joints of the sheet metal mandrels.

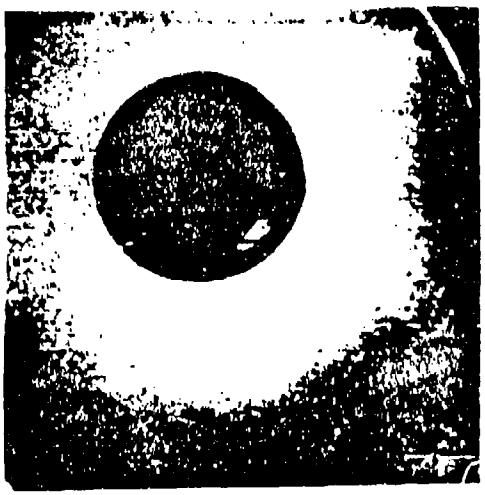

Figure 2-30. X404362-1 DC-93-104 Chamber looking forward (U) (65908-69-6)

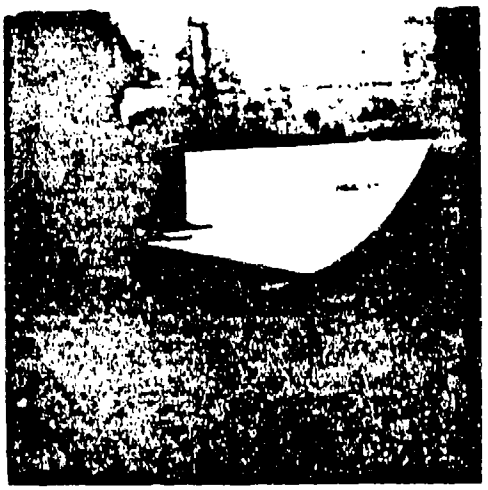

Figure 2-31. X404362-1 DC-93-104 Chamber looking aft from chamber end. (U) (65908-69-7)

2.3.4 Ablative Liner No. 3

2.3.4.1 Design

(U) The design of the X404363-1 ablative liner was based on the use of a MX-2600 silica-phenolic throat insert fabricated in the same manner as the throat insert used in the number 1 configuration liner (see 2.3.2.1). The original design of the number 3 liner was based on the use of either Haveg-41 (asbestos phenolic) or GE-223-50 (epoxy-novalak) in the chamber and exit cone in conjunction with the MX-2600 throat insert.

(U) The AFRPL approved design consisted of an MX-2600 silica-phenolic throat insert, a DP5-161 silica-phenolic chamber section and an MXA-150 asbestos-phenolic exit-cone liner. Neither material had been tested in the TRW Systems sub-scale program; data furnished by the AFRPL indicated that the MXA-150 material was at least comparable, in terms of performance, to the Haveg-41 asbestos-phenolic material used in the sizing studies. Therefore, the thickness for the exit cone was sized the same as for the Haveg-41 material. The performance of the Ironsides Resin Co. DP5-161 (formerly designated DP5-160) silica-phenolic material in the AFRPL material screening program indicated an erosion-char rate of 0.90 inches/60 seconds under the most severe conditions. Therefore, the chamber liner was designed for 2.0 inch thickness which would result in about 0.25 inches of virgin material at the end of the 120 second firing duration.

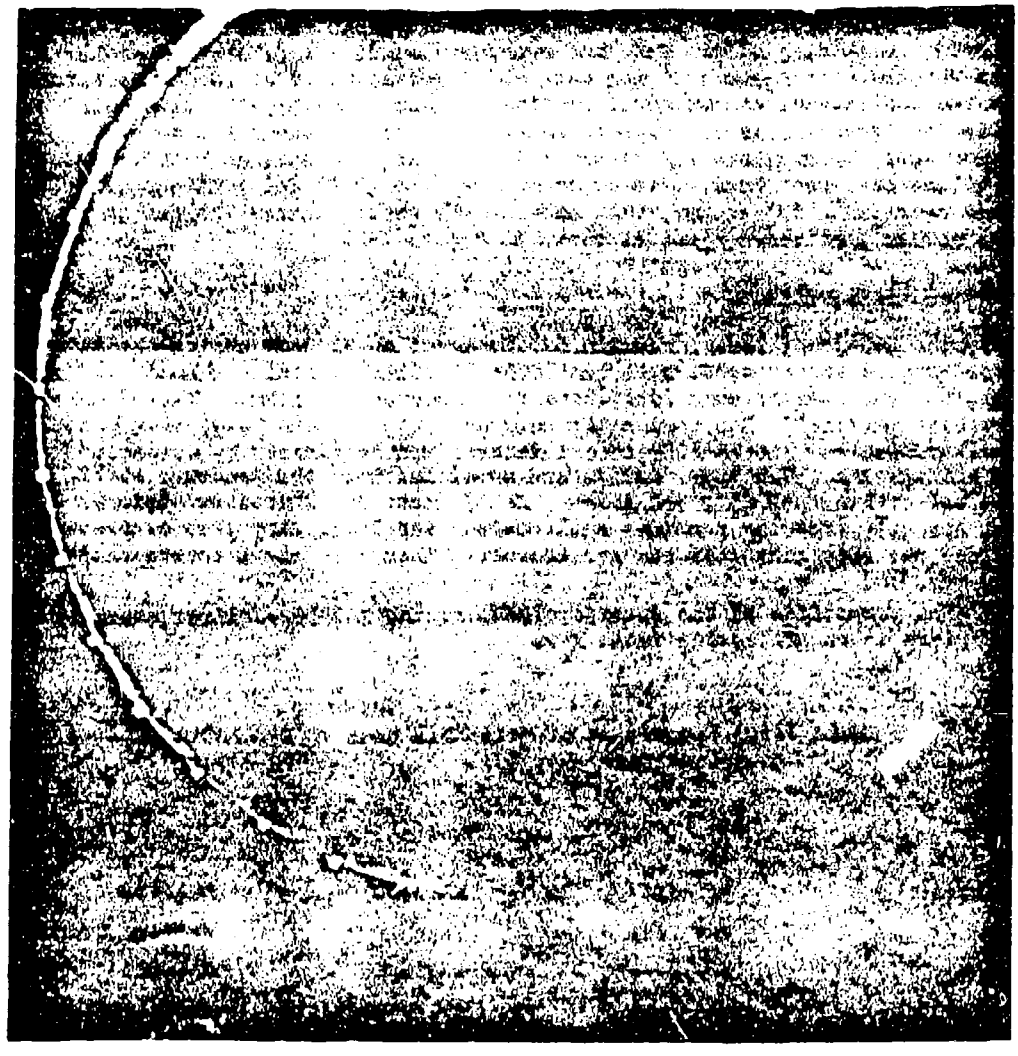

Figure 2-17. [illegible] Exit cone-throat section
(65909-69-1)

(U) The fabrication methods proposed for the number 3 chamber liner were tape-wrapping of throat insert at 60° orientation to the centerline, autoclaving, machining of the O.D. and secondary bonding to the steel shell. The DP5-161 silica-phenolic was cast and cured in place at room temperature in the same manner as the configuration 2 liner. The MXA-150 exit cone liner was designed as compression molded (1000 psi), segmented panels, secondarily bonded into the pressure shell. Nine panels, each covering a 40° sector, were used to an expansion ratio of 2.25 and twelve panels, each covering a 30° sector, were used to the nozzle exit. The design of the number 3 ablative liner is shown in Figure 2-33.

2.3.4.2 Fabrication

(U) The X404363-2 liner assembly consisted of an MX-2600 silica-phenolic tape wrapped throat section, a cast DP5-161 silica-phenolic chamber and dome section, and an exit cone fabricated from compression molded MXA-150 asbestos-phenolic material. The components were assembled into an X404342-2 pressure shell assembly. The MX-2600 throat section was fabricated by Composite Technology Inc., Van Nuys, Calif. and assembled into the pressure shell. San Rafael Plastics Co., San Rafael, Calif. cast the Ironsides Resin DP-5-161 directly into the pressure shell in two sections; they also compression molded the exit cone segments and assembled them into the pressure shell.

(U) The properties of the materials used in the X404362-2 liner assembly are given in the following Table 2-5.

Table 2-5. Properties of Materials Used in X404363-2 Liner Assembly (U)

Material	DP5-161	MX-2600	MXA-150
Form	Two Part Mixture	Tape	Molding Compound
Lot No.	--------	H-355	H-4492
Resin	--------	MIL-R-9299(II)	MIL-R-9299(II)
Filler	Silica-Silica flour	Silica (7.8%)	--------
Fabric Reinforcement	None	Silica (96.0% min)	Asbestos
Resin Solids, %	-------	31.0	49.0
Volatile content, %	-------	7.0	4.3
Specific Gravity	1.40	1.71	1.65*

*Molded @ 1000 psi

(U) The throat section (X404361-4) was tape-wrapped on a net, male mandrel at 60° to centerline using techniques identical to those described in Section 2.3.2.1. Following completion of wrapping the part was vacuum bagged and cured in an autoclave at 100 psi and 290-310°F for five hours.

(U) The part was then machined, using the mandrel on which it was wrapped, to fit the X404342-2 pressure shell. Figure 2-34 shows the finished throat section prior to assembly into the shell. Figure 2-35 shows the throat section with adhesive being lowered into the shell. The adhesive used in bonding the throat to the shell was Epon 901/B3.

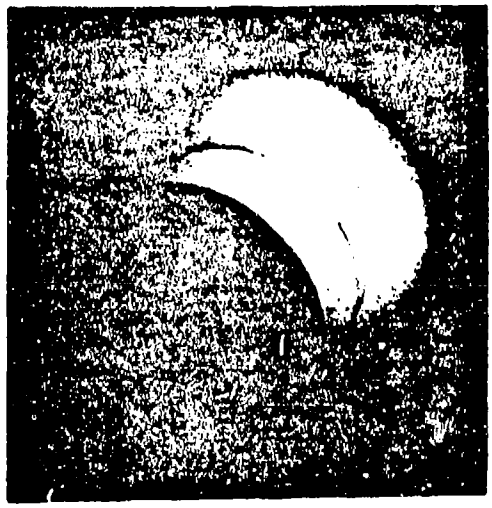

Figure 2-34. X404361-4 Throat section prior to assembly (U) (65543-69-7)

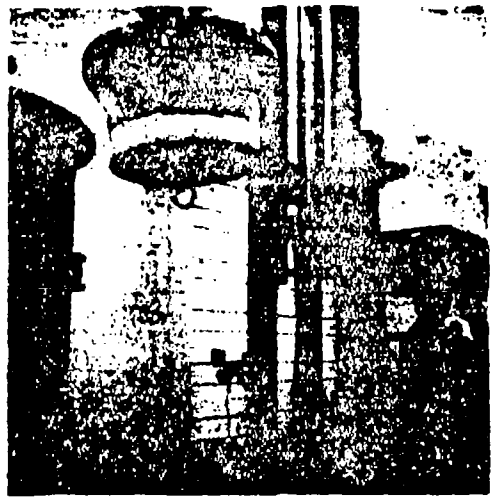

Figure 2-35. X404361-4 Throat section being installed in pressure shell (U) (65543-69-9)

(U) The throat assembly, X404363-7, was cured overnight at room temperature, then cured in an oven at 240°F for approximately 2 hours. Figure 2-36 shows the cured throat in place prior to shipment to San Rafael Plastics Co. San Rafael, California.

(U) Following receipt of the X404363-7 partial thrust chamber assembly by San Rafael Plastics the interior metal surfaces were sandblasted and degreased, then rinsed with MEK to prepare a scale-free, lint-free substrate. No primer was used in the chamber-dome sections. Samples made of material cast against both primed and unprimed surfaces showed no differences in

(U) adhesive quality. The samples also showed good adhesive qualities between cured and cast DP5-161. The throat insert was cleaned with MEK at the interface between the DP5-161 and the throat insert.

(U) DP 5-161 is a two-component ablative system consisting of a viscous phenolic type resin (DP 5-161R) and a solid hardener (DP 5-161H). The hardener contains silica fiber-silica flour fillers in addition to the hardening agent. The two components are mixed in the ratio of 0.7 parts hardener to 2.0 parts resin. This results in a very viscous mixture which is difficult to mix as shown in Figure 2-37. Two different types of mixers were tried. A Reynolds Electric Mixer (Model 114) was used to achieve a smooth consistency shown in Figure 2-38. This mixer operated at a higher mixing speed then the Kol M-58 mixer and heated the mix to a slightly higher temperature (about 90°F). A total of 21 batches of DP5-161 were mixed and cast on a single day. A sample of batch 20 was taken and cured for two weeks at room temperature to check cure properties. Table 2-6 shows the weights of resin and hardener for each of the mixtures.

Figure 2-36. X404363-7 Partial Thrust (65543-69-12) Chamber Ass'y (U)

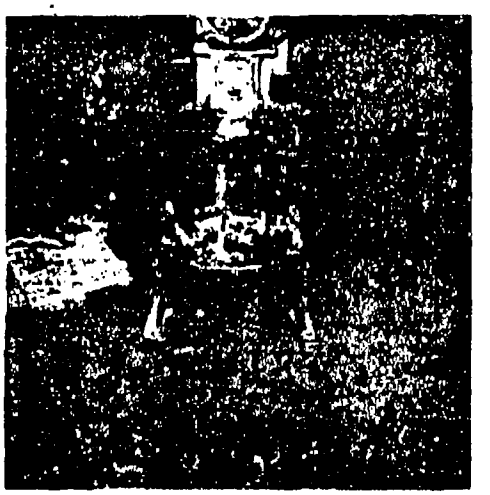

Figure 2-37. DP5-161 Mix at start (66841-69-2) of mixing cycle (U)

(U) The mixed-resin-filler system was cast in much the same manner as the DC-93-104 silicone rubber used in the number 2 liner assembly. The mixes were not deaerated prior to casting since laboratory tests indicated considerable frothing of both the mix and resin under vacuum. Entrapped air came out of the mix quite readily as the mixture was cast.

Table 2-6

DP5-161 Batch Mixtures (U)

Batch No.	Resin Wt., lbs	Hardener Wt., lbs	Wt.Resin/Wt.Hardener
1	14.50	5.063	2/0.70
2	14.88	5.186	2/0.696
3	21.06	7.312	2/0.696
4	22.06	7.75	2/0.705
5	19.13	6.75	2/0.705
6	14.63	5.125	2/0.70
7	14.06	5.00	2/0.713
8	17.88	6.25	2/0.703
9	16.63	5.685	2/0.684
10	17.57	6.125	2/0.699
11	13.43	4.75	2/0.707
12	18.68	6.50	2/0.697
13	16.82	5.68	2/0.676
14	23.62	8.06	2/0.685
15	15.93	5.62	2/0.704
16	16.68	5.81	2/0.696
17	19.18	6.75	2/0.704
18	16.03	5.56	2/0.694
19	16.94	5.94	2/0.701
20	18.68	6.50	2/0.696
21	16.82	5.68	2/0.676
TOTALS	365.21	127.10	2/0.696

NOTE: Estimated 14 lbs of mix not used in casting chamber and dome section.

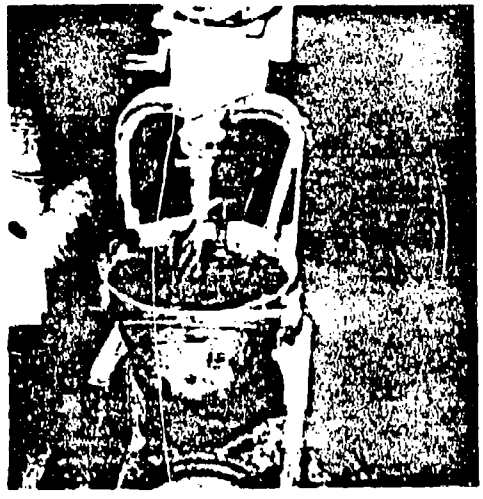

(U) The dome section was cast first using batches 1-6. A plaster mold was used to form the internal contour. This mold had only four injection ports for introducing the DP5-161 into the void. Some difficulty occurred during the casting; the resin flowed up and under the polyethylene tape used as a release film on the plaster mold. This section was broken out when the mold was broken out and later repaired. Figure 2-39 shows the dome section at the completion of the casting, and Figure 2-40 shows the dome section after removal of the plaster mold and prior to assembly with the chamber section.

Figure 2-38. (66841-69-3) DP5-161 Mix prior to casting (U)

Figure 2-39. (66841-69-1) X404363-1 Dome section at completion of casting (U)

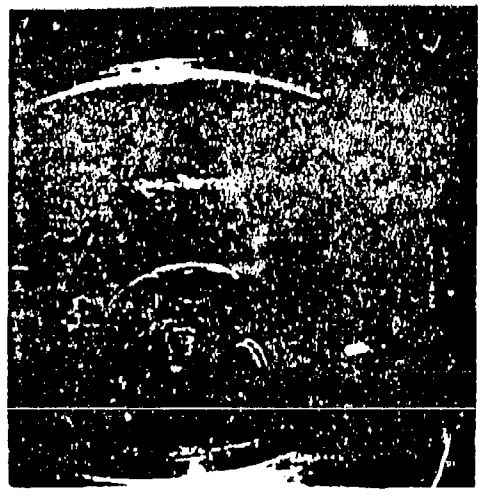

Figure 2-40. (67989-69-6) X404363 Dome section prior to assembly (U)

(U) The chamber section was cast using a sheet metal-plywood mandrel to form the internal contour. The mandrel was secured in place using the X404361-4 throat section, which had been installed previously, as an anchor for the cylindrical section Batches 7-21 were used to cast the two-inch thick section. Figure 2-41 shows the cast DP5-161 near the top of the flange; Figure 2-42 shows the completion of casting of the step-joint in the cylindrical section. The cast material was allowed to cure for approximately 10 days at room temperature prior to removal of the mold and mandrel. Figure 2-43 shows the chamber (DP5-161)/throat (MX-2600) interface after removal of the casting mandrel.

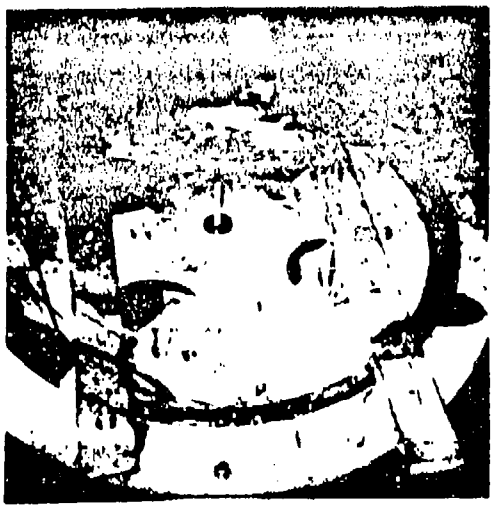

Figure 2-41. X404363-1 2 inch thick cylindrical chamber section. (U)
(66841-69-6)

Figure 2-42. X404363-1 Completion of casting chamber section (U)
(66841-69-8)

(67989-69-11)

Figure 2-43. DP5-161/MX-2600 Interface looking aft. (U)

(U) The exit cone was fabricated from MXA-150 molded segments, secondarily bonded into the pressure shell using GLOM-O-N RT high temperature adhesive. The forward exit cone segments covered a 40 degree segment while the aft exit cone segments covered a 30 degree segment. The segments were molded in matched cast-iron dies using a 200 ton press. Figure 2-44 shows the two punches (forward and aft segments) prior to clean-up. The molding cavity was put in place on a steam-heated platen on the base of the press, while the punch was attached to a steam heated platen on the ram. Temperature of the casting molds were held at 325°F. The MXA-150 was preheated to 190°F prior to charging into the cavity. Figure 2-45 shows the forward segment after molding and prior to release from the cavity.

Figure 2-44. MXA-150 Segment Punches (66841-69-4) (U)

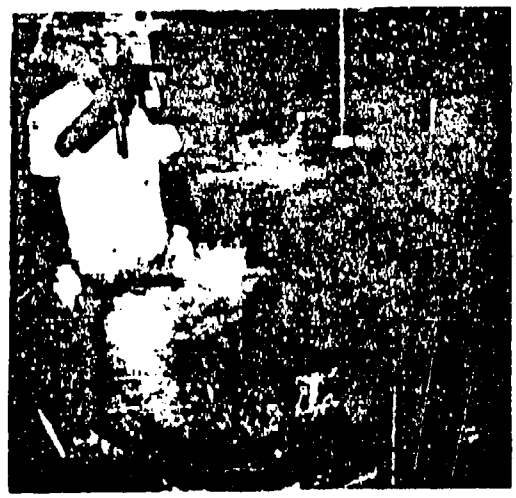

Figure 2-45. Molded MXA-150 Fwd (67989-69-10) segment cavity (U)

(U) Both the forward and aft exit cone segments were molded oversize and required trimming. Figures 2-46 and 2-47 show a molded forward exit cone segment set up for trimming. The trim lines are clearly visible in the photograph. The nine 40° forward cone, segments and twelve 30° aft cone segments were dry fitted in the pressure shell and final trimming made on the key pieces. The weights of the various segments are given in Table 2-7.

(U) A 3/4 inch wide by 1/16 inch deep recess was routed into the backside of each segment and 1 1/2 inch wide silica phenolic doubler strip was attached to each longitudinal joint with adhesive.

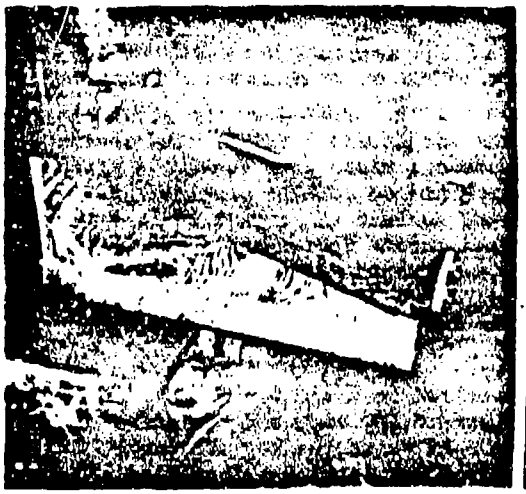

Figure 2-46. (67989-69-7) Rough molded MXA-150 fwd segment set-up for trimming (U)

Figure 2-47. (67989-69-8) Molded MXA-150 fwd segment (rough) set-up for trimming (U)

Table 2-7

Weights of Molded MXA-150 Segments*(U)

Panel No.	Forward Cone (40°)	Panel No.	Aft. Cone (30°)
1	22.19	1	17.50
2	22.19	2	16.82
3	22.38	3	17.00
4	22.19	4	17.06
5	22.38	5	16.63
6	21.82	6	16.63
7	21.44	7	16.82
8	22.13	8	16.69
0(1)	21.94	9	16.82
		10	16.75
		11	16.69
		0(1)	16.13
Total	198.66	Total	201.54 = 400.20 lbs

*Includes weight of silica doubler strips
(1) Key panel

(U) Prior to the start of installation of the segments the steel shell was sandblasted and wiped clean with MEK. GLOM-ON RT adhesive mixed in the ratio of 40 parts of A to 100 parts of B was applied to the pressure shell and backside of each panel plus the longitudinal joint. The panels were put in place starting with the number one panel (two doubler strips) and finishing with the key panel (0) which had no doubler panel strips. Panels were slid forward until they butted against the throat section (X404361-4) until the measured gap between throat insert and forward panels became essentially zero. Figure 2-48 shows all forward panels in place and bottomed out on the throat insert. A plywood ring which fit against the individual panels was used to hold the panels in the proper position until the adhesive had set.

(U) The aft exit cone segments were installed in a similar manner. The panels were put in place with an approximate 0.100 inch wedge holding the panel from the forward segments. Figure 2-49 shows the key aft panel being installed in the exit cone. After the key panel was installed all wedges were pulled and the 12 segments were allowed to bottom out on the forward panels. The panels were held in place with a plywood bonding fixture and C-clamps. Approximately 35 pounds of adhesive were used in the secondary bonding operation resulting in an exit cone weight of approximately 435 pounds.

Figure 2-48. (70053-70-4) 9 Forward panels in place (U)

Figure 2-49. (70053-70-6) Key aft panel being installed in the exit cone (U)

(U) Finishing operations consisted of cutting the aft segments to length and installing the retainer clips. All longitudinal joints and circumferential interfaces were ground smooth. Figures 2-50 and 2-51 show the

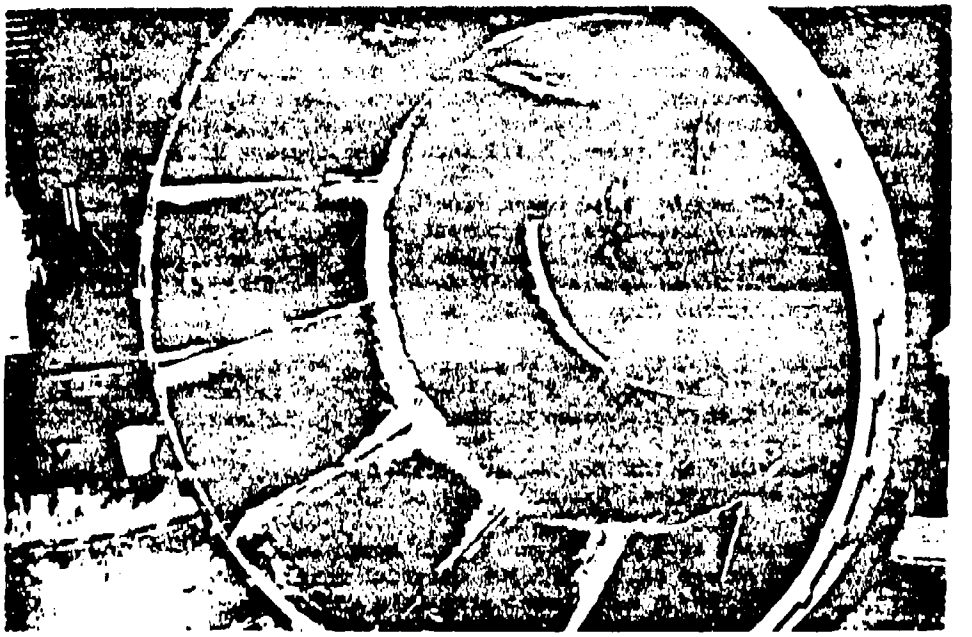

(70054-70-4)

Figure 2-50. X404363-1 Chamber prior to shipment to the AFRPL (U)

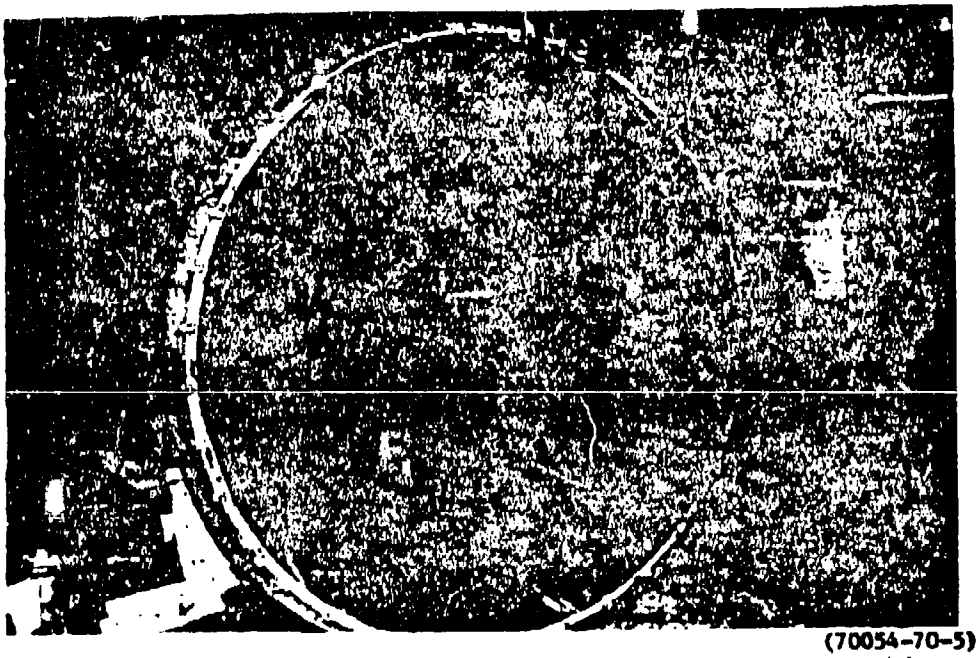

(70054-70-5)

Figure 2-51. X404363-1 Chamber prior to shipment to the AFRPL (U)

(U) finished part prior to shipment to the AFRPL.

(U) Measurements were taken of the exit plane diameter, throat diameter, chamber diameter and location of the throat plane prior to shipment. The throat diameter was 26 1/8 inches, ± 1/16 inch, while the exit plane diameter was 52 1/8 inches, ± 1/8 inch. The chamber diameter was 35 inches.

(U) Material samples were taken from each end of the MX-2600 throat. Specific gravity samples of the throat indicate a Sp. Gr. of 1.71 for both samples. The throat was also weighed (183.5 lbs); using the calculated volume results in an apparent bulk density of 1.735. The specification requirement for the throat Sp. Gr. was 1.65 (min).

(U) The Sp. Gr. of the MXA-150 panels was 1.54 compared to a specification requirement of 1.60 (min). A small sample piece molded at 1000 psi had a Sp. Gr. of 1.65. The cause of the difference is unknown.

(U) The Sp. Gr. of the DP5-161 cast material was 1.38. The material supplier had suggested a nominal Sp. Gr. value of 1.40.

(U) Examination of the configuration 3 liner assembly at AFRPL showed considerable shrinkage of the DP5-161 material from the time the material was cast. This shrinkage manifested itself in two ways; the bond between the dome and cast material was broken and cracking of the liner was experienced. Prior to the test firing the repair of the chamber dome liner was attempted. The repair consisted of the back-filling of the void between insulation and shell with a 50:50 mixture of Epon 828-Versamid 115 adhesive using a SEMCO hand applicator to inject the adhesive mixture into the void. This repair was only partially successful as noted in Section 3.3.3.3.

SECTION 3

TEST RESULTS

3.1 GENERAL

(U) The results of the Task II test effort are summarized in this section. Detailed discussions of each checkout test series and each long duration test firing are given in the following sections. In addition, the summary of the performance of the S/N 001 and S/N 002 demonstration injectors which were checked out in Task I are included for completeness. The hardware used in Task II is tabulated in Section 3.2. The test results presented herein were derived from computer printout data furnished TRW Systems by the AFRPL. Detailed data reduction procedures used at arriving at the test results are given in Appendix E.

3.2 TEST HARDWARE

(U) The test hardware, including injector configurations, used in the Task II test program is tabulated as Table 3-1. The initial four test firings (103-106) employed the X404056-1 (S/N 003) demonstration injector and the Dev-1A heat-sink combustion chamber. The S/N 001 and S/N 002 demonstration injectors had been checked out previously in Task I (see Volume 1). The first ablative liner firing (107) employed the S/N 003 demonstration injector and the number 1 ablative thrust chamber assembly.

(U) Following test firing 107 the development injector with the 06/F2 orifice configuration was checked out with the heat-sink combustion chamber to determine if acceptable performance could be achieved in a finer pattern injector. This configuration failed to produce satisfactory performance and the X404056-1 (S/N 001) demonstration injector was used with the number 3 ablative thrust chamber assembly for firing 111.

(U) The X404056-1 (S/N 002) demonstration injector was used with the number 2 ablative thrust chamber assembly for the third long duration firing (117). The demonstration injectors weigh approximately 1500 pounds. The ablative thrust chamber pressure vessels weigh approximately 2850 pounds and the ablative liners weigh from 680 to 1130 pounds. The number 2 ablative liner is the lightest weight design.

3.3 TEST RESULTS

3.3.1 Checkout Firings - S/N 003 Demonstration Injector

3.3.1.1 Performance Data

(U) The only demonstration injector which was not test fired during the Task I test program was the S/N 003 injector. This injector was essentially identical to the S/N 001 and S/N 002 injectors. This injector was used to calibrate the system following facility modification and was fired four times (103-106) prior to installation of the first ablative chamber.

(U) Figure 3-1 shows the measured thrust as a function of the nozzle stagnation pressure (Po). Po is computed from the average of PC-1/PC-2 (Figure E-2 of Appendix E shows the location of the instrumentation ports) corrected to throat stagnation pressure for an $\epsilon_c = 2.25$ and a $\gamma = 1.235$. The data for the checkout firings of the S/N 001 and S/N 002 demonstration injectors is shown for comparative purposes. Substantial agreement is shown between the S/N 001 injector checkout data and the data from firings

(U) Table 3-1. Test Hardware Configurations (U)

Test Firings / Hardware	103-106	107	108-110	111	117
Injector Assembly					
X403829-20			X		
X404056-1 (S/N 1)				X	
X404056-1 (S/N 2)					X
X404056-1 (S/N 3)	X	X			
Pintle Tip Assembly					
X404408-6			X		
X404280-1	X	X		X	X
Oxidizer Orifice Ring					
X404108-1			X		
X404693-1	X	X		X	X
Fuel Orifice Ring					
X403832-4			X		
Thrust Chamber Ass'y					
X403646-11	X		X		
X404361-1		X			
X404362-1					X
X404363-1				X	

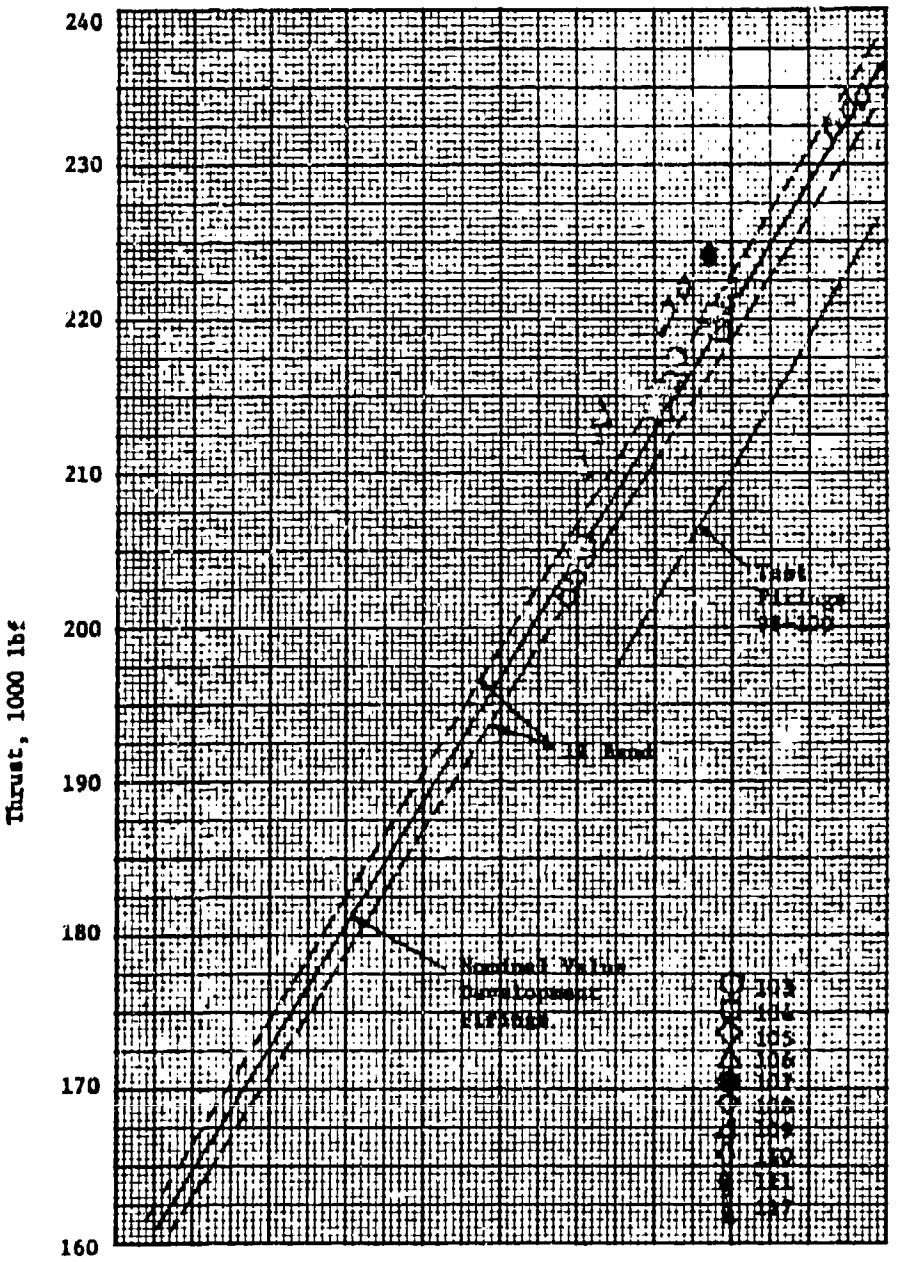

(C) Figure 3-1. Measured Thrust, Task II Test Program (U)

(U) 103-106 while the data from firings 98-100 with the S/N 002 injector show a loss in the thrust coefficient of about 4 to 5 percent.

(U) The computed specific impulse efficiency, η_{Isp}, for the S/N 003 injector is shown in Figure 3-2 as a function of the operating mixture ratio. The data is well ordered except for the data of firing 103 which was of short duration and was terminated prematurely. The data from the S/N 001 injector checkout firings is shown for comparative purposes.

(U) The computed combustion efficiency, η_{C^*}, for the S/N 003 injector is shown in Figure 3-3 as a function of the operating mixture ratio. The throat stagnation pressure is computed from the average of PC-1/PC-2 as described in Appendix E, Section 2. Again, with the exception of test firing 103, the data are well ordered. The data for the S/N 001 and S/N 002 injector checkout firings are shown for comparative purposes. The agreement between the S/N 001 and S/N 003 injectors is very good while the combustion efficiency of the S/N 002 injector is about 1 percent greater than either the S/N 001 or S/N 003 injectors.

3.3.1.2 Injector Characteristics

(U) The fuel injector conductance, KLJCF, for test firings 103-106 is shown in Figure 3-4 as a function of the volumetric flow rate. The fuel orifice discharge coefficient computed from the average conductance is 0.955 which is in essential agreement with the value measured with the S/N 002 injector during water-flow. The indicated conductance for the S/N 001 and S/N 002 injectors during the checkout firings is shown for comparative purposes. Both these injectors have indicated discharge coefficients greater than 1.0. The internal manifold losses [(PIF-2) - (PIF-1)] show good agreement with those measured during the S/N 001 injector checkout firings.

(U) The oxidizer injector conductance, KLJCO, for test firings 103-106 is shown in Figure 3-5 as a function of the volumetric flow rate. The oxidizer orifice discharge coefficient computed from the average conductance is 0.652 which is approximately 5 percent lower than the average conductance measured with the S/N 001 and S/N 002 demonstration injectors. The differences in conductances between the injectors is attributed to errors in the measurement of injection pressures (or chamber pressures) and propellant flow rates. Errors in propellant densities do not result in significant changes in the conductances.

(C) The specific impulse efficiency for the X404056-1 (S/N 003) demonstration injector is shown in Figure 3-6 as a function of $(\Delta P_r)^{0.5}(\mu)^{0.4}$, which is the performance correlating parameter used in Task I. The apparent peak performance occurs at a nominal value of 1.80 although insufficient data was taken to define the exact peak.

3.3.2 Long Duration Firing No. 1 - X405090-1 Engine Assembly

(U) The X405090-1 250,000 lbf thrust (vacuum engine assembly was fired on December 1969 for 66 seconds. The engine assembly consisted of an initial combustion chamber length to diameter ratio of 1.54, a contraction ratio of 1.8 and characteristic length of 89 inches. The thrust chamber liner consisted of MXA-150 (asbestos-phenolic) in the chamber-dome section, MX-2600 (silica-phenolic) tape-wrapped throat insert, and MX-2600 (silica-phenolic)

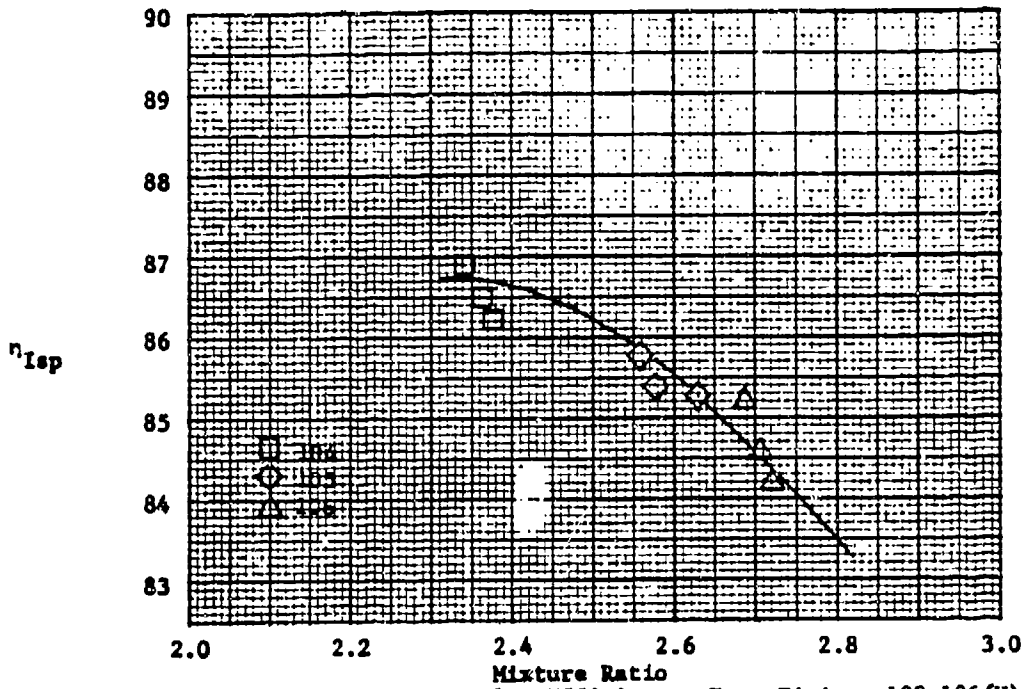

(C) Figure 3-2. Specific Impulse Efficiency, Test Firings 103-106(U)

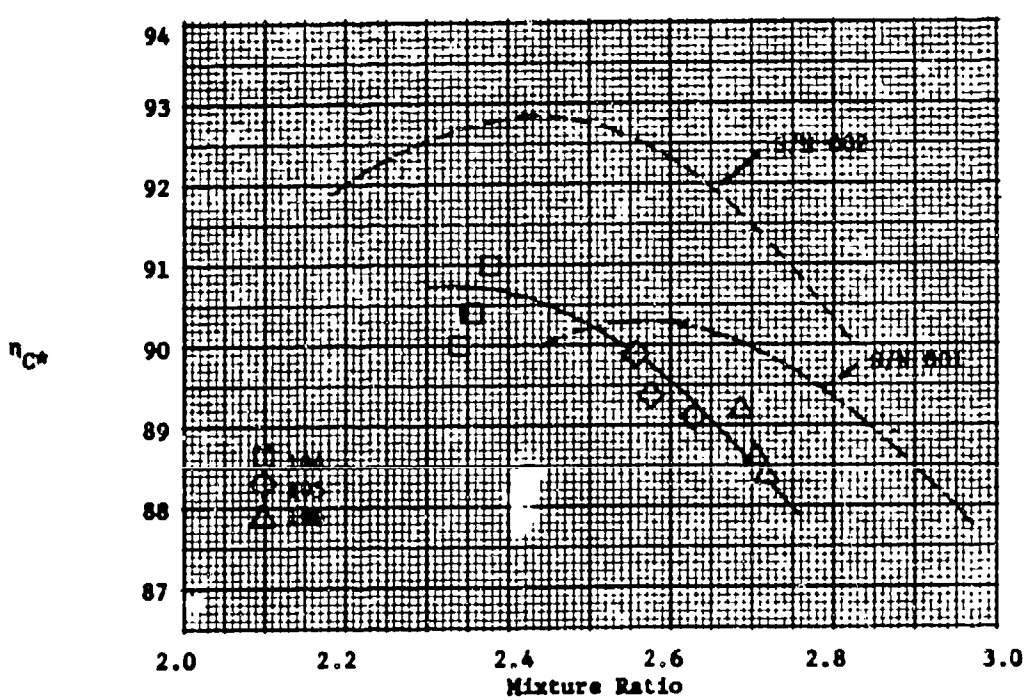

(C) Figure 3-3. Combustion Efficiency, S/N 003 Injector (U)

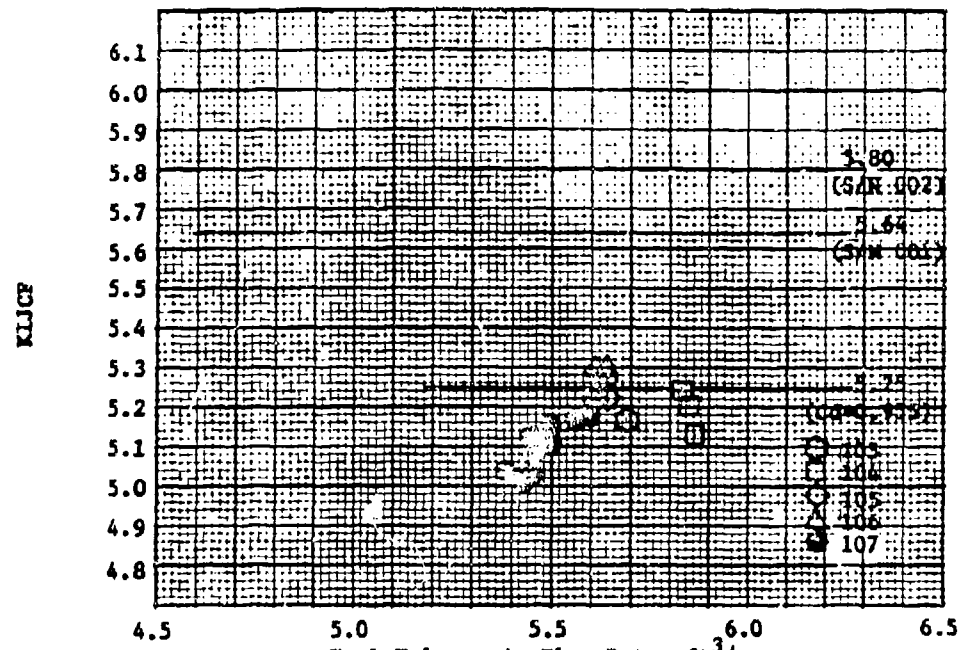

Figure 3-4. Fuel Injector Conductance, S/N 003 Injector (U)

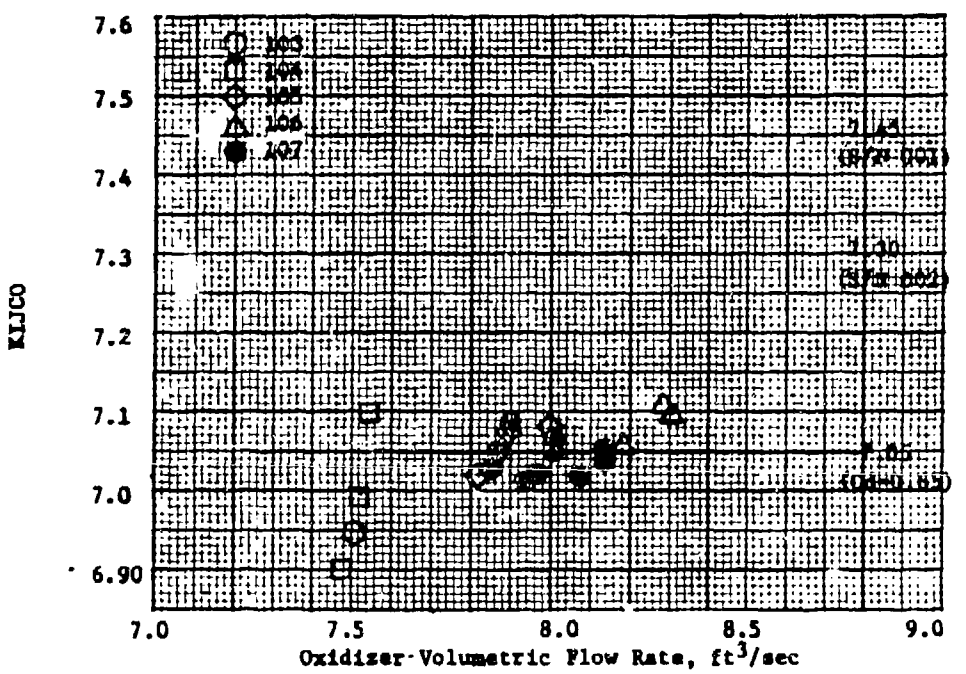

Figure 3-5. Oxidizer Injector Conductance, S/N 003 Injector (U)

(This page is unclassified.)

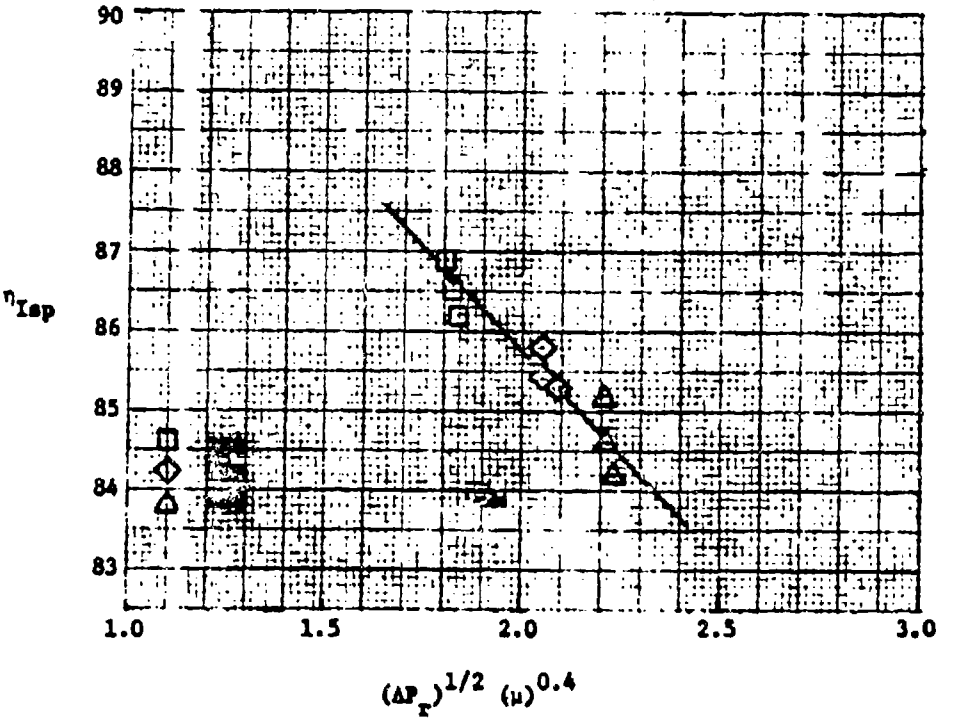

(C) Figure 3-6. Specific Impulse Efficiency, S/N-003 Injector (U)

(U) layed-up in a rosette pattern in the exit c[illegible]. The firing (107) was scheduled for 120 seconds but was terminated pre[illegible]y by a burn through of the pressure shell behind the throat insert. The burn through was believed due to excessive erosion of the MXA-150 asbestos-phenolic material in one quadrant of the chamber with subsequent ejection of the remaining MXA-150 material and a number of MX-2600 silica-phenolic laminations of the throat insert. This allowed the bond line to be exposed to hot combustion gases which subsequently allowed hot gases behind the throat. The pressure differential across the insert (from O.D. to I.D.) cracked the insert, allowing gas flow, and resulting in a burn through. The test is discussed further in the following sections.

3.3.2.1 Performance Data

(U) The initial 250,000 lb_F thrust (vacuum) engine assembly tested in Task II consisted of the X404056-1 (S/N-003) demonstration injector and the X404361-1 thrust chamber assembly. Checkout firings of the S/N-003 injector were made just prior to the firing (107) and the results are given in Section 3.3.1.

(U) The thrust-throat stagnation pressure relationship calculated for the initial 1.5 seconds of the firing is essentially in agreement with the data obtained during the checkout firings (see Figure 3-1). This would be expected since erosion is not expected until a steady-state ablation process has been established. This process has been estimated to take about 5 seconds. The computed specific impulse efficiency, η_{Isp}, for firing 107 is shown in Figure 3-7 as a function of mixture ratio. At comparable mixture ratios the performance is about one percent greater than measured in the cold wall (heat-sink) combustion chamber. This is due to an increase of 1.0 percent in combustion efficiency since the nozzle efficiency remained essentially the same as measured in test firings 103-106.

(U) The initial throat diameter was 26.2 inches which increased to approximately 27.0 inches at the end of the firing. The chamber I.D. was 35.0 inches at the start of the firing and was estimated to be 38.5 inches post-test. These values were used to determine the contraction ratio as a function of time which in turn was used to correct the head-end pressure to throat stagnation pressure. The throat stagnation pressure and measured thrust are shown in Figure 3-8 as a function of time. These values were differentiated as discussed in Appendix E, Section 5 to arrive at the erosion rate (dr/dt) as a function of time which is shown in Figure 3-9. The erosion rate of the MX-2600 throat insert is somewhat lower than predicted from the sub-scale test results (see Appendix B).

3.3.2.2 Injector Characteristics

(U) The fuel injector conductance, KIJCF, for test firing 107 is shown in Figure 3-4 as a function of the volumetric flow rate. The data for the checkout firings is shown for comparative purposes.

(U) The oxidizer injector conductance, KIJCO, for test firing 107 is shown in Figure 3-5 as a function of the volumetric flow rate. The data for the checkout firings is shown for comparative purposes.

3.3.2.3 Ablative Material Performance

(C) The average erosion rate of the MX-2600 silica-phenolic throat insert (tape-wrapped at 60° to ℄ was 6.0 mils/second. This is slightly lower than the predicted value of 7.3 mils/second which was obtained in the sub-scale test program (see Appendix B). The throat erosion was nearly completely symmetrical with one cool streak of approximately 1.0 inches width located at 270° from the fuel inlet (clockwise). Although the insert was cracked and portions were ejected it is believed that these cracks and loss of material were the result of the failure of the material upstream of the throat insert.

(C) The erosion rate of the MX-2600 silica-phenolic exit cone liner (rosette lay-up) was slightly higher than predicted (~2 mils/sec) due to localized heating. The 36 streak pattern created by the injector and observed in the chamber section was observed in the exit cone. The observed erosion rate in these streak areas was 3-4 mils/second. Some

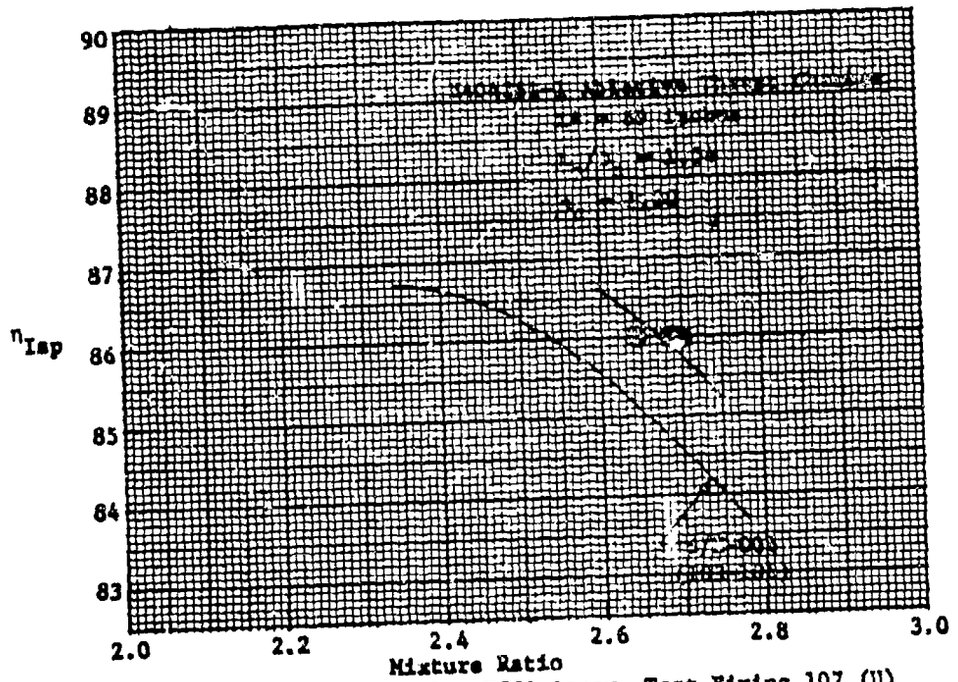

(C) Figure 3-7. Specific Impulse Efficiency, Test Firing 107 (U)

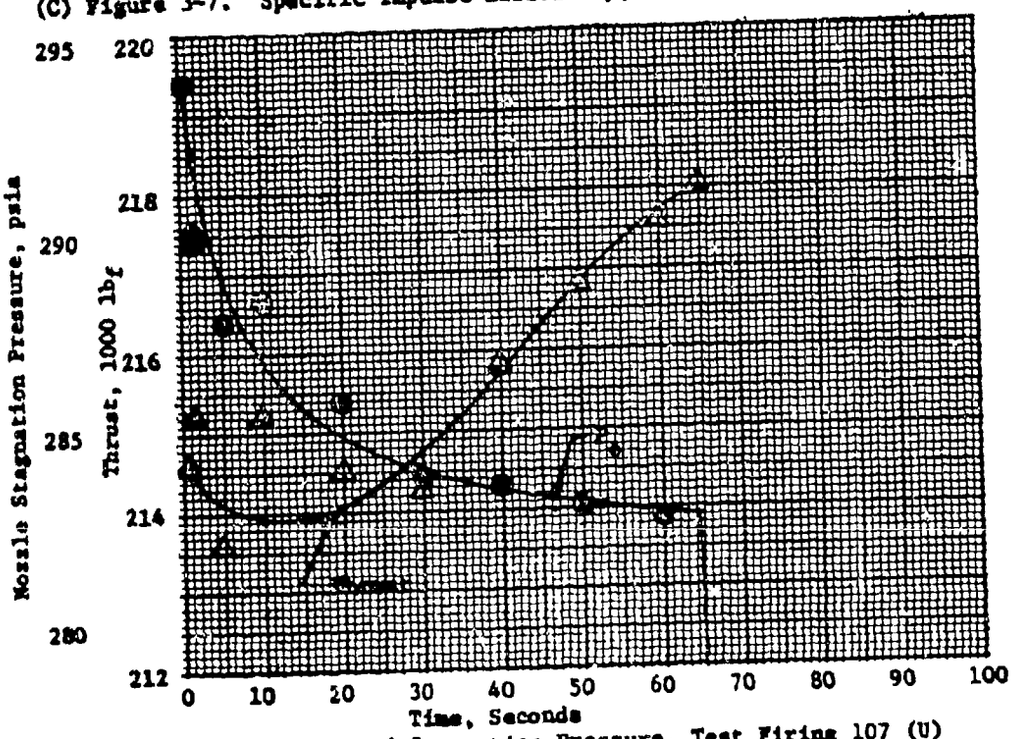

(C) Figure 3-8. Thrust and Stagnation Pressure, Test Firing 107 (U)

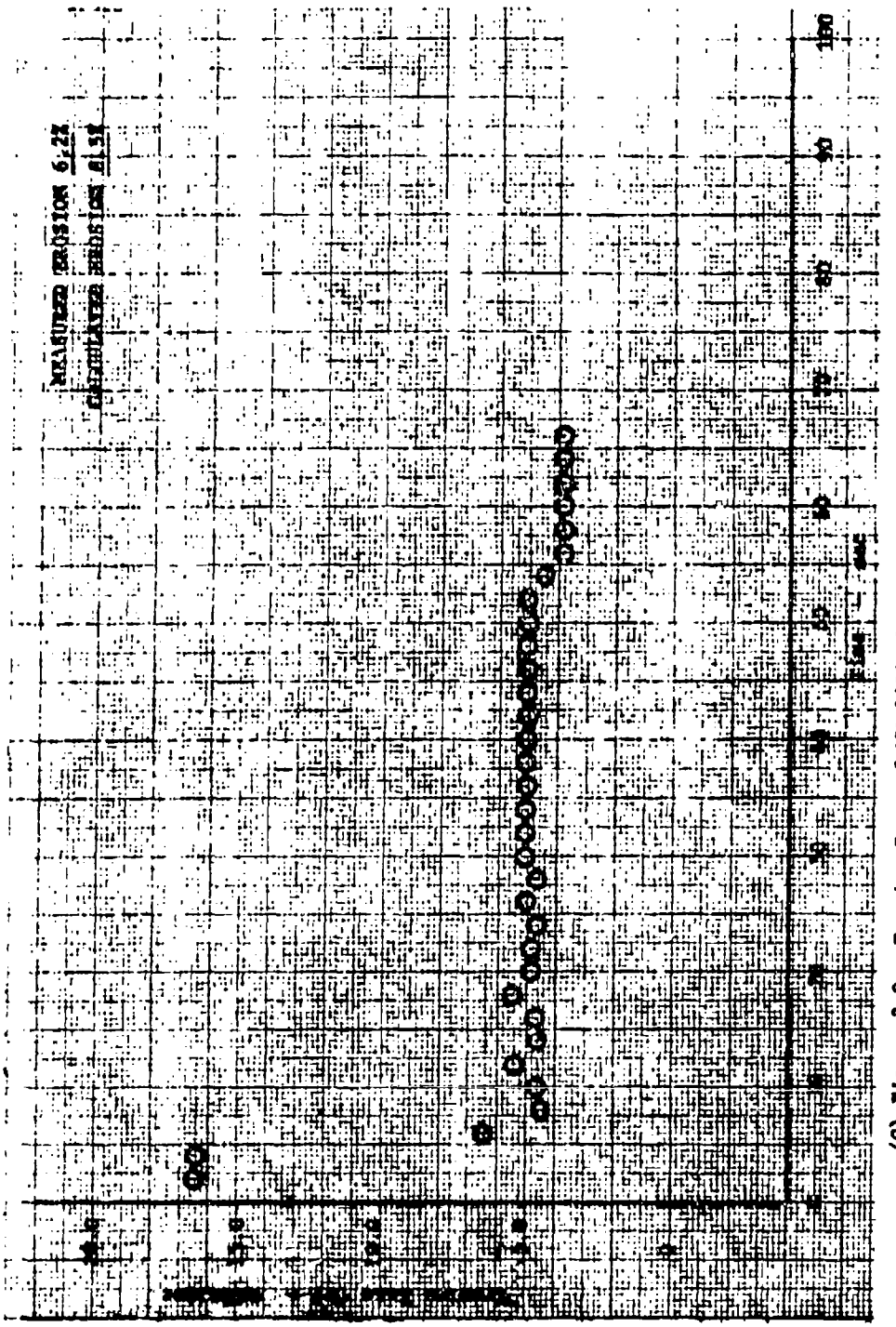

(C) Figure 3-9. Erosion Rate of MX-2600 Throat Insert, Test Firing 107 (U)

(C) delamination of the exit cone plies occurred near the exit plane. This separation is typical of rosette lay-ups.

(C) The erosion rate of the MXA-150 (parallel-to-surface layup) in the chamber at a point 24 inches upstream of the throat averaged 17.5 mils/second (8.0 to 28.3 mils/second). The greatest erosion occurred at 150° (clockwise) from the fuel inlet which corresponds to the section where a portion of the liner was ejected during the firing. At a point 12 inches upstream of the throat (start of convergent section) the average erosion rate was 10.8 mils/second (5.5 to 15.6 mils/second) with the greatest erosion again being at 150° from the fuel inlet. The circumferential variation in erosion rate is probably due to a combination of mixture ratio variation caused by the manifold maldistribution, and material nonuniformity due to the method of fabrication (molded insitu at 100 psi). Examination of the test hardware post-test indicated that the portion of the chamber liner (80° to 150° clockwise from the fuel inlet) which was jected during the firing probably delaminated the upstream portion of the throat insert. This exposed the bond line to hot combustion gases which eventually led to gas flow behind the insert and burn through of the pressure shell.

3.3.3 Long Duration Firing No. 2 - X405090-3 Engine Assembly

(U) The X405090-3 250,000 lbf thrust (vacuum) engine assembly was fired on 12 December 1969 for 83 seconds. The engine had an initial combustion chamber configuration identical to the first long duration firing. (L^* = 89 inches, L/D = 1.54 and ε_c = 1.80.) The firing (111) was scheduled for 120 seconds but was terminated prematurely by a burn through of the pressure shell in the exit cone. This burn through was believed due to excessive erosion of one of the forward, molded MXA-150 panels (~150° clockwise from the fuel inlet) which resulted in ejection of the aft, molded panel just downstream. Ejection of the first aft segment led to the subsequent ejection of four (4) additional segments during the firing and the remaining seven (7) segments were ejected during the shutdown sequence. The loss of insulation in the one 40° sector resulted in two local burn throughs of the pressure shell. The test firing is discussed in further detail in the following sections.

3.3.3.1 Performance Data

(U) The second 250,000 lbf thrust (vacuum) engine assembly tested in Task II consisted of the X404056-1 (S/N 001) demonstration injector and the X404363-1 thrust chamber assembly. The checkout firings of this injector were made during Task I and are reported in Reference 1. This injector was also used in the durability firing (number 78) with the low-cost insulated heat-sink combustion chamber. Prior to test firing 111 the char layer on the pintle tip was removed by grinding and the pintle tip was refurbished using V-61 rubber. The thrust chamber liner consisted of DP5-151 (silica-phenolic) in the dome-chamber section, MX-2600 (silica-phenolic) tape-wrapped throat insert, and MXA-150 (asbestos-phenolic) molded segments in the exit cone.

(U) The measured thrust-throat stagnation pressure relationship shown in Figure 3-1 for firing 111 indicates a thrust coefficient approximately 1.5 percent greater than that measured during the checkout firings. This data is for the initial 5 second period; (as noted) in Section 3.3.2.1 no erosion of the throat was expected until a steady-state, ablation process is established. The computed specific impulse efficiency, $\eta_{I_{sp}}$, for firing 111 is shown in Figure 3-10 as a function of mixture ratio. At comparable mixture ratios the performance is a maximum of two percent greater than measured in the cold wall (heat-sink) combustion chamber during firings

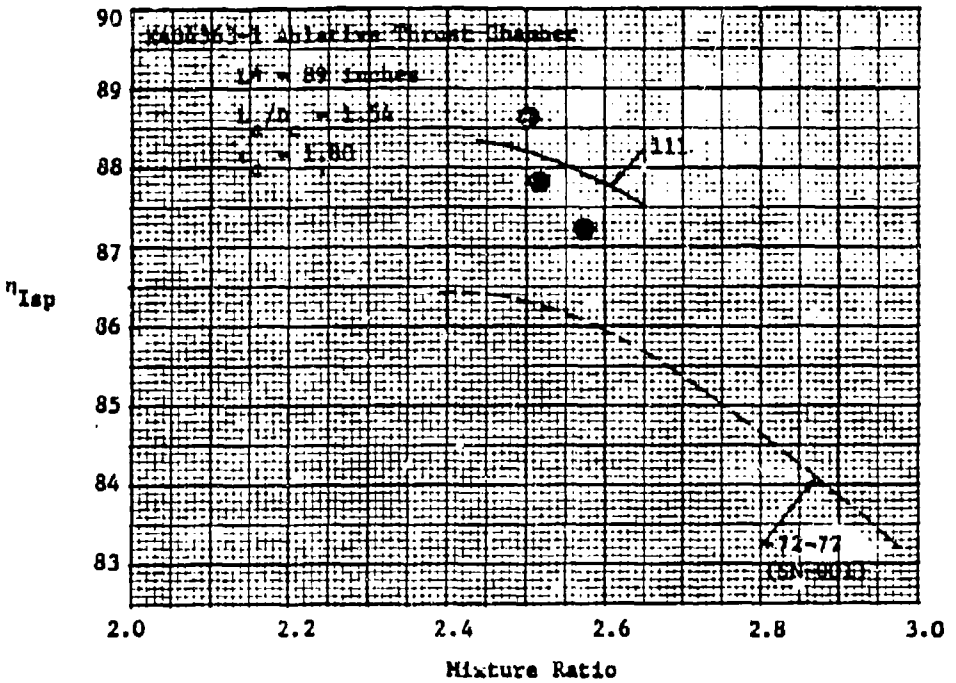

(C) Figure 3-10. Specific Impulse Efficiency, Firing 111 (U)

(U) 72-75. This is due to an increase of approximately one percent in combustion efficiency and approximately one percent in the apparent nozzle effeciency over that measured in test firings 72-75.

(U) The measured thrust and nozzle stagnation pressure are shown in Figure 3-11 as a function of the firing time. These plots indicate a uniform erosion with time. No by-passing of the throat insert occurred as in test firing 107 and in fact no rapid pressure decay was observed until propellant valves were closed upon visual observation of the burn through.

(U) The initial throat diameter was 26.168 inches. Post-test inspection of the throat showed some nonuniformity as indicated in Figure 3-12. The average diameter post-test is approximately 26.4 inches. The chamber internal diameter at the start of the firing was 35.0 inches. Post-test the diameter was estimated to be 36.0 inches. These values were used to determine the contraction ratio as a function of time which in turn was used to correct the head-end pressure to throat stagnation pressure. The throat stagnation pressure and thrust values shown in Figure 3-11 as a function of time were differentiated as discussed in Appendix E, Section 5 to arrive at the erosion rate (dr/dt) which is shown in Figure 3-13. The erosion rate of the MX-2600 throat insert is considerably lower than predicted from the subscale results and is also less than measured on test firing 107.

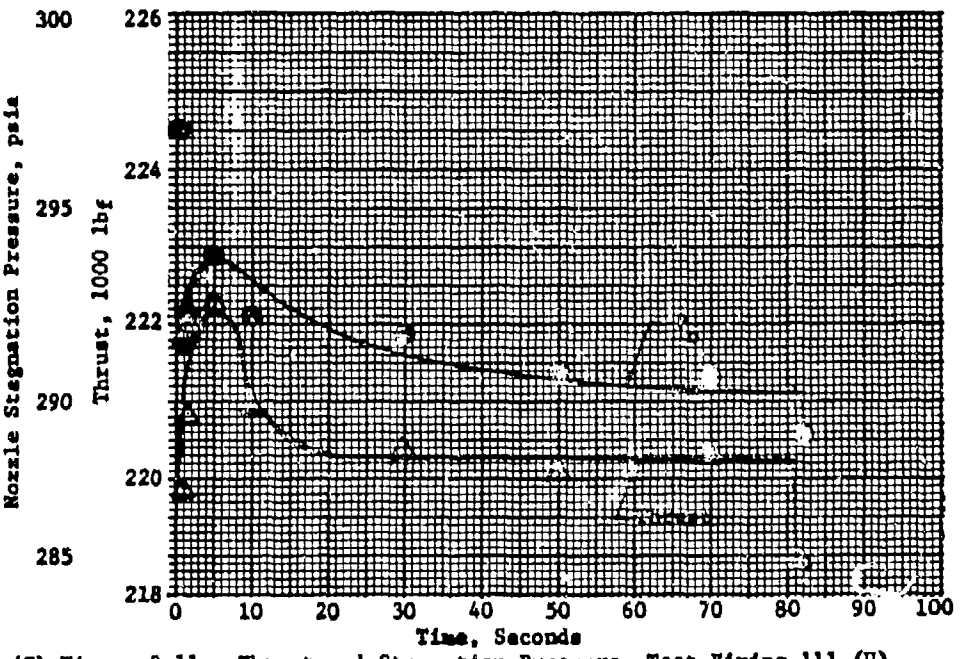

(C) Figure 3-11. Thrust and Stagnation Pressure, Test Firing 111 (U)

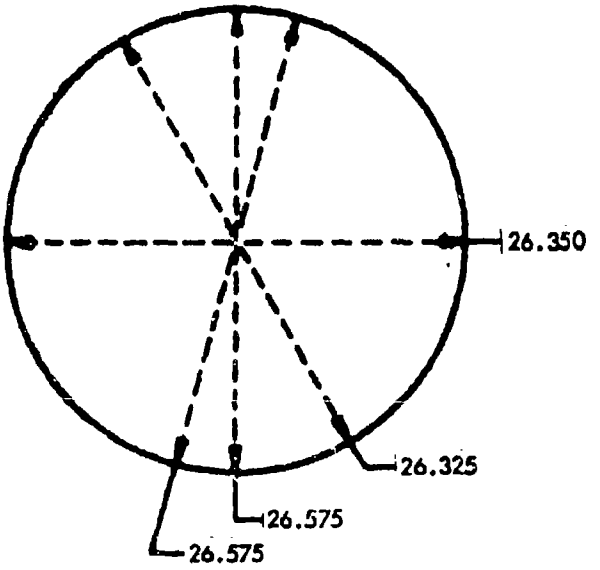

(C) Figure 3-12. X404363-1 Post-Test Throat Measurements (U)

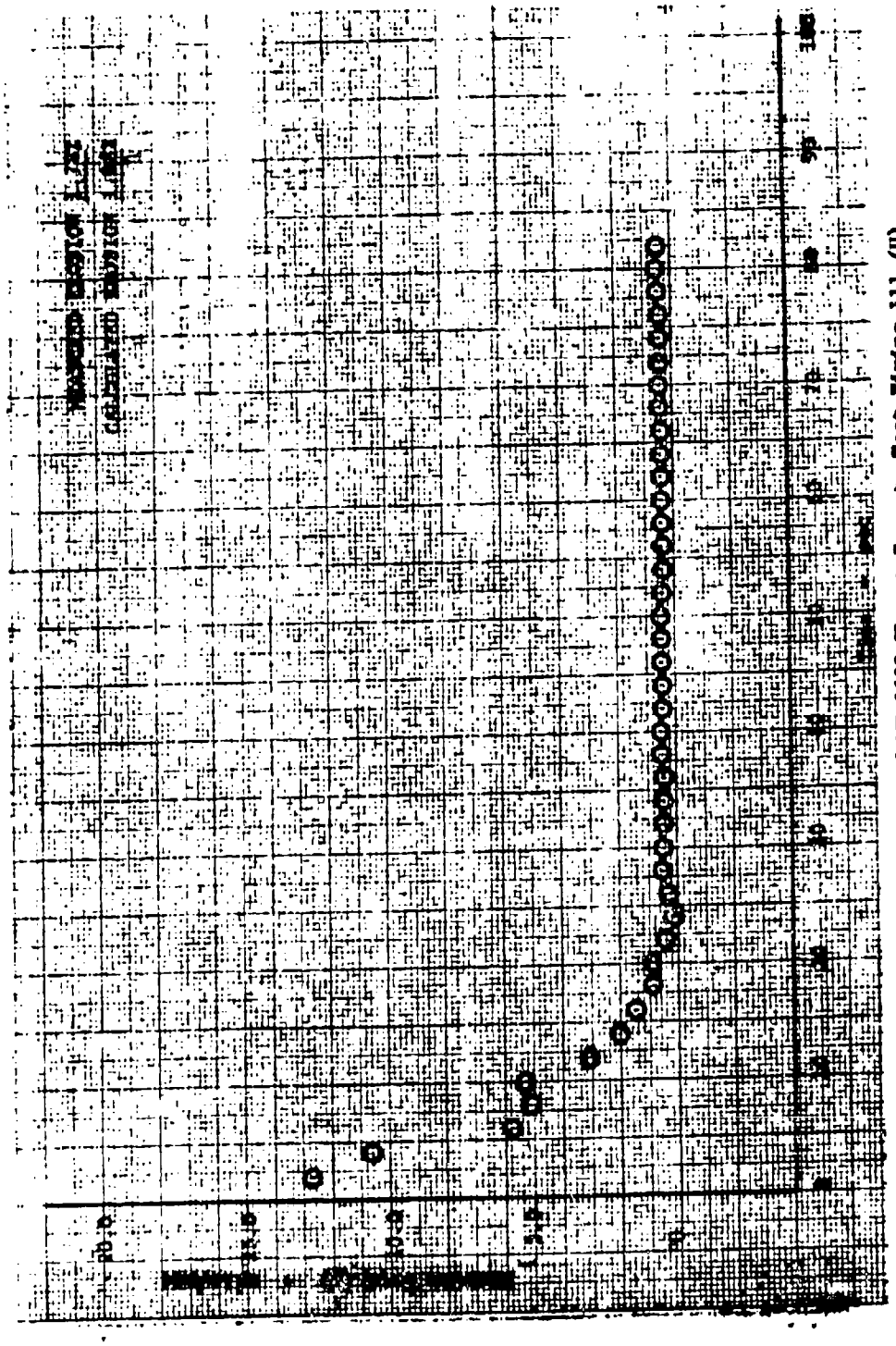

(C) Figure 3-13. Erosion Rate of MX-2600 Throat Insert, Test Firing 111 (U)

3.3.3.2 Injector Characteristics

(U) The fuel injector conductance, KIJCF, for test firing 111 is shown in Figure 3-14 as a function of the volumetric flow rate. The data for the checkout firings (72-77) is shown for comparative purposes.

(U) The oxidizer injector conductance, KIJCO, for test firing 111 is shown in Figure 3-15 as a function of the volumetric flow rate. The data for the checkout firings is shown for comparative purposes.

(U) The injector conductances measured during firing 111 are both considerably lower than those measured during the checkout firings of the S/N-001 injector. There is insufficient data to ascertain whether the difference is due to errors in the volumetric flow rate measurement or in the pressure measurements, or in both measurements.

3.3.3.3 Ablative Material Performance

(C) The average erosion rate of the MX-2600 silica-phenolic throat insert (tape-wrapped at 60° to ℄) was approximately 2.0 mils/second which is considerably lower than the measured value of 6.0 mils/second obtained on test firing 107. The throat erosion was nearly symmetrical with slightly greater erosion occurring in the 260°-300° (clockwise from fuel inlet) section of the insert. There is nothing in either the fabricating process or the operating conditions to indicate a reason for this difference in erosion rate. Therefore, it is postulated that the ablated material from the combustion chamber was substantially cooling the boundary layer which in turn flowed through the throat region with a greatly reduced local recovery temperature. Both inserts used in the 107 test firing and the 111 test firing were wrapped by the same fabricator using material from the same lot. Process variables were identical and the apparent density of the two parts were nearly identical. The operating conditions were within the normal design range and although the mixture ratio on firing 111 was slightly lower than on firing 107 it was not expected that the erosion rate of the silica-phenolic throat insert would be extremely sensitive to mixture ratio.

The erosion rate of the molded MXA-150 asbestos-phenolic segments 20 inches downstream of the throat averaged 10.15 mils/second (5.25 to 11.15 mils/second). The 40° segment at 150° (clockwise from the fuel inlet) was completely eroded (16.15 mils/second). The high erosion in this 40° sector caused ejection of the molded aft segment just downstream and subsequent loss of four additional panels during the firing. Seven aft panels were ejected upon shutdown. The erosion pattern at the throat/exit cone interface is shown in Figure 3-16. The erosion rate of the MX-2600 throat insert at a point 6.5 inches downstream of the throat plane was 1 mil/second; just downstream of the interface the erosion rate of the MXA-150 is estimated at 12 mils/second. This corresponds fairly well with the predicted erosion rate used in the preliminary design studies as discussed in Appendix B.

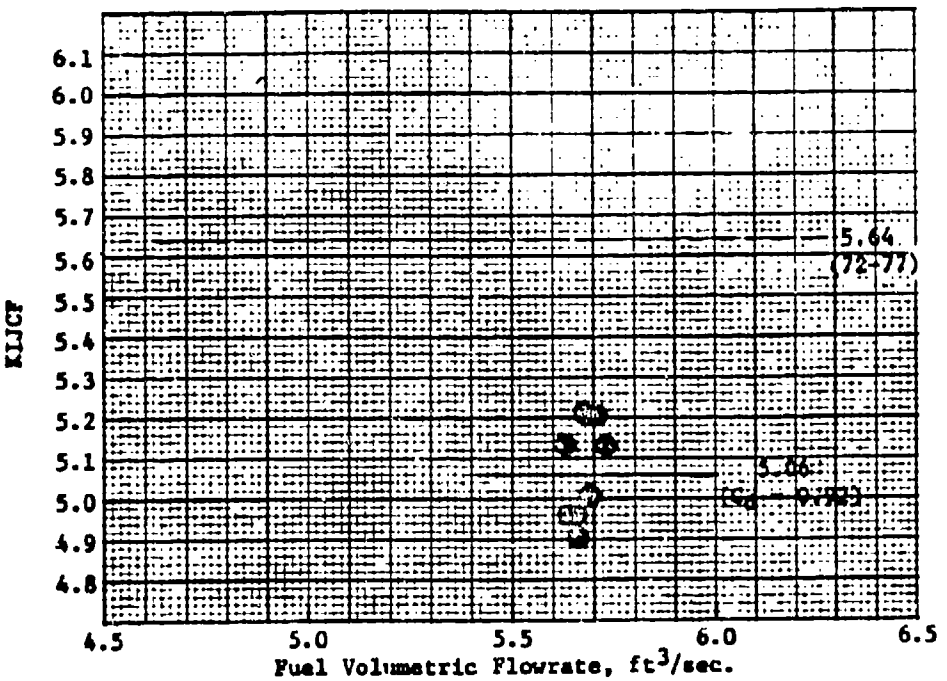

(U) Figure 3-14. Fuel Injector Conductance, S/N-001 Injector (U)

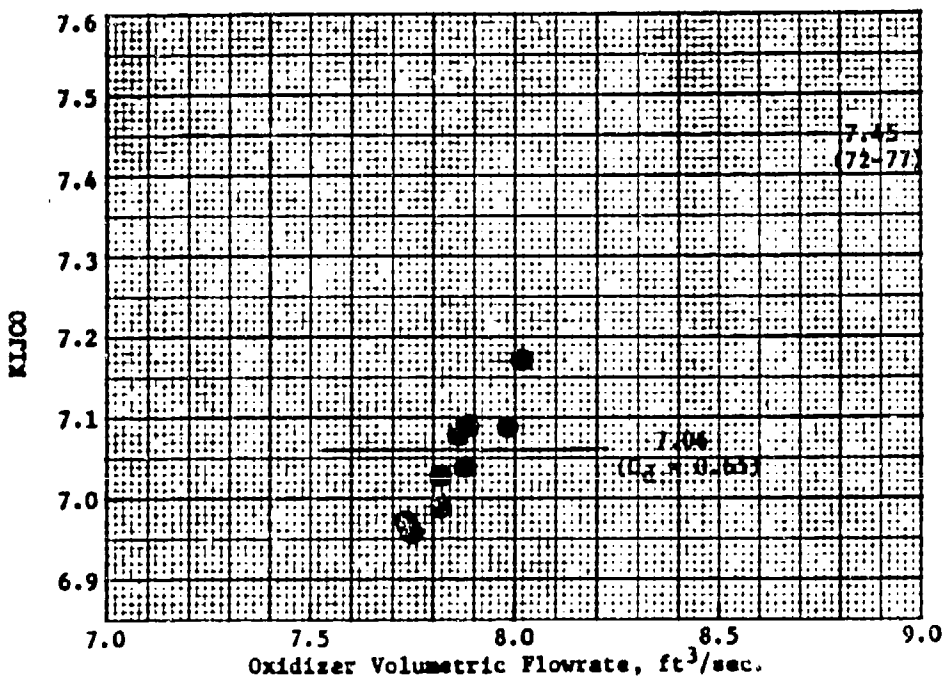

(U) Figure 3-15. Oxidizer Injector Conductance, S/N-001 Injector (U)

(This page is unclassified.)

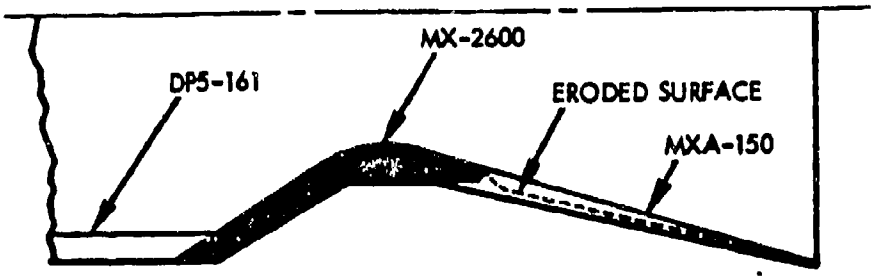

(U) Figure 3-16. Erosion Pattern of X404363 Exit Cone Liner (C)

(C) The erosion rate of the DP5-161 silica-phenolic material in the chamber at a point 24 inches upstream of the throat was 3.3 mils/second which was considerably less than would be predicted from the AFRPL material screening program. There were no deep gouges at the point of impingement of the reacting streams on the chamber wall as was experienced in test firing 107. As has been noted previously the mixture ratio was slightly lower than the design mixture ratio; this would result in a slightly cooler wall environment than was experienced on test firing 107.

(U) One large portion of the dome liner (covering ~15°) was ejected either during the test firing or the post-test purging. The chamber liner was also cracked and smaller segments of the liner from an area just adjacent to the chamber liner/throat insert interface were ejected also. These failures were due to the shrinkage of the DP5-161 during cure as noted in Section 2.3.4.2.

3.3.4 Long Duration Firing No. 3 - X405090-2 Engine Assembly

(U) The X405090-2, 250,000 lb_f thrust (vacuum), engine assembly was fired on 7 January 1970 for 98 seconds. The initial combustion chamber configuration consisted of a 104 inch L^*, 1.44 chamber length to diameter ratio and a 2.07 contraction ratio. The ablative liner, the thrust chamber, and the total engine weights were approximately 680, 3250 and 5030 pounds, respectively. The test firing (117) was scheduled for 120 seconds but was terminated prematurely by a burn through of the pressure shell in the convergent section of the nozzle. This burn through was due to a high localized erosion rate of the silicone rubber at the cylindrical/convergent section intersection which exposed the metal shell and caused the burn through. The test firing is discussed in greater detail in the following sections.

3.3.4.1 Performance Data

(U) The final 250,000 lb_f thrust (vacuum) engine assembly tested in Task II consisted of the X404056-1 (S/N-002) demonstration injector and the

(U) X404362-1 thrust chamber assembly. The checkout firings of this injector were made during Task I and are reported in Volume I. The char layer on the pintle tip from the checkout firings was removed by grinding and the pintle tip was refurbished using DC-93-104 filled-silicone rubber. The thrust chamber liner consisted of DC-93-104 filled-silicone rubber throughout.

(C) The measured thrust-throat stagnation pressure relationship shown in Figure 3-1 was not verified during the initial 5.0 second period. As noted in Section 3.3.2.1 no erosion of the throat was expected until a steady-state, ablation process is established. The computed specific impulse efficiency, η_{Isp}, for test firing 117 is shown in Figure 3-1 as a function of mixture ratio. At comparable mixture ratios the performance is approximately 4.0 percent greater than measured in the cold wall (heat-sink) combustion chamber during firings 98-100. This is due to an increase in nozzle efficiency of 4.0 percent over that measured in test firings 98-100 (see Figure 3-1).

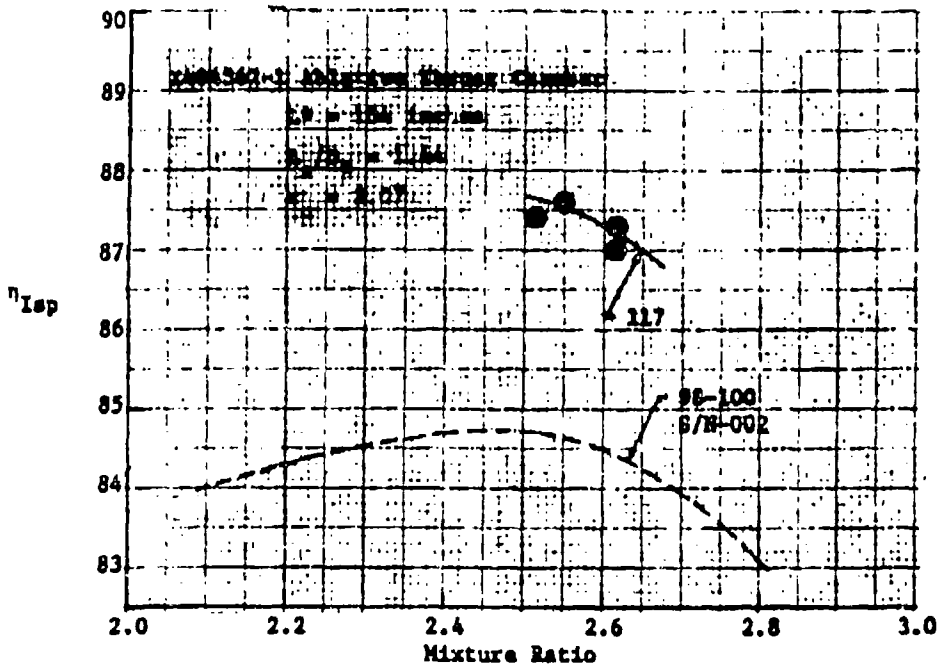

(C) Figure 3-17. Specific Impulse Efficiency, Test Firing 117 (U)

(U) The measured thrust and throat stagnation pressure are shown in Figure 3-18 as a function of the firing time. These plots show a uniform erosion of the throat, with time, up to the time of burn through in the convergent section. No rapid pressure decay was observed until propellant valves were closed upon visual observation of the burn through.

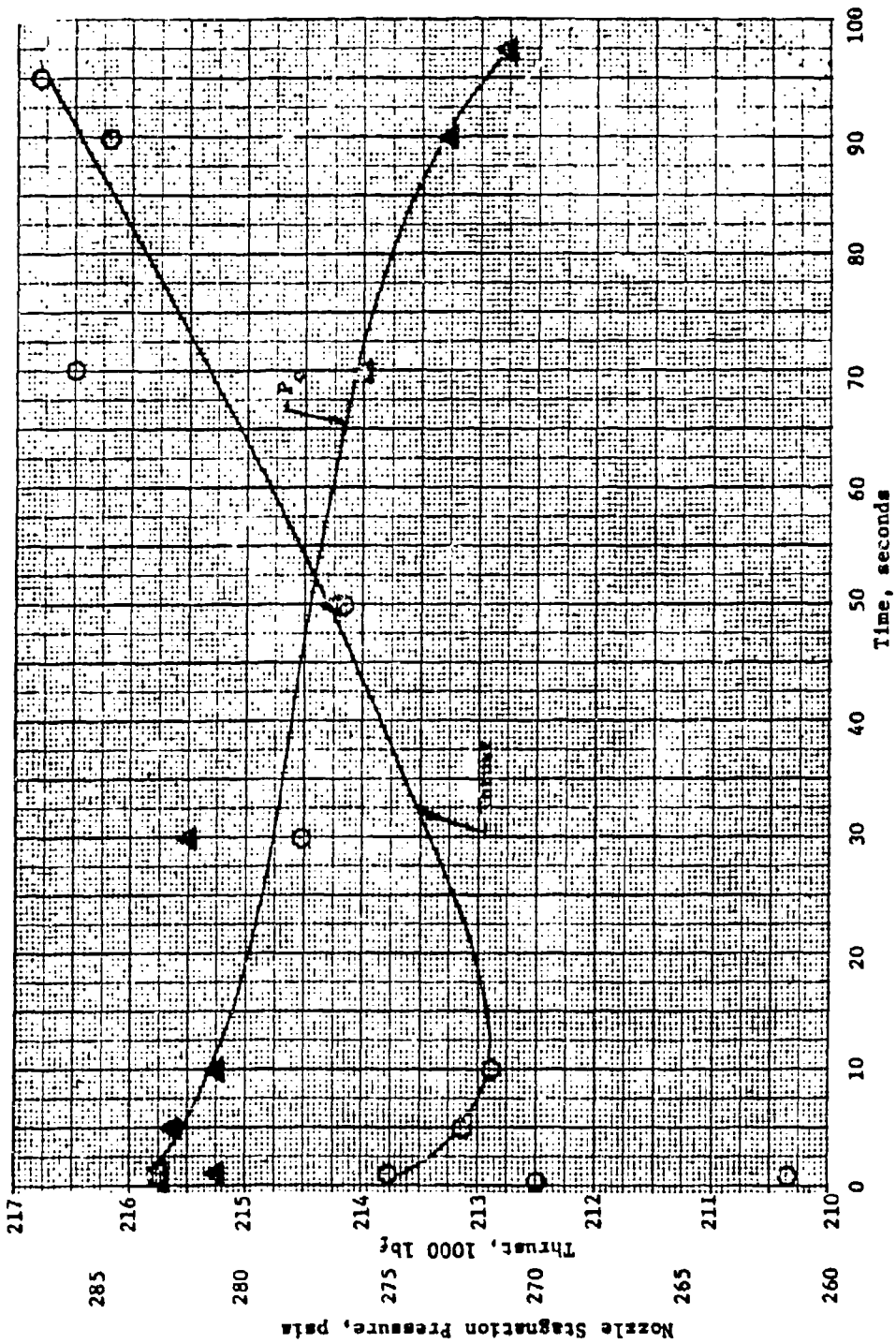

(C) Figure 3-1E. Thrust and Stagnation Pressure, Test Firing 117 (U)

(C) The initial throat diameter was 26.050 inches. Post-test inspection showed some nonuniformity as indicated in Figure 3-19. The average diameter post-test is approximately 27.330 inches, which includes the loss of char and molten silica associated with engine shutdown and the engine purging sequence. Post-test inspection showed little or no change in the ID at sections where the char layer was still evident. These values were used to determine the contraction ratio as a function of time which in turn was used to correct the head-end pressure to throat stagnation pressure. The throat stagnation pressure and thrust values shown in Figure 3-18 as a function of time were differentiated as discussed in Appendix E, Section 5.0 to arrive at the erosion rate of the DC-93-104 material at the throat is lower than predicted from the subscale results.

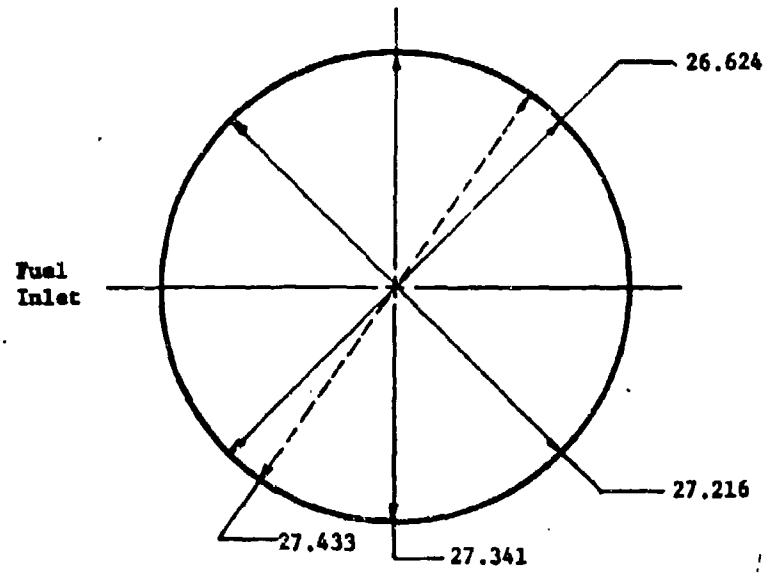

(C) Figure 3-19. Post-Test Measurements, X404362 Throat (U)

3.3.4.2 Injector Characteristics

(U) The fuel injector conductance, KIJCF, for test firing 117 is shown in Figure 3-21 as a function of the volumetric flow rate. The data for the checkout firings (98-100) is shown for comparative purposes.

(U) The oxidizer injector conductance, KIJCO, for test firing 117 is shown in Figure 3-22 as a function of the volumetric flow rate. The data for the checkout firings is shown for comparative purposes.

3.3.4.3 Ablative Material Performance

(C) The average erosion rate of the DC-93-104 filled silicone rubber at the throat plane was approximately 3.0 mils/second which is considerably

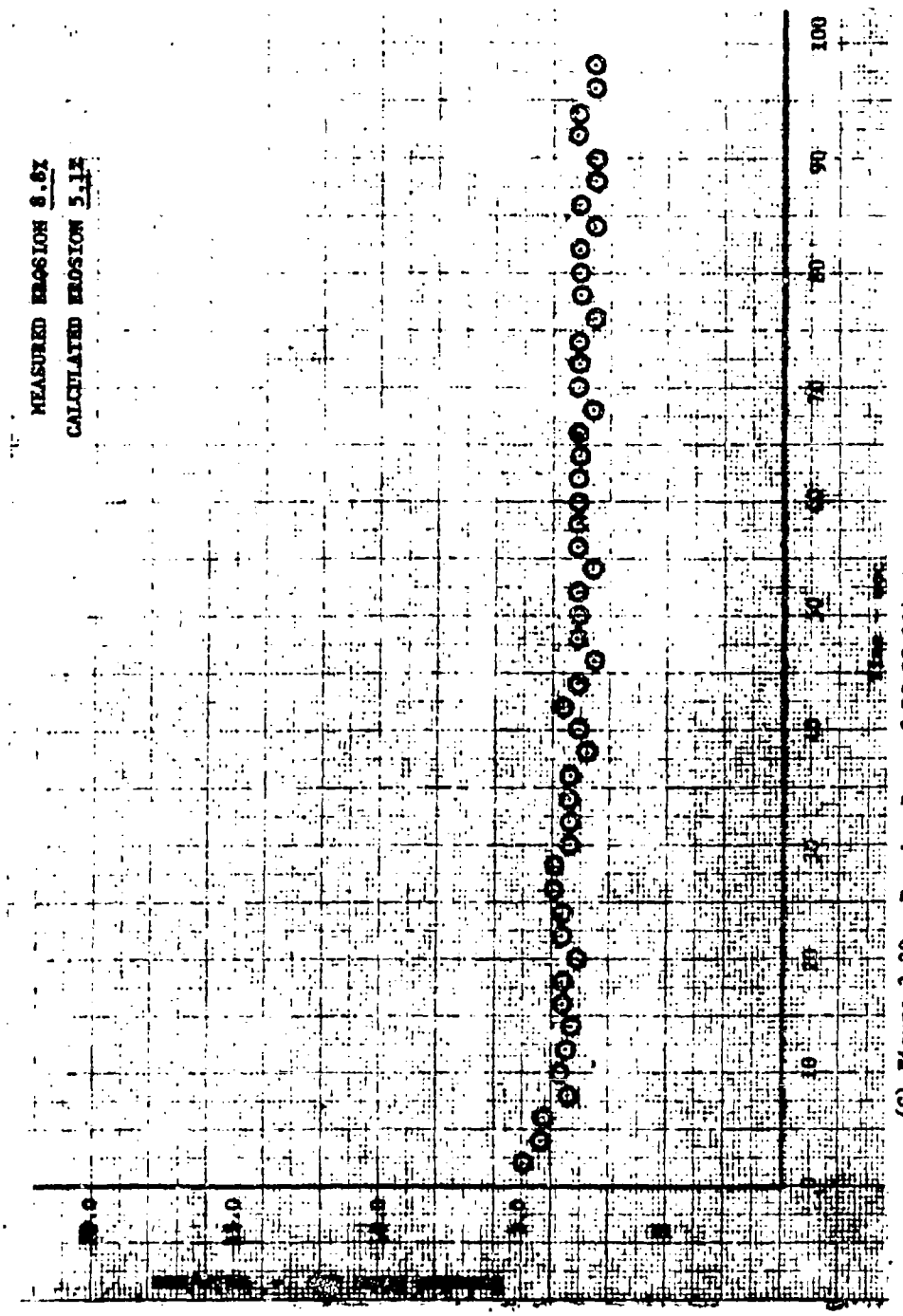

(C) Figure 3-20. Erosion Rate of DC-93-104 Throat Insert, Test Firing 117 (U)

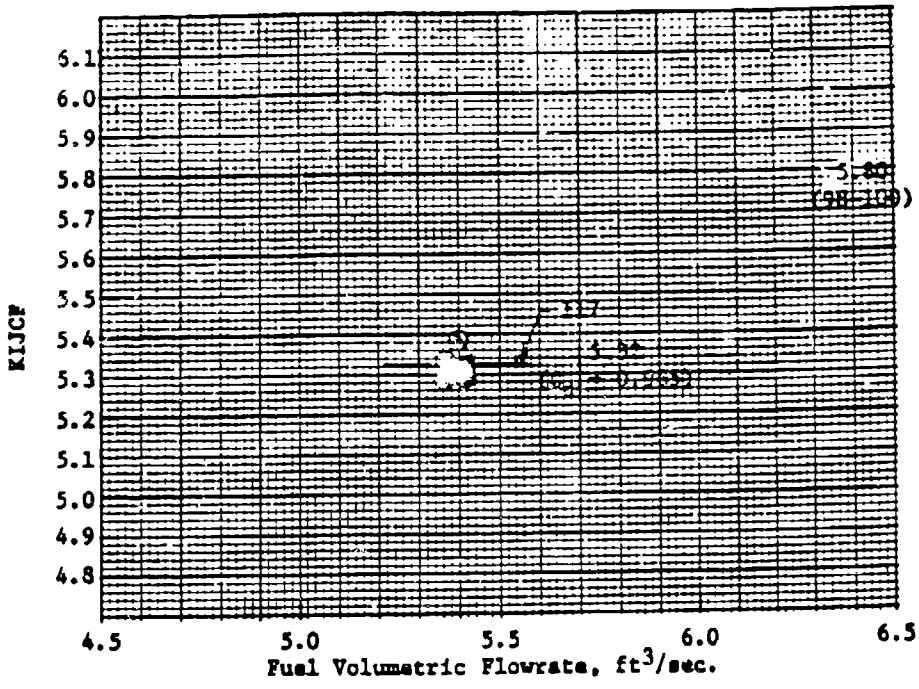

(U) Figure 3-21. Fuel Injector Conductance, S/N-002 Injector (U)

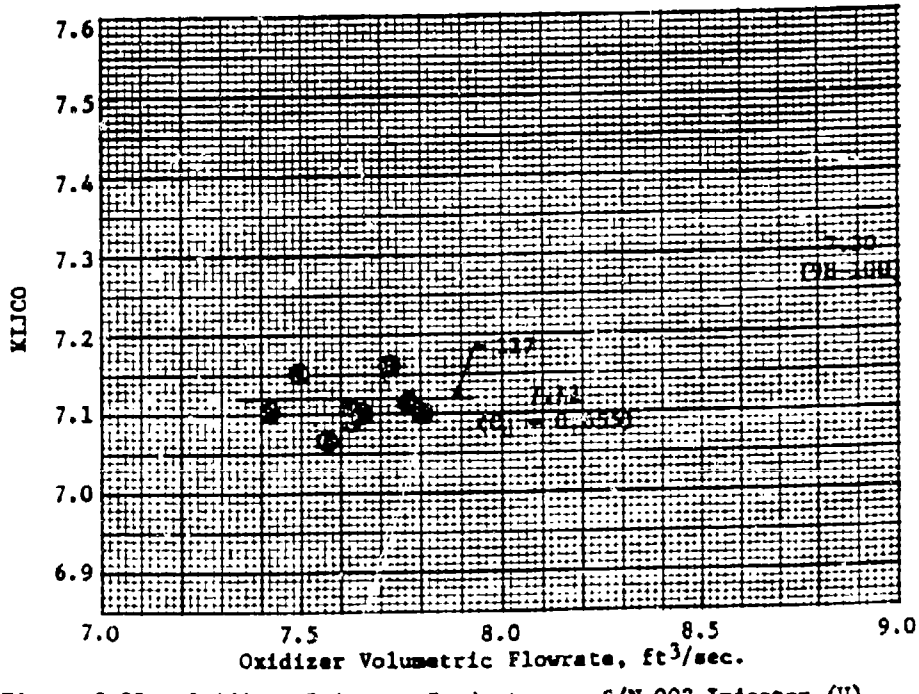

(U) Figure 3-22. Oxidizer Injector Conductance, S/N-002 Injector (U)

(This page is unclassified.)

(C) lower than the 10 mils/second value measured in the subscale test program. The throat erosion pattern was nonuniform as has been indicated. Some of the nonuniformity appears to be due to the persistence of streaks through the throat. These streaks are also apparent in the exit cone.

(C) Approximately 0.25 inch erosion had been expected at the exit plane. Preliminary evaluation of the liner indicates that the erosion of the material in the exit cone was almost nil. The char layer was intact and approximately 0.20 inch of virgin material remained. There was considerable evidence of silica flow in the nozzle (exit cone) and one additional hot streak (in addition to the one in line with the burn through).

(C) Very little erosion was experienced in the chamber section with the exception of the one streak in the throat approach section. It appears that most of the char layer from the chamber was lost during the shutdown and purging sequence. The char that remained amounted to about 0.45 inches thick with about 0.40 inches of virgin material beneath the char. The char showed very good adhesion to the virgin rubber. From the appearance of the throat section the DC 93-104 material appears to be more environment sensitive than the MX-2600 silica-phenolic material.

SECTION 4

CONCLUSIONS

(U) This section presents TRW Systems conclusions based on the results of design studies, evaluation of fabrication methods, and analysis of hardware performance during the Task II phase of the Injector/Chamber Sealing Feasibility Program.

(C) The measured vacuum specific impulse for the three ablative engines during the long duration firings was 88 percent, ± 0.5 percent at the nominal design mixture ratio of 2.60 (O/F). The average weight of these engines is approximately 5290 pounds each with the all DC-93-104 ablative liner being the lightest weight design. This engine is estimated to weigh 5030 pounds and demonstrated a sea level thrust to weight ratio of 43. The maximum performance measured during the Task II long duration firings was 89 percent which is one percent lower than that measured during Task I in the 60-inch heat sink combustion. The one dimensional vaporization rate limited combustion model developed in Task I for sizing low cost booster engines predicted the one percent loss in delivered performance for the 54-inch long ablative chambers. During the checkout of the S/N 002 demonstration injector in Task I a lowered performance level was observed. Subsequent checkout firings of the S/N 003 demonstration injector and the three long duration firings indicate that the lowered performance was due to erroneous thrust measurements.

(C) Long duration firings of the two tape-wrapped MX-2600 silica-phenolic throat inserts indicate an average erosion rate of 4.0 mils/second (2.0 to 6.0 mil/second) which is slightly better than predicted from the subscale material evaluation program. In the exit cone the performance of the MX-2600 silica-phenolic material was essentially as predicted although the pattern created by the 36 element injector was discernible. Delamination of the rosette plies occurred near the exit plane.

(C) The performance of the DC93-104 filled silicone rubber was slightly better than predicted from the subscale material evaluation program for the most severe condition. The erosion of the DC-93-104 in the chamber and exit cone sections was almost negligible. In the throat section the design thickness was adequate. The char depths ranged from 0.4 inches in the chamber and at the exit plane to approximately 0.8 inches at the throat plane. The char layer showed excellent adhesion to the virgin rubber which in turn was still bonded to the pressure shell. DC-93-104 filled silicone rubber was shown to be an effective low-cost ablator for rocket engines of this size even though the current raw material cost is about 50 percent greater than the raw material cost of the silica-phenolic material. This is due to the significantly lower fabrication (labor plus processing) costs for the DC-93-104 material. The MXA-150 components were fabricated by two different methods; the low-pressure, molded insitu chamber liner had a maximum erosion rate of about 28 mils/second while the maximum erosion rate of the compression molded exit cone segments was about 16 mils/second. Both of these erosion rates are greater than measured in the AFRPL material screening program at the most severe test conditions.

(C) The fourth material evaluated in the program, Ironsides Resin Co. DP-5-161, which was used as a chamber liner in the configuration 3 ablative thrust chamber had acceptable performance (~3.3 mils/second) as a chamber insulator. However, the cure mechanism for the material results in a volume change (shrinkage) which takes an indeterminate period of time and thus results in a dimensionally unstable part. Elevated temperature cure of the cast material results in cracking of the material which is also detrimental to performance. It is concluded that the present DP 5-161 formulation is not satisfactory for use in ablative liners even through its erosion characteristics are acceptable.

(U) The casting techniques used in fabricating the ablative components from DP-5-161 and DC-93-104 were limited only by the mixing equipment. Both mixtures are viscous and there is some degree of difficulty in obtaining uniform mixtures. The greatest difficulty occurred in mixing the DP-5-161 which requires the addition of a large amount of solid (0.7 lbs) to 2.0 lbs of viscous resin. The DP-5-161 mixing process is exothermic and requires jacketed mixing equipment for temperature control.

(U) The segmented, molded panel approach (often referred to as the "building-block" approach) to fabricating large ablative components appears to be a feasible technique. Tapered joints do not provide sufficient retention force to hold the panels in place and positive interlocking of each panel appears to be a requirement. In addition, a thick bond line technology must be developed to hold the panels to the pressure shell.

(U) Tape-wrapping of throat inserts, especially for engine thrust sizes below 250,000 lbf thrust, appears to be the best technique. For booster size engines, with burn times of approximately 120 seconds, both the tape-wrapped silica phenolic (MX-2600) throat insert and the cast filled-silicone rubber (DC-93-104) have erosion rates (~5 mils/second) which result in minimum throat area change. For example, the throat area of a 3×10^6 lbf thrust ablative chamber would increase approximately 1 percent in 120 seconds at these erosion rates.

(U) The program showed that acceptable hardware could be fabricated with a minimum of quality control. It is not anticipated that fabrication of multi-million pound thrust ablative liners would require any greater quality control than employed during this program.

(U) There were no instances of combustion stability with any of the demonstration injectors during any of the checkout firings or the three long duration firings.

APPENDIX A

STRESS ANALYSIS OF 250K LONG DURATION THRUST CHAMBER SHELL ASSEMBLY (404342)

(U) The structural elements of the development injector and heat-sink combustion chamber were analyzed for a static pressure loading of 600 psi at ambient temperature with a minimum required margin of safety of one against pressure loading. The analytical results are given in Reference 1.

(U) The 250,000 lbf Long Duration Thrust Chamber Shell Assembly, P/N X404342, is a revised design of the original heat-sink combustion chamber which was analyzed previously. The major changes in the redesign are (1) the addition of flanges in the chamber section to allow for installation of the throat inserts and (2) the reduction of material thickness in the exit cone. The stress analysis was made for a pressure loading of 600 psi at ambient temperature.

(U) The analytical results are summarized in Table I and detailed calculations are given in the following pages.

Reference 1. G. A. Voorhees, Jr., "Injector/Chamber Scaling Feasibility Program", AFRPL-TR-70-86, Volume I; TRW Systems, Redondo Beach, California; April 1970; Confidential Report.

Table I. Stress Analysis Summary (U)

Description	Material	Available Ultimate PSI	Stress Yield PSI	Max. Calculated Stress PSI	Margin of Safety	Page No.
Chamber Shell	1/2" T-1 Steel	135,000	100,000	23,700	4.7	A-3
Chamber Flange Bolts	Steel	125,000		63,500	0.97	A-5
Chamber at Flange Joint	1/2" T-1 Steel	135,000	100,000	67,500	1.00	A-14
Nozzle Extension	1/4" T-1 Steel	135,000	100,000	20,678	5.52	A-18

PREPARED P Y HSIEH
CHECKED
MODEL

REPORT NO.

250 K LONG DURATION THRUST CHAMBER
X 40481

CHAMBER STRESSES

$P = 300 \cdot 2 = 600$ PSI.

T = AMBIENT TEMP.

MAT'L. T-1 STEEL

$f_{tu} = 135{,}000$ PSI.

$f_{ty} = 100{,}000$ PSI.

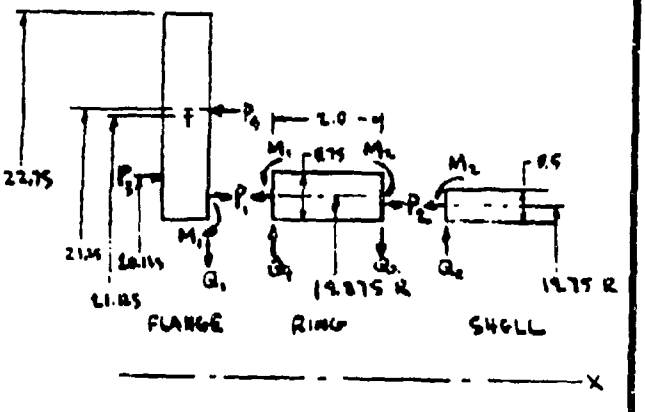

SHELL

$$D = \frac{Et^3}{12(1-\nu^2)}$$

$$= \frac{30 \cdot 10^6 \cdot .5^3}{12(1-.3^2)}$$

$$= 0.344 \cdot 10^6$$

$$\lambda = \sqrt[4]{\frac{3(1-\nu^2)}{R^2 t^2}}$$

$$= \sqrt[4]{\frac{3(1-.3^2)}{19.75^2 \cdot .5^2}}$$

$$= 0.409$$

$$\lambda^2 = 0.1675$$

$$\lambda^3 = 0.0685$$

$$P_2 = \frac{600 \cdot \pi (19.75^2 - 15.75^2)}{2\pi \cdot 19.75}$$

$$= 1340 \text{ LB/IN}$$

SYSTEMS 1441 REV. 6-67

PREPARED P Y HSIEH
CHECKED
MODEL
REPORT NO.

MEMBRANE STRESSES

$$\sigma_1' = \frac{P_2}{t}$$

$$= \frac{2340}{0.5}$$

$$= 4680 \text{ psi.}$$

$$\sigma_2' = \frac{P_2 R}{t}$$

$$= \frac{400 \cdot 19.75}{0.5}$$

$$= 23700 \text{ psi.}$$

END DISPLACEMENT

$$\delta_2 = \frac{R}{E}(\sigma_2' - \nu\sigma_1') - \frac{M_2}{2D\lambda^2} + \frac{Q_2}{2D\lambda^3}$$

$$= \frac{19.75}{30 \cdot 10^6}(23700 - .3 \cdot 4680) - \frac{M_2}{2 \cdot 0.3744 \cdot 10^6 \cdot 0.1675} + \frac{Q_2}{2 \cdot 0.7446 \cdot 10^6 \cdot .00685}$$

$$= 10^{-6}(14900 - 8.7 M_2 + 21.2 Q_2)$$

END ROTATION

$$\theta_2 = -\frac{M_2}{2D\lambda} + \frac{Q_2}{2D\lambda^2}$$

$$= -\frac{M_2}{.409 \cdot 0.3744 \cdot 10^6} + \frac{Q_2}{2 \cdot 0.1446 \cdot 10^6 \cdot 0.1675}$$

$$= 10^{-6}(-7.1 M_2 + 8.7 Q_2)$$

PREPARED P Y HSIEH
CHECKED
MODEL
REPORT NO.

RING

$$M_T = -M_1 + M_2 + Q_1 + Q_2 - 0.125\,P_i$$
$$= -M_1 + M_2 + Q_1 + Q_2 - 272$$

$$I_y = \frac{1}{12}\,0.75 \cdot 2.0^3$$
$$= 0.5\ \text{in}^4$$

$$\theta_R = \frac{M_T r^2}{G I_y}$$
$$= \frac{19.875^2}{30\cdot10^6\cdot 0.5}\,(-M_1 + M_2 + Q_1 + Q_2 - 272)$$
$$= 10^{-6}\,(-26.35\,M_1 + 26.35\,M_2 + 26.35\,Q_1 + 26.35\,Q_2 - 7100)$$

RING DISPLACEMENT AT SHELL

$$(\Delta_R)_s = \frac{S\,P\,r^2}{A\,E} - L\,\theta_R$$
$$= \frac{(600\cdot 2 + Q_1 - Q_2)\,19.875^2}{1.5\cdot 30\cdot 10^6} - 10^{-6}\,(-26.35\,M_1 + 26.35\,M_2 + 26.35\,Q_1 - 26.35\,Q_2 - 7700)$$
$$= 10^{-6}\,(10540 + 8.78\,Q_1 - 8.78\,Q_2) - 10^{-6}\,(-26.35\,M_1 + 26.35\,M_2 + 26.35\,Q_1 + 26.35\,Q_2 - 7700)$$
$$= 10^{-6}\,(26.35\,M_1 - 17.57\,Q_1 - 26.35\,M_2 - 35.13\,Q_2 + 18240)$$

RING DISPLACEMENT AT FLANGE

$$(\Delta_R)_F = 10^{-6}\,(10540 + 8.78\,Q_1 - 8.78\,Q_2) + 10^{-6}\,(-26.35\,M_1 + 26.35\,M_2 + 26.35\,Q_1 + 26.35\,Q_2 - 7700)$$
$$= 10^{-6}\,(-26.35\,M_1 + 35.13\,Q_1 + 26.35\,M_2 + 17.57\,Q_2 + 2840)$$

PREPARED P Y HSIEH
CHECKED
MODEL
REPORT NO.

FLANGE FOR 0.88 IN. THICKNESS

$A = .88(2175 - 19.5) = 1.86\ in^2$

$I_y = \frac{1}{12} 325 \cdot 0.88^3 = 0.184\ in^4$

$P_1 = \frac{1975}{19875} 2140$

$= 2720\ lb/in$

$P_1 = 0.75 \cdot 3000$

$= 2250\ lb/in$

$P_4 = \frac{1}{2175}\left(19.875 \cdot 2720 + 2.125 \cdot 2250 \right)$

$= 4320\ lb/in$

72 - ½ φ Bolts $A_{bolt} = 72 \cdot 0.126 = 9.08\ in^2$

Bolt stress $\sigma_{bolt} = \frac{4320 \cdot 28 \cdot 2175}{9.08}$

$= 67500\ psi.$ (9000 lb/bolt) $M.S. = \frac{127000}{67500} - 1 = 1.0$

Torque $= \frac{67500}{47.1} = 655\ in\text{-}lb$ (54.6 ft-lb)

$M_F = \frac{1}{21.125}\left[19.875\left(-.75 \cdot 2720 + M_1 + 0.44\, Q_1 \right) - 2.125\left(1.0 \cdot 2250 \right) - 2.125\left(.75 \cdot 4320 \right) \right]$

$= -2720 + 0.94\, M_1 + 0.419\, Q_1 - 2140 - 940$

$= 0.94\, M_1 + 0.419\, Q_1 - 5410$

$\theta_F = \frac{M_F Y_{CG}}{E I_y}$

$= \frac{21.125^2}{30 \cdot 10^6 \cdot 0.184}\left(0.94\, M_1 + 0.419\, Q_1 - 5410 \right)$

$= 10^{-6}\left(76\, M_1 + 33.6\, Q_1 - 437{,}000 \right)$

FLANGE DISPLACEMENT AT RING

$\delta_F = \frac{\Sigma P Y Y_{CG}}{AE} - 0.375\, \theta_F$

$= \frac{(600 \cdot .938 \cdot 195 - Q_1 \cdot 19.875) 21.125}{2.86 \cdot 30 \cdot 10^6} - 0.44 \cdot 10^{-6}(76\, M_1 + 33.6\, Q_1 - 417{,}000)$

$= 10^{-6}\left(2540 - 4.9\, Q_1 - 33.4\, M_1 - 14.8\, Q_1 + 192{,}500 \right)$

$= 10^{-6}\left(-33.4\, M_1 - 19.7\, Q_1 + 195{,}040 \right)$

ONE SPACE PARK • REDONDO BEACH, CALIFORNIA

PREPARED P Y HSIEH

CHECKED

MODEL

REPORT NO.

$\partial_S = (\partial_D)_S$

$10^{-6}(14{,}700 - 8.7\,M_2 + 2.2\,Q_2) = 10^{-6}(26.35\,M_1 - 17.57\,Q_1 - 26.35\,M_2 - 35.13\,Q_2 + 18240)$

$-26.35\,M_1 + 17.57\,Q_1 + 17.65\,M_2 + 56.33\,Q_2 = 1540$ (1)

$\theta_S = \theta_R$

$10^{-6}(-7.1\,M_2 + 9.1\,Q_2) = 10^{-6}(-26.35\,M_1 + 26.35\,M_2 + 26.35\,Q_1 + 26.35\,Q_2 - 7700)$

$26.35\,M_1 - 26.35\,Q_1 - 33.45\,M_2 - 17.05\,Q_2 = -7700$ (2)

$(\partial_R)_F = \partial_F$

$10^{-6}(-26.35\,M_1 + 35.11\,Q_1 + 26.35\,M_2 + 17.57\,Q_2 + 2840) = 10^{-6}(-73.4\,M_1 - 19.7\,Q_1 + 195{,}040)$

$7.05\,M_1 + 54.83\,Q_1 + 26.35\,M_2 + 17.57\,Q_2 = 192{,}200$ (3)

$\theta_R = \theta_F$

$10^{-6}(-26.35\,M_1 + 26.35\,M_2 + 26.35\,Q_1 + 26.35\,Q_2 - 7700) = 10^{-6}(-76\,M_1 + 33.6\,Q_1 - 437{,}000)$

$-102.35\,M_1 - 7.25\,Q_1 + 26.35\,M_2 + 26.35\,Q_2 = -429{,}300$ (4)

(1) + (3) $\quad -8.78\,Q_1 - 15.80\,M_2 + 39.68\,Q_2 = -4160$ (5)

$7.05\,M_1 - 7.05\,Q_1 - 9.95\,M_2 - 4.72\,Q_2 = -2060$ (2)

(3) − (2) $\quad 61.88\,Q_1 + 35.30\,M_2 + 22.29\,Q_2 = 194{,}260$ (6)

$-7.05\,M_1 - 0.50\,Q_1 + 1.81\,M_2 + 1.81\,Q_2 = -29{,}600$ (4)

(3) + (4) $\quad 54.33\,Q_1 + 28.16\,M_2 + 19.38\,Q_2 = 162{,}600$ (7)

$-61.88\,Q_1 - 111.50\,M_2 + 279.0\,Q_2 = -29{,}400$ (5)

(5) + (6) $\quad -76.20\,M_2 + 295.19\,Q_2 = 164{,}960$ (8)

$54.33\,Q_1 + 31.0\,M_2 + 19.38\,Q_2 = 170{,}600$ (6)

(6) − (7) $\quad 2.44\,M_2 + 0.2\,Q_2 = 8{,}000$ (9)

$76.20\,M_2 + 5.37\,Q_2 = 215{,}000$

TRW
ONE SPACE PARK • REDONDO BEACH, CALIFORNIA

PREPARED P Y HSIEH
CHECKED
MODEL
REPORT NO.

$$700.66\,Q_2 = 379860$$

$$Q_2 = 1262 \text{ LB/IN}$$

FROM (9) $$M_2 = \frac{5000 - 62(1262)}{2.84} = 2770 \text{ IN-LB/IN}$$

FROM (7) $$Q_1 = \frac{162{,}600 - 19.38(1262) - 24.16(2770)}{54.93} = 1130 \text{ LB/IN}$$

FROM (7) $$M_1 = \frac{192200 - 17.57(1262) - 26.15(2770) - 54.93(1130)}{7.05}$$

$$= 5110 \text{ IN-LB/IN.}$$

UNCLASSIFIED

ONE SPACE PARK · [illegible] · CALIFORNIA

PREPARED P Y HSIEH

CHECKED

MODEL

REPORT NO.

FLANGE THICKNESS INCREASED TO 1.00 IN.

$A = \frac{1.0}{\cancel{144}}(21.75 - 19.5) = \frac{3.25}{\cancel{144}}$ IN^4

$I_y = \frac{1}{12} 3.25 \cdot \frac{1.0}{\cancel{1000}^3} = \frac{0.271}{\cancel{0.194}}$ IN^4

$P_1 = \frac{19.75}{19.875} 2340$

$= 2320$ LB/IN

$P_3 = 0.75 \cdot 3000$

$= 2250$ LB/IN

$P_4 = \frac{1}{21.75}(19.875 \cdot 2320 + 20.125 \cdot 2250)$

$= 4320$ LB/IN

$72 - \frac{1}{2}\phi$ BOLTS $\quad A_{bolt} = 72 \cdot 0.126 = 9.08$ IN^2

BOLT STRESS $\quad \sigma_{bolt} = \frac{4320 \cdot 24 \cdot 21.25}{1.0 \cdot \delta}$

$= 63500$ PSI. $\quad (9000$ LB/BOLT$)$

$M_F = \frac{1}{21.125}\left(19.875\left(-.125 \cdot 2320 + M_1 + \frac{0.5}{\cancel{0.444}} Q_1\right) - 20.125(10 \cdot 2250) - 2.5(10 \cdot 4320)\right)$

$= -2730 + 0.94 M_1 + \frac{0.47}{\cancel{0.444}} Q_1 - 2160 - 540$

$= 0.94 M_1 + \frac{0.47}{\cancel{0.444}} Q_1 - 5410$

$\theta_F = \frac{M_F Y_{cc}^2}{E I_y}$

$= \frac{21.125^2}{30 \cdot 10^6 \cdot \cancel{0.271}}\left(0.94 M_1 + \frac{0.47}{\cancel{0.444}} Q_1 - 5410\right)$

$= 10^{-6}\left(\frac{51.9}{\cancel{56}} M_1 + \frac{25.9}{\cancel{27.6}} Q_1 - \frac{296000}{\cancel{\quad\quad}}\right)$

$\delta_F = \frac{\Sigma P Y_{cc}}{AE} - 0.375\,\theta_F$

$= \frac{(600 \cdot \cancel{\quad} \cdot 1.95 - Q_1 \cdot 19.875) 21.125}{\cancel{3.25} \cdot 30 \cdot 10^6} - \frac{0.5}{\cancel{0.444}} \cdot 10^{-6}\left(\frac{51.9}{\cancel{56}} M_1 + \frac{25.9}{\cancel{27.6}} Q_1 - \frac{296000}{\cancel{\quad\quad}}\right)$

$= 10^{-6}\left(2540 - \frac{0.7}{\cancel{0.444}} Q_1 - \frac{29.75}{\cancel{32.4}} M_1 - \frac{17.9}{\cancel{19.7}} Q_1 + \frac{148000}{\cancel{\quad\quad}}\right)$

$= 10^{-6}\left(-\frac{25.75}{\cancel{32.4}} M_1 - \frac{17.2}{\cancel{19.7}} Q_1 + \frac{150540}{\cancel{\quad\quad}}\right)$

PREPARED P Y HSIEH

CHECKED

MODEL

REPORT NO.

$\partial_s = (\partial_R)_s$

$10^{-6}(14700 - 8.7 M_2 + 2.2 Q_2) = 10^{-6}(26.35 M_1 - 17.57 Q_1 - 26.35 M_2 - 15.13 Q_2 + 18240)$

$-26.35 M_1 + 17.57 Q_1 + 17.65 M_2 + 56.33 Q_2 = 3540$ (1)

$\theta_s = \theta_R$

$10^{-6}(-7.1 M_2 + 8.7 Q_2) = 10^{-6}(-26.35 M_1 + 26.35 M_2 + 26.35 Q_1 + 26.35 Q_2 - 7700)$

$26.35 M_1 - 26.35 Q_1 - 33.45 M_2 - 17.65 Q_2 = -7700$ (2)

$(\partial_R)_F = \partial_F$

$10^{-6}(-26.35 M_1 + 35.13 Q_1 + 26.35 M_2 + 17.57 Q_2 + 2840) = 10^{-6}(-\frac{26.35}{7344} M_1 - \frac{17.2}{1000} Q_1 + \frac{190540}{1000000})$

$-0.60 M_1 + 52.33 Q_1 + 26.35 M_2 + 17.57 Q_2 = 147700$ (3)

$\theta_R = \theta_F$

$10^{-6}(-26.35 M_1 + 26.35 M_2 + 26.35 Q_1 + 26.35 Q_2 - 7700) = 10^{-6}(\frac{515}{10} M_1 + \frac{35.8}{5000} Q_1 - \frac{296000}{1000000})$

$-77.85 M_1 + 8.55 Q_1 + 26.35 M_2 + 26.35 Q_2 = -283700$ (4)

$(1) + (2)$ $\quad -8.78 Q_1 - 15.80 M_2 + 35.68 Q_2 = -4160$ (5)

$\frac{0.60}{7345} M_1 - \frac{8.60}{2006} Q_1 - \frac{0.761}{0.845} M_2 - \frac{0.702}{4000} Q_2 = -\frac{175}{2000}$ (6)

$(3) + (2)$ $\quad \frac{51.73}{1000} Q_1 + \frac{26.59}{1000} M_2 + \frac{17.168}{2000} Q_2 = \frac{147.815}{1000}$ (7)

$-\frac{0.60}{7345} M_1 + \frac{0.00841}{0.956} Q_1 + \frac{0.703}{1034} M_2 + \frac{0.703}{1000} Q_2 = -\frac{2221}{24000}$ (8)

$(7) \wedge (8)$ $\quad \frac{52.316}{1000} Q_1 + \frac{26.191}{38.10} M_2 + \frac{17.369}{1000} Q_2 = \frac{149.922}{1000}$ (9)

$-\frac{51.73}{1000} Q_1 - \frac{93.0}{1000} M_2 + \frac{228.0}{1000} Q_2 = -\frac{24500}{24000}$ (10)

$(5) + (6)$ $\quad -\frac{57.441}{1000} M_2 + \frac{249.17}{2000} Q_2 = \frac{123.025}{1000}$ (11)

$\frac{52.326}{1000} Q_1 + \frac{25.86}{1000} M_2 + \frac{17.37}{1000} Q_2 = \frac{149.200}{1000}$ (12)

$(6) - (7)$ $\quad -\frac{0.247}{2000} M_2 + \frac{0.003}{0.82} Q_2 = -\frac{722}{2000}$ (13)

$\frac{17.84}{1000} M_2 + \frac{0.32}{1000} Q_2 = -\frac{137000}{215000}$ (14)

PREPARED P Y HSIEH

CHECKED

MODEL

REPORT NO.

$$-8.25\ M_1 + 5.5\ Q_1 + 5.52\ M_2 + 17.65\ Q_2 = 1110 \qquad (1)$$

(1)+(3) $\quad 18.10\ M_1 - 20.85\ Q_1 - 27.93\ M_2 = -6590 \qquad (5)$

$$26.20\ M_1 - 26.20\ Q_1 - 33.70\ M_2 - 17.57\ Q_2 = -7660 \qquad (2)$$

(2)+(1) $\quad 25.60\ M_1 + 26.13\ Q_1 - 6.95\ M_2 = 140040 \qquad (6)$

$$-0.90\ M_1 + 78.50\ Q_1 + 39.52\ M_2 + 26.35\ Q_2 = 221,500 \qquad (7)$$

(3)-(4) $\quad 76.95\ M_1 + 77.95\ Q_1 + 13.17\ M_2 = 509,800 \qquad (7)$

$$4.50\ M_1 - 5.18\ Q_1 - 6.95\ M_2 = -1640 \qquad (5)$$

6)-(5) $\quad 21.10\ M_1 + 31.31\ Q_1 = 141,660$

$$48.50\ M_1 + 49.50\ Q_1 - 13.17\ M_2 = 269,500 \qquad (6)$$

(6)+(7) $\quad 125.45\ M_1 + 127.45\ Q_1 = 775300$

$\quad 30.8\ M_1 + 31.31\ Q_1 = 190,180$

$$9.70\ M_1 = 48,500$$

$$M_1 = 5000 \text{ IN-LB/IN}$$

$$Q_1 = \frac{190180 - 30.8(5000)}{31.31} = 1156 \text{ LB/IN}$$

FROM (7) $\quad M_2 = \frac{509,800 - 76.95(5000) - 77.95(1156)}{13.17} = 2625 \text{ IN-LB/IN}$

FROM (1) $\quad Q_2 = \frac{3540 + 26.35(5000) - 17.57(1156) - 17.65(2625)}{56.33} = 1710 \text{ LB/IN}$

TRW
ONE SPACE PARK • REDONDO BEACH, CALIFORNIA

PREPARED P Y HSIEH
CHECKED
MODEL
REPORT NO.

STRESSES IN SHELL

$\sigma_1 = \sigma_1' \pm \frac{6M_2}{t^2}$

$= 4680 \pm \frac{6(2625)}{0.5^2}$

$= 4680 \pm 62820$

$= 67{,}500$ psi. MAX. OUTER SURFACE M.S. $= \frac{135000}{67500} - 1 = 1.00$

710 psi. Safety Factor $= \frac{135000}{67500} = 4.00$

$\sigma_2 = \sigma_2' + \frac{2Q_2}{t} \times Y - \frac{2M_2}{t} \times^2 Y \pm \nu \frac{6M_2}{t^2}$

$= 27700 + \frac{2(1310)}{0.5} 0.809 \cdot 19.75 - \frac{2(2625)}{0.5} 0.1675 \cdot 19.75 \pm 0.3(62820)$

$= 27700 + 41300 - 34700 \pm 18800$

$= 49100$ psi. MAX.

STRESSES IN RING

$M_r = -M_1 + M_2 + Q_1 + Q_2 - 292$

$= -6000 + 2625 + 1156 + 1310 - 292$

$= -201$

$\sigma_b = \frac{M_2 Y K'}{I_y}$

$= \frac{-201 \cdot 19.675 (\pm 1.0)}{0.5}$

$= \pm 8000$ psi.

$\sigma_a = \frac{\Sigma P Y}{2A}$

$= \frac{(600 \cdot 2 + 1156 - 1310) 19.675}{2 \cdot 1.5}$

$= 6950$ psi.

$\sigma_{TOTAL} = -8000 + 6950 = -1050$ psi. INNER END

$= 8000 + 6950 = 14950$ psi. SHELL END

UNCLASSIFIED

PREPARED P Y HSIEH
CHECKED
MODEL
REPORT NO.

STRESSES IN FLANGE.

$M_T = 0.44\, M_1 + 0.47\, R_1 - 5410$

$= 0.44 \cdot 5000 + 0.47 \cdot 1156 - 5410$

$= -167$

$\sigma_b = \frac{-167 \cdot 21.175\ (\pm 0.5)}{1.291}$

$= \mp 6500$ psi.

$\sigma_b = \frac{(600 \cdot 1.0 - 1156)\, 19.375}{2 \cdot 7.25}$

$= -1700$ psi

$\sigma_{TOTAL} = -6500 - 1700 = -8200$ psi. GASKET SIDE

$= 6500 - 1700 = 4800$ psi. RING SIDE

SYSTEMS 1441 REV. 867

PREPARED P Y HSIEH
CHECKED
MODEL
REPORT NO.

THROAT - NOZZLE STRESSES

MAT'L. T-1 STEEL

f_{tu} = 175000 PSI

f_{ty} = 100000 PSI

THROAT AT NOZZLE

$$D = \frac{E t^3}{12(1-\nu^2)}$$

$$= \frac{30\cdot10^6 \cdot 0.5^3}{12(1-0.3^2)}$$

$$= 0.344\cdot10^6$$

$$\lambda = \sqrt[4]{\frac{3(1-\nu^2)}{a^2 t^2}}$$

$$= \sqrt[4]{\frac{3(1-0.3^2)}{15.15^2 \cdot 0.5^2}}$$

$$= 0.414$$

λ^1 = 0.715

λ^2 = 0.10

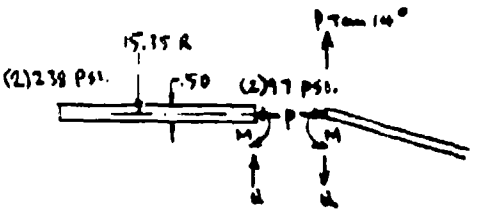

$$P = 2\,\frac{485\,\pi\,(24.6^2 - 15.15^2)}{2\pi \cdot 15.15}$$

= 1490 LB/IN

MEMBRANE STRESSES

$$\sigma_1' = -\frac{P}{t}$$

$$= -\frac{1490}{0.5}$$

= -2980 PSI.

$$\sigma_2' = \frac{2.97 \cdot 15.15}{0.5}$$

= 5960 PSI. NOZZLE SIDE

$$\frac{2.378 - 15.15}{0.5}$$

= 14600 PSI CHAMBER SIDE

SYSTEMS 1441 REV. 5-67

TRW

PREPARED P Y HSIEH

CHECKED

MODEL

REPORT NO.

THROAT DISPLACEMENT DUE TO PRESSURE

$$\partial_p \text{ AT CHAMBER} = \frac{R}{E}(\sigma_2' - \nu\sigma_1')$$

$$= \frac{15.15}{30\cdot10^6}(14600 + 0.3\cdot2980)$$

$$= 10^{-6}(7960)$$

$$\partial_p \text{ AT NOZZLE} = \frac{15.75}{30\cdot10^6}(5960 + 0.3\cdot2980)$$

$$= 10^{-6}(3520)$$

THROAT DISPLACEMENT AT NOZZLE

$$\partial_T = 10^{-6}(3520) + \frac{M}{2D\lambda^3} - \frac{Q}{2D\lambda^2}$$

$$= 10^{-6}(3520) + \frac{M}{2\cdot0.744\cdot10^6\cdot0.215} - \frac{Q}{2\cdot0.744\cdot10^6\cdot0.10}$$

$$= 10^{-6}(3520 + 6.15M - 1.45Q)$$

THROAT ROTATION AT NOZZLE

$$\theta_T = \frac{10^{-6}(3520-7960)}{1.8} + \frac{M}{\lambda D} - \frac{Q}{2D\lambda^2}$$

$$= 10^{-6}(-565) + \frac{M}{0.468\cdot0.744\cdot10^6} - \frac{Q}{2\cdot0.744\cdot10^6\cdot0.215}$$

$$= 10^{-6}(-565 + 6.27M - 6.75Q)$$

UNCLASSIFIED

PREPARED P Y HSIEH
CHECKED
DATE
REPORT NO.

NOZZLE

$$R_2 = \frac{R}{\cos 14^\circ} = \frac{15.75}{\cos 14^\circ} = 15.8$$

$$\beta = \sqrt[4]{3(1-\nu^2)\left(\frac{R_2}{t}\right)^2}$$

$$= \sqrt[4]{3(1-0.3^2)\left(\frac{15.8}{0.25}\right)^2}$$

$$= 10.22$$

$$\beta^2 = 104.5$$

$$\beta^3 = 1070$$

MEMBRANE STRESSES

$$\sigma_1' = \frac{-p}{t\cos 14^\circ}$$

$$= \frac{-1490}{0.25\cos 14^\circ}$$

$$= -6150 \text{ psi}$$

$$\sigma_2' = \frac{pR}{t\cos 14^\circ}$$

$$= \frac{2.97 \cdot 15.75}{0.25 \cdot \cos 14^\circ}$$

$$= 12300 \text{ psi}$$

NOZZLE DISPLACEMENT DUE TO PRESSURE

$$\delta_p \text{ AT THROAT} = \frac{R^2}{E}(\sigma_2' - \nu\sigma_1')$$

$$= \frac{15.75}{30\cdot 10^6}(12300 + 0.3 \cdot 6150)$$

$$= 10^{-3}(773.0)$$

NOZZLE ROTATION DUE TO PRESSURE

$$\theta_p \text{ AT THROAT} = -\frac{10^{-3}(773.0-0)}{446.8}$$

$$= 10^{-6}(-157)$$

PREPARED P Y HSIEH
CHECKED
MODEL
REPORT NO.

NOZZLE DISPLACEMENT AT THROAT

$$\delta_N = 10^{-6}(7230) + \frac{M}{E t} 2R^2 \sin\phi + (Q - P_{min}\,10^6)\frac{2R R_t \sin^2\phi}{E t}$$

$$= 10^{-6}(7230) + \frac{M}{30\cdot10^6\cdot0.25} 2\cdot104.5\cdot0.97 + (Q - 1440\cdot0.244)^2\frac{2\cdot10.22\cdot15.9\cdot0.94}{30\cdot10^6\cdot0.25}$$

$$= 10^{-6}(7230 + 27.0\,M + 40.5\,Q - 15000)$$

$$= 10^{-6}(-7770 + 27.0\,M + 40.5\,Q)$$

NOZZLE ROTATION AT THROAT

$$\theta_N = 10^{-6}(-157) - \frac{M}{E t}\frac{4R^3}{R_t^2} - (Q - P_{min}\,10^6)\frac{2R^2\sin\phi}{E t}$$

$$= 10^{-6}(-157) - \frac{M}{30\cdot10^6\cdot0.25}\frac{4\cdot10.22^3}{15.8} - (Q - 1440\cdot0.244)\frac{2\cdot104.5\cdot0.97}{30\cdot10^6\cdot0.25}$$

$$= 10^{-6}(-157 - 36.1\,M - 27.0\,Q + 10000)$$

$$= 10^{-6}(9843 - 36.1\,M - 27.0\,Q)$$

FOR $\delta_T = \delta_N$

$$10^{-6}(3320 + 6.75\,M - 1.45\,Q) = 10^{-6}(-7770 + 27.0\,M + 40.5\,Q)$$

$$20.25\,M + 41.95\,Q = 11290$$

FOR $\theta_T = \theta_N$

$$10^{-6}(-565 + 6.27\,M - 6.75\,Q) = 10^{-6}(9843 - 36.1\,M - 27.0\,Q)$$

$$42.37\,M + 20.25\,Q = 10408$$

$$97.1\,M + 41.95\,Q = 21600$$

$$67.45\,M = 10310$$

$$M = 153 \text{ LB/IN} \qquad \text{REV. 1}$$

$$Q = \frac{10408 - 42.37(153)}{20.25} = 193 \text{ LB/IN} \qquad \text{REV. 1}$$

PREPARED P Y HSIEH
CHECKED
MODEL
REPORT NO.

STRESSES IN NOZZLE

$$\sigma_1 = \sigma_1' \pm \frac{6M}{t^2} - (Q - P\pi m)\frac{\cot\phi}{t}$$

$$= -\frac{1490}{0.25 \cdot 0.97} \pm \frac{6 \cdot 153}{0.25^2} - (193 - 1490 \cdot 0.349)\frac{.342}{.25}$$

$$= -6150 \pm 14700 - 172$$

$$= -20678 \text{ psi}$$

$$M.S. = \frac{135000}{20678} - 1 = 5.52$$

REV. 1

$$\sigma_2 = \sigma_2' + (Q - P\pi m\cos\phi)\frac{1}{t}M\sin\psi + \frac{M}{tR_2}\lambda R^2 \pm \nu\frac{6M}{t^2}$$

$$= 12300 + (193 - 1490 \cdot 0.349)\frac{1}{0.25}1072 \cdot 1.94 + \frac{153}{.25 \cdot 152.9}2 \cdot 1045 \pm 0.3(14700)$$

$$= 12300 - 14100 + 8070 \pm 4400$$

$$= 10670 \text{ psi MAX.} \quad (12300 \text{ psi MEMBRANE STRESS})$$

STRESSES IN THROAT

$$\sigma_1 = -\frac{P}{t} \pm \frac{6M}{t^2}$$

$$= -\frac{1490}{0.5} \pm \frac{6 \cdot 153}{0.5^2}$$

$$= -2980 \pm 3670$$

$$= -6650 \text{ psi MAX}$$

$$\sigma_2 = \sigma_1' - \frac{2Q}{\phi}\lambda R + \frac{2M}{t}\lambda^2 R \pm \nu\frac{6M}{t^2}$$

$$= 5960 - \frac{2(193)}{0.5}0.444 \cdot 15.15 + \frac{2(153)}{0.5}0.215 \cdot 15.15 \pm 0.3(3670)$$

$$= 5960 - 5450 + 2030 \pm 1100$$

$$= 3640 \text{ psi MAX.}$$

APPENDIX B

SUBSCALE CHAMBER LINER MATERIALS
EVALUATION PROGRAM

1. INTRODUCTION AND SUMMARY

1.1 INTRODUCTION

(U) TRW's Science and Technology Division has been investigating new technology related to the goal of developing low-cost space launch vehicles. The major technological effort has been the demonstration of an engine design concept which would be scaleable in terms of performance, stability, and durability and which could be manufactured using industrial rather than aerospace fabrication techniques.

(U) In support of the Air Force funded Injector/Chamber Scaling Feasibility Program (Contract No. F04611-68-C-0085) TRW Systems undertook an IR&D program to investigate the feasibility of low-cost ablative liners for the 250,000 lbf thrust engine designs. The Subscale Chamber Liner Materials Evaluation Program had the following objectives:

- Evaluate candidate 250,000 lbf thrust ablative chamber liners at a reduced thrust level (1500 lbf)
- Generate ablative performance data necessary for designing the 120 second firing duration, 250,000 lbf thrust chamber liners.
- Recommend additional materials for future material evaluation programs.

(U) The materials evaluated are the result of an industry search of potential candidate tank lining materials, reentry heat shield materials, launch pad protective coating materials and high temperature ablative materials. The current raw material costs ranged from $2.00/lb. to $10.00/lb. and all candidate materials showed the potential of an in-place cost of less than $10.00/lb. for production quantities.

(U) The program was conducted in two phases. Phase I (injector characterization phase) consisted of determining the smooth wall thermodynamic environment as a function of injector operating conditions for fixed injection orifices. Heat sink hardware was used to determine the local thermodynamic environment throughout the combustion chamber and converging-diverging nozzle section. Phase II (material evaluation phase) consisted of evaluating the candidate low-cost materials to determine (1) char formation characteristics of the char forming materials, (2) chamber, throat, and exit cone erosion rates, (3) circumferential variations in the erosion rates, and (4) the virgin materials insulative ability from the standpoint of minimizing chamber backwall temperature.

(U) Limited laboratory investigations were also conducted to obtain additional thermodynamic data on the candidate materials. An oxygen/methane (C_2/CH_4) torch was used (in the laboratory) to simulate oxidizer-rich and fuel-rich chemical environments. Steady-state ablation surface temperatures were measured with an optical pyrometer. This surface temperature was then used with the known gas recovery temperature, a Bartz value of convective film coefficient, and the measured throat mass loss rate to calculate the effective heats of ablation of the various candidate materials. The effective heat of ablation is a lumped parameter used to describe the ablation process by a purely thermal model. This parameter includes all forms of mass loss such as chemical erosion, mechanical erosion, and thermal erosion.

1.2 SUMMARY

1.2.1 General

(U) All testing was conducted using the TRW 1500 lbf vacuum thrust coaxial injector (see Figure B-1), operating with oxidizer (N_2O_4) flow through the center circuit and fuel (UDMH) flow through the outside circuit. The flow passages and injection orifices of this injector are similar to those of the 250,000 lbf injector used in the Air Force sponsored Injector/Chamber Scaling Feasibility Program.

(U) The nominal test conditions were based on matching the 1500 lbf subscale thermodynamic and gas dynamic throat environments to those anticipated in the 250,000 lbf low-cost rocket engine. Section 3 describes in detail this scaling procedure. The resultant test conditions were:

Propellants	N_2O_4/UDMH
Chamber pressure	190 psia
Total flow rate	4.5 lb/sec
Mixture ratio	2.0 to 2.7 (O/F)
Contraction ratio	2.4
Expansion ratio	2.8 (optimum at sea level)

Cavitating venturis were used to maintain constant propellant flow rates during each test. Redundant measurements were taken on all critical engine performance parameters.

(U) Seven injector characterization tests were made in a heat-sink thrust chamber to determine the smooth wall thermodynamic environment throughout the thrust chamber as a function of injector operating conditions. Figure B-2 shows the heat-sink thrust chamber assembly; the assembly was instrumented with three steel Nanmac thermocouple probes in the chamber and six isolated copper calorimeter plugs in the nozzle section.

(U) The results of the seven heat-sink injector characterization tests are presented in Table I. Test firings HA1-489-HA1-491 were used to determine the chamber thermal environment over the mixture ratio (O/F) range of 2.0

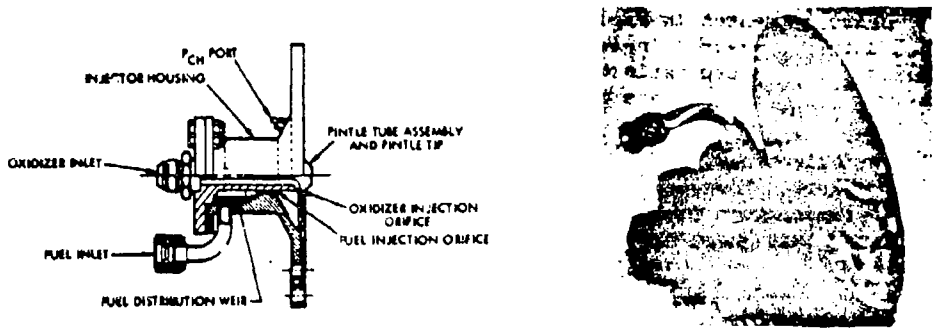

Figure B-1. 1500 lbf Thrust (vacuum) Single-Element Coaxial Injector Assembly (U)

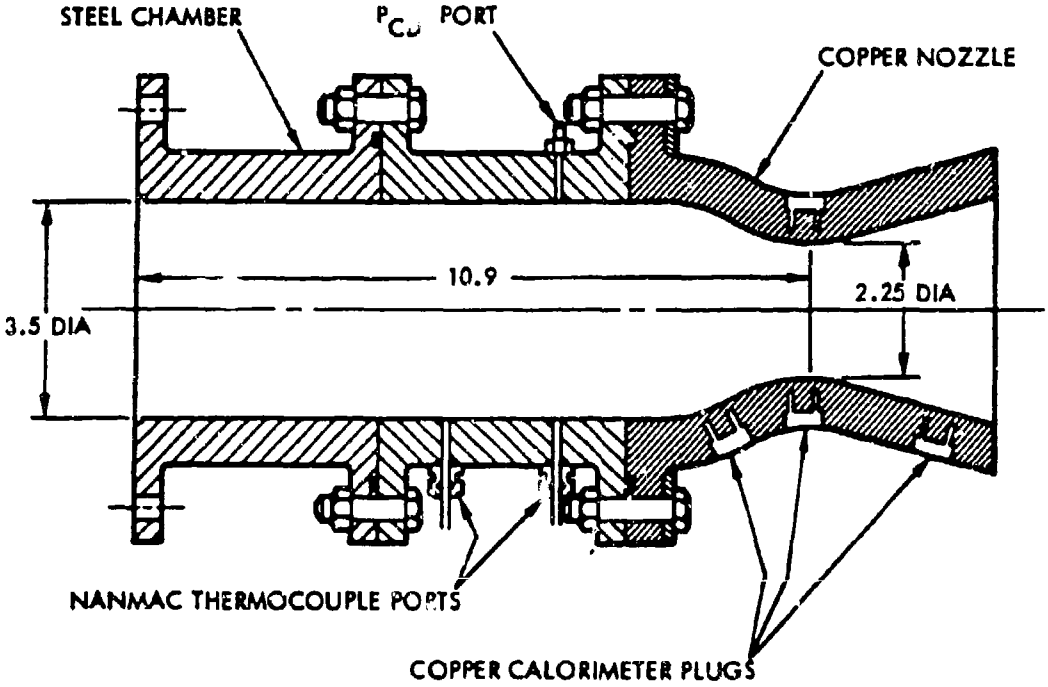

Figure B-2. 1500 lbf Heat Sink Thrust Chamber Assembly Used for the Injector Characterization Firings (U)

(U) to 2.7 Figure B-3 presents the combustion efficiency (η_{C^*}) based on theoretical shifting equilibrium calculations as a function of mixture ratio. Also presented in Figure B-3 are the chamber and throat heat rejection data as measured in line with the injector fuel inlet. Both curves maximized at a mixture ratio of 2.4 (oxidizer/fuel). The measured gas recovery temperature at this mixture ratio was 4850°F in the chamber section. The throat copper calorimeter plugs resulted in longitudinal heat losses which removed the possibility of measuring the throat gas recovery temperature. However, since a value equal to 90 percent of the theoretical flame temperature was measured in the chamber section it was assumed to be constant throughout the thrust chamber.

Table I. Subscale Chamber Liner Materials Evaluation Program Injector Characterization Test Results (U)

Run No.	Test Duration (sec)	Mixture Ratio (O/F)	Total Flow Rate (lb/sec)	ΔPIO (psia)	ΔPIF (psia)	Nozzle Stagnation Pressure (psia)	Characteristic* Exhaust Velocity (ft/sec)	Combustion** Efficiency (%)
HA1-432	2.0	2.43	4.49	121	40	186.2	5314	93.8
HA1-433	3.0	2.09	4.51	108	51	191.5	5447	96.1
HA1-434	4.3	2.44	4.51	124	39	189.1	5380	94.9
HA1-435	6.3	2.43	4.50	116	39	188.6	5368	94.7
HA1-489	4.2	2.46	4.54	122	40	186.2	5241	92.6
HA1-490	3.9	2.08	4.49	104	49	187.1	5337	94.3
HA1-491	4.2	2.76	4.48	124	33	175.7	5012	88.6

* Performance is based on downstream chamber pressure corrected to nozzle stagnation.

** Percent performance is based on theoretical shifting equilibrium calculations.

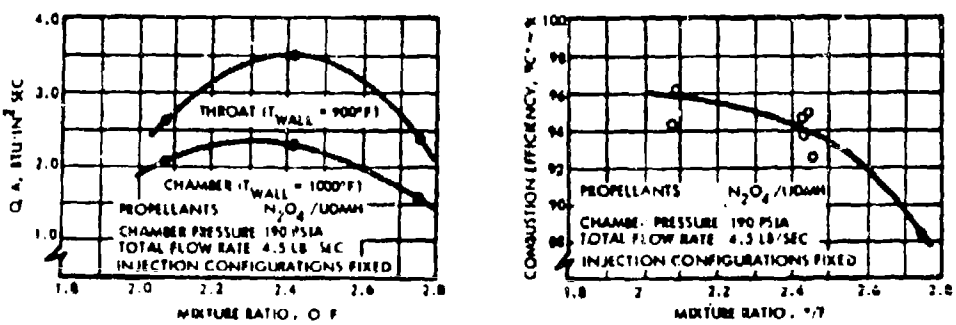

Figure B-3. Chamber and Throat Heat Rejection Data and Combustion Performance (η_{C^*}) as a Function of Mixture Ratio for the 1500 lbf Injector with Fixed Injection Orifices (U)

1.2.2 Ablative Material Evaluation Firings

(U) The purpose of the ablative material evaluation tests was to screen and evaluate various candidate low-cost ablative materials for possible use in the 250,000 lbf low-cost long-duration thrust chamber assemblies. All materials evaluated showed promise of less than $10/lb "in-place" costs for large quantities. The ablative performance data generated for these candidate materials were used to design baseline thrust chamber liner assemblies capable of ablatively cooling the 250,000 lbf rocket engine for a single 120-second continuous burn. A mixture ratio of 2.4 (oxidizer/fuel) was chosen for evaluating the ablative materials since this corresponds to the most severe thermal environment measured in the subscale injector characterization test firings. At this mixture ratio, the thermodynamic and gas dynamic environments were:

Gas Recovery Temperature	4850°F
Smooth Wall Shear Stress	
Chamber	4psf
Throat	36psf
Exit Plane	27psf

(U) Twelve low-cost ablative liners and a baseline silica-phenolic liner were tested. The ablative thrust chamber assembly employed on these tests is shown in Figure B-4. All tests were terminated after essentially the same amount (percent) of throat erosion had occurred. The calculated changes in the thermodynamic and gas dynamic environments because of this erosion are shown in Figure B-5. The throat convective film coefficient decreased 35 percent and the throat smooth wall shear stress level decreased 45 percent. The materials evaluated are described in Table II.

(U) The measured head end chamber pressure decay rates for the four most promising ablative materials are shown in Figure B-6. For constant propellant flow rates and assuming constant combustion performance (characteristic exhaust velocity) the instantaneous throat erosion rate can be calculated from the measurable instantaneous chamber pressure decay rate. Figure B-7 presents the instantaneous throat erosion rates of the four candidate materials. The throat erosion rate decreases nearly linearly with the measured head end chamber pressure. Since the convective film coefficient is dependent upon chamber pressure to the 0.8 power (see Section 3), it appears that the throat erosion can be described by a simplified thermal model. In essence, the model defines the effective heat of ablation which groups the thermal, chemical, and mechanical erosion into a lumped parameter. Table III presents the effective heats of ablation and steady-state ablation surface temperatures for the candidate ablative materials. The surface temperatures were measured with an optical pyrometer in controlled chemical environment laboratory torch tests (see Section 3.3.6).

(U) Figure B-8 shows the throat radius history as determined by integrating the instantaneous throat erosion rate and the calculated value using the effective heat of ablation presented in Table III. The agreement in the two curves verifies the validity of the thermal model for describing the throat erosion process.

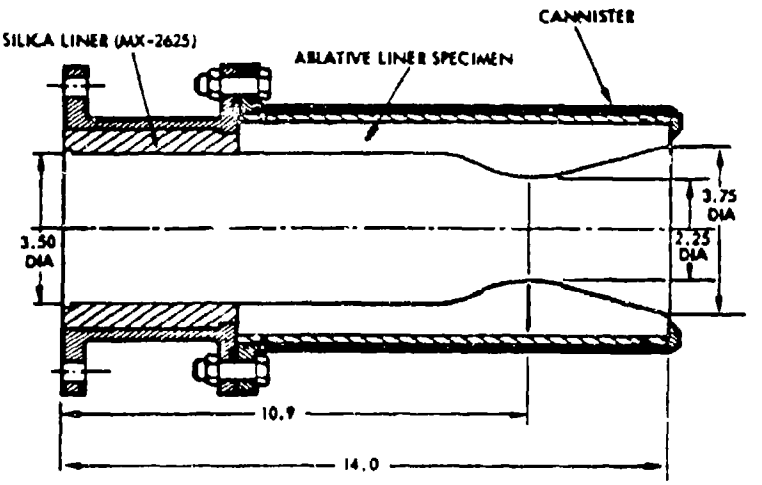

Figure B-4. 1500 lbf Ablative Thrust Chamber Assembly Used for the Ablative Material Evaluation Firings (U)

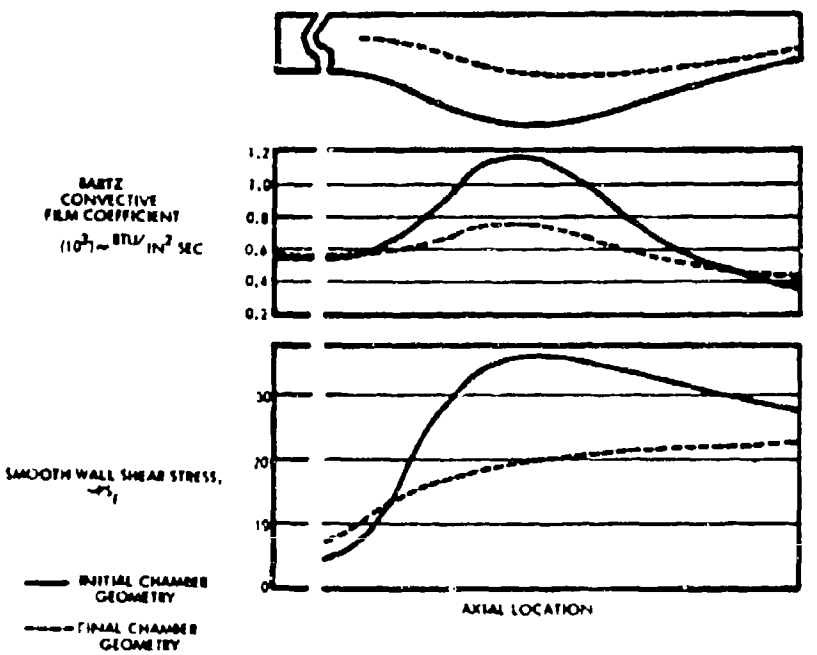

Figure B-5. The Change in the Thermodynamic and Gas Dynamic Environments Because of 70% Throat Erosion (Recovery Temperature = 4850°F) (U)

Table II. Description of Materials Evaluated During Subscale Chamber Liner Materials Evaluation Program (U)

Material	Source	Type	Filler	Resin	Fabrication Method	Cure	
						Temp. (°F)	Pressure (psia)
MX-2600	Fiberite	Rigid	Silica Fabric	Phenolic	Tape Wrap	300	--
DC-93-104	Dow Corning	Elastomeric	C.P.[1]	Silicone	Cast in Place	R.T.[2]	Amb.[3]
HAVEG-41	HAVEG	Rigid	Abestos Fiber	Phenolic	Molded Segments	300	200
GE-223-50	General Elect.	Rigid	Silica Flour/Fiber	Epoxy Novalak	Molded Segments	R.T.	Amb.
HAVEG-41F	HAVEG	Rigid	Asbestos Fiber	Phenolic	Molded Segments	R.T.	Amb.
AVCOAT 4011	AVCO	Rigid	Silica Fiber	Epoxy Novalak	Molded Segments	350	Amb.
T-500-113	Thermal Syst.	Rigid	C.P.	Phenolic	Cast/Mold		
DE-350	Dyna Therm	Elastomeric	Refrasil	Mod. Epoxy	Trowellable	R.T.	Amb.
T-500-7	Thermal Syst.	Rigid	C.P.	Phenolic	Cast/Mold		
AVCOAT 8021	AVCO	Elastomeric	None	Epoxy-Urethane	Cast in Place	200	Amb.
E-742NT	See-Co Plastics	Rigid	Asbestos	Epoxy-Neoprene	Trowellable	R.T.	Amb.

(1) C.P. = Company Proprietary
(2) R.T. = Room Temperature
(3) Amb. = Ambient Pressure

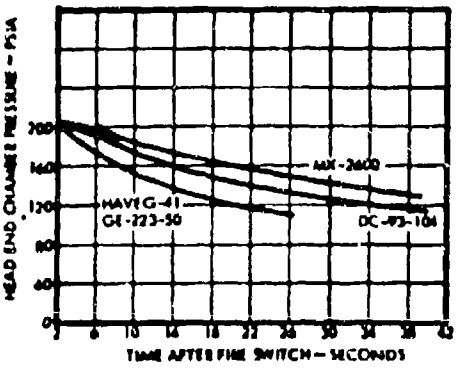

Figure B-6. Experimental Chamber Pressure Decay Rates for the Four Best Performing Ablative Materials (U)

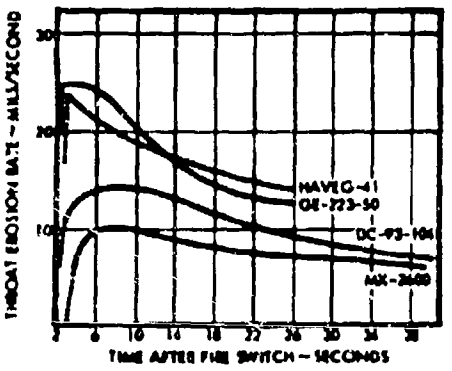

Figure B-7. Calculated Instantaneous Throat Erosion Rate for Candidate Materials (U)

Table III. Subscale Chamber Liner Materials Evaluation Program Ablative Test Results for the Candidate Materials (U)

Material	Steady-State Surface Temperature (°F)	Effective Heat of Ablation (Btu/lbm)
MX-2600	3340	2400
DC-93-104	3200	1600
HAVEG-41	2880	1000
GE-223-50	3130	875

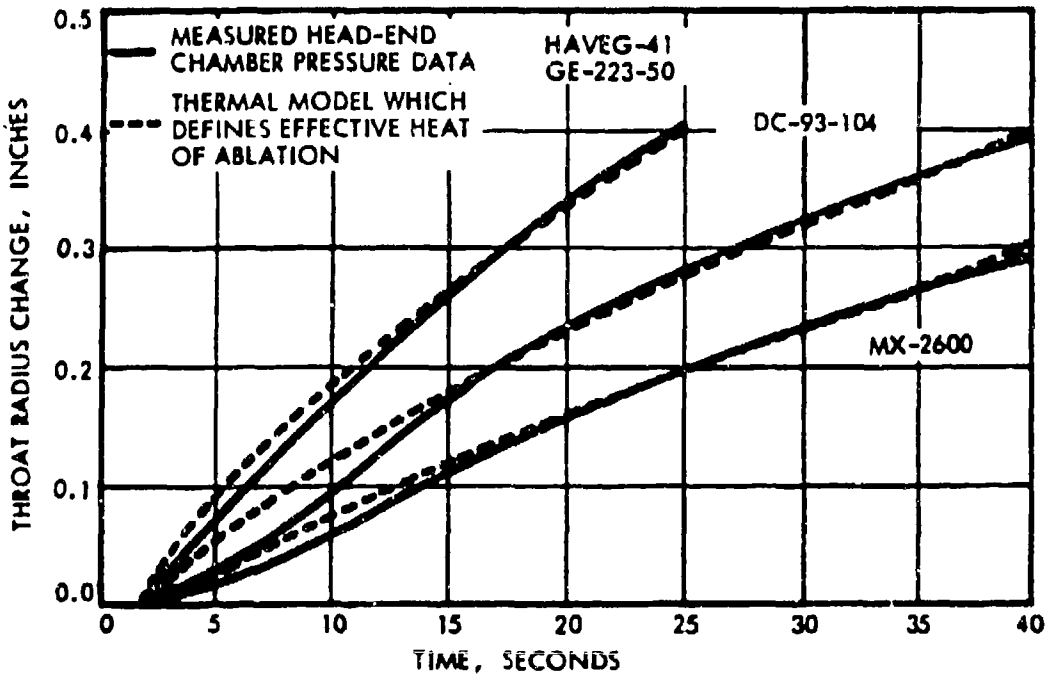

Figure B-8. Throat Radius History as Calculated From Measured Head End Chamber Pressure Decay (solid line). Also described by the thermal model which includes mechanical, chemical and thermal erosion as a lumped parameter-defined as the effective heat of ablation (dashed line) (U)

2. MATERIALS EVALUATED

2.1 GENERAL

(U) The materials evaluated in the program are presented in Table VI and are the result of an industry search of the following:

- Chemical tank lining materials
- Reentry heat shield materials
- Launch pad protective coating materials
- Aerodynamic structure protective coating materials
- Conventional high temperature ablative materials

(U) The resin systems include phenolics, numerous epoxies, and silicone, urethane, and neoprene elastomers. The fillers include silica fabrics, silica flour, silica fibers, asbestos fibers, and other company proprietary fillers. The current raw material costs ranged from $2.00/lb. to $10.00/lb. and all materials evaluated showed promise of reaching $10.00/lb. or less in-place cost for production quantities. The following paragraphs describe the five most promising materials.

2.1.1 MX 2600 Silica-Phenolic (Fiberite Corp)

(U) The MX-2600 material consists of a silica fabric impregnated with a silica-filled phenolic resin. It is a conventional rocket engine ablative material which can be tape-wrapped, using a tape wrapping machine, or hand laid-up by building up a number of plies of previously cut fabric. The tooling costs for tape wrapping a part and the labor costs for hand lay-up processes make it a high-cost material when installed in a thrust chamber. It requires both elevated temperature (300°F) and pressure (depending upon geometry of part) for curing.

2.1.2 DC-93-104 Filled Silicone Rubber (Dow Corning)

(U) The DC-93-104 is a filled silicone rubber. The silicone rubber is a cross-linking of phenyl-methyl polysiloxane polymers and the added fillers are company proprietary. The addition of these fillers increases the material's resistance to shear loads without inhibiting its elongation characteristics and reduces the thermal conductivity of the material.

(U) The material is available in both a thixotropic and nonthixotropic version. It is room temperature curable and has a 70 percent elongation capability. The high elongation rate allows it to expand or contract with its backup substrate. The use of DC primer solution will result in self-bonding of the material to its back-up substrate during cure. The amount of shrinkage during cure is minimal because the catalyst becomes an integral part of the polymer.

Table IV. Subscale Materials Evaluation Program Description of Materials Evaluated (U)

Material	Source	Type	Resin	Filler (%)	Density[1] (S.G.)	Specific[2] Heat (Btu/lbm-°R)	Thermal[2] Conductivity (Btu/ft-hr-°F)	Thermal Coefficient of Expansion (in./in.-°F)	Cure Temp (°F)	Cure Pressure (psi)
MX-2600	Fiberite Corp	Rigid	Phenolic	Silica Fabric (70%)	(1.7)				300	-
DC-93-104	Dow Corning	Elastomeric	Silicone	C.P.[3]	1.44	0.29	0.20	3×10^{-4}	R.T.[4]	Ambient
HAVEG-61	HAVEG Industries	Rigid	Phenolic	Asbestos (60%)	1.62	-	0.11	10^{-5}	300	200
GE-223-50	General Electric	Rigid	Epoxy Novolak	Silica Flour / Silica Fiber (50%)	1.7	0.29	0.13	-	R.T.	Ambient
HAVEG-61F	HAVEG Industries	Rigid	Phenolic	Asbestos	1.47	-	-	-	R.T. (24 hr)	Ambient
AVCOAT-6011	AVCO Corp	Rigid	Epoxy Novolak	Silica (16%)	1.12	0.28	0.14	-	350	Ambient
T-500-115	Thermal Systems	Rigid	Phenolic Rubber	C.P.	1.47	0.25	0.08	-		
DE-350	Dyna Therm	Elastomeric	Epoxy	Refrasil (6%)	(1.85)	0.45	0.085		R.T. (7 days)	Ambient
T-100..	Thermal Systems	Rigid	Phenolic Rubber	C.P.	1.37	0.25	0.08	-		
AVCOAT-6021	AVCO Corp.	Rigid	Epoxy Urethane	None	1.06	0.41	0.11	10^{-4}	200	Ambient
K-76/MT	BarCo Plastics	Rigid	Epoxy Neoprene	Asbestos	1.34	-	-	-	R.T. (5 days)	Ambient

1. All density values are as measured except those in parenthesis which are quoted information from source
2. Values listed are taken at room temperature
3. Company proprietary
4. Room temperature

2.1.3 HAVEG-41 Asbestos-Phenolic (Haveg Industries)

(U) HAVEG-41 is an asbestos fiber-filled phenolic resin system. The asbestos fiber content is 40 percent by weight. The out-gassing of catalytic reactions during cure causes about 2 percent volumetric shrinkage of the material. It requires both temperature (300°F) and pressure (200 psi) for curing.

(U) HAVEG-41 is a commercial molding compound used primarily for lining chemical tanks and pipelines. It is a char forming material and the presence of the asbestos fibers retain this char. Very little data have been generated on this material as an ablative liner for rocket engine thrust chambers.

2.1.4 HAVEG-41F Asbestos-Phenolic (Haveg Industries)

(U) The HAVEG-41F asbestos-phenolic is a room temperature catalytically cured version of the HAVEG-41. Its primary use is as an ablative cement for bonding compression molded segments of the HAVEG-41 material. It is a two-part system consisting of a hardener solution plus the asbestos phenolic cement. The hardener solution must be thoroughly mixed with the cement to insure complete curing of the material.

2.1.5 GE-223-50 Silica Filled Epoxy Novalak (General Electric Co.)

(U) The GE-223-50 is a silica filled epoxy Novalak system. It contains a mixture of silica flour and milled silica fibers as fillers for the epoxylated Novalak resin base. The filler content is 50 percent by weight. It is a castable material which can be cured at room temperature. The silica fibers are spread uniformly throughout the resin and increase the resistance to shear forces for retaining the char layer.

3. EXPERIMENTAL PROGRAM

3.1 BACKGROUND

(U) To effectively evaluate, on a subscale basis, low-cost ablative liner materials, the thermodynamic and gas dynamic environment of the subscale rocket engine must be comparable to the full-scale hardware. The Air Force sponsored Injector/Chamber Scaling Feasibility Program consists of demonstrating the feasibility of the low-cost ablative liner concept at a 250,000 lbf thrust level. The operating conditions of this engine are:

Thrust level	250,000 lbf
Propellants	N_2O_4/UDMH
Chamber pressure	300 psia
Mixture ratio	2.3 to 2.9 (O/F)
Contraction ratio	2.1
Expansion ratio	4.0

3.1.1 Throat Gas Dynamic Environment

(U) The smooth wall shear stress profile throughout any thrust chamber may be calculated using Equation 3-1 where this equation is applicable for gases with a specific heat ratio of 1.2 and a Prandtl number of 0.83.

$$T_w = 2\left(\frac{\rho V^2}{2g}\right)\left(0.026Re^{-0.2}\right)\left[1.0 + 1.64\left(0.161^{-0.1}\right)\right] \qquad (3\text{-}1)$$

(U) The Reynolds number at the throat is calculated from the following equation:

$$Re_t = 1580\ P_o\ D_t \qquad (3\text{-}2)$$

(U) In terms of nozzle stagnation pressure and throat diameter the smooth wall shear stress at the throat is given by Equation 3-3

$$T_w = P_o\left[0.58\left(P_o D_t\right)^{-0.2} + 0.0737\ \ P_o D_t^{\ -0.3}\right] \qquad (3\text{-}3)$$

The units to be used in Equation 3-3 are:

P_o, psia
D_t, inches
T_w, lbf/ft^2

3.1.2 Throat Thermodynamic Environment

(U) Using Bartz' equation (Reference 1) for the convective heat transfer film coefficient (hg) and assuming constant viscosity (μ), constant specific heat (Cp), constant Prandtl number (Pr) and constant property variation across the boundary layer (σ), the throat convective film coefficient becomes dependent upon nozzle stagnation pressure, throat diameter and throat radius of curvature as follows:

$$hg = 2.22 \times 10^{-5}\ \frac{P_o^{0.8}}{D_t^{0.1}\ r_c^{0.1}} \qquad (3\text{-}4)$$

where:

hg is the convective heat transfer film coefficient, $Btu/in^2\ sec°R$

r_c is the nozzle throat radius of curvature, inches

Reference 1. D. R. Bartz, "An Approximate Solution of Compressible Turbulent Boundary-Layer Development and Convective Heat Transfer in Convergent-Divergent Nozzles," Trans.ASME, Nov.'55

P_o is the nozzle stagnation pressure, psia

D_t is the nozzle throat diameter, inches

(U) The nozzle stagnation pressure, throat diameter and throat radius of curvature of the 250,000 lbf low-cost rocket engine are 300 psia, 26.2 inches, and 11.5 inches, respectively. According to Equations (3-3) and (3-4) this corresponds to a smooth wall shear stress at the throat of 31 lbf/ft^2 and a throat convective film coefficient of 0.0012 $Btu/in^2sec°R$.

3.2 1500 ENGINE OPERATING CONDITIONS

(U) The 1500 lbf rocket engine was designed to operate at a nozzle stagnation pressure of 300 psia and throat diameter of 1.8 inches. For a constant ratio of thrust level to thrust coefficient the operating level of the 1500 lbf rocket engine is:

$$P_o D_t^{2.0} = 974.5 \text{ (lbf)} \qquad (3\text{-}5)$$

Figure B-9 shows the relationships between nozzle stagnation pressure and throat diameter for constant smooth wall shear stress at the throat, constant convective film coefficient at the throat, and the operating level of the 1500 lbf rocket engine. At a nozzle stagnation pressure of 170 psia and a throat diameter of 2.30 inches, the smooth wall shear stress at the throat and the throat convective film coefficient of the 1500 lbf rocket engine are equal to the values for the 250,000 lbf rocket engine.

(U) A slightly higher nozzle stagnation pressure was selected for evaluating the ablative liners. The reason for this was that as the throat erodes this pressure will decrease and a greater initial pressure will result in a longer test duration before reaching a minimum head end chamber pressure shutdown criteria. A nozzle stagnation pressure of 190 psia, throat diameter of 2.25 inches, and throat radius of curvature of 2.5 inches were selected.

(U) Table V shows the calculated smooth wall shear stress at the throat and the throat convective film coefficient for both the 250,000 lbf and the 1500 lbf rocket engines.

3.3 ABLATIVE MATERIAL EVALUATION FIRINGS

(U) Thirteen ablative liners were tested. Figure B-10 shows the 1500 lbf ablative rocket engine assembly mounted in the HEPTS A1 test cell.

(U) Table VI presents the ablative material evaluation test results. All tests were conducted at a mixture ratio of 2.4 (O/F) and a total propellant flow rate of 4.5 lb/sec. This corresponds to the most severe chamber and throat thermal environments measured in the injector characterization firings. All tests were terminated after essentially the same amount of throat erosion had occurred. The changes in the thermodynamic and gas dynamic environments because of the throat erosion were calculated by

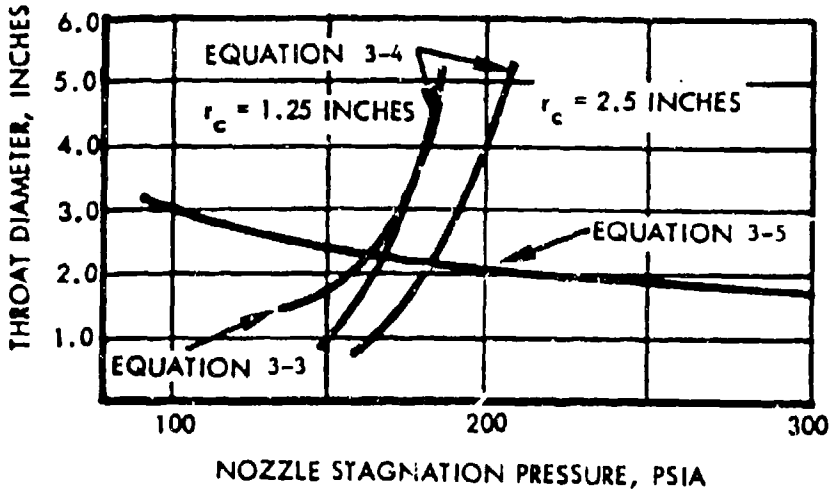

Figure B-9. Throat Diameter Versus Nozzle Stagnation Pressure for Constant Smooth Wall Shear Stress at the Throat Constant Convective Film Coefficient at the Throat and the Operating Level of the 1500 lbf Engine (U)

Table V. Subscale Chamber Liner Materials Evaluation Program Thermodynamic and Gas Dynamic Environments (U)

Parameter	Engine	
	250,000 lbf	1500 lbf
Smooth Wall Shear Stress [Equation (3-3]	31 psf	36 psf
Throat Convective Film Coefficient [(Equation (3-4]	0.0012 $\frac{\text{Btu}}{\text{in}^2\ \text{sec}\ ^\circ\text{R}}$	0.0012 $\frac{\text{Btu}}{\text{in}^2\ \text{sec}\ ^\circ\text{R}}$

(U) assuming that the wall chemical environment did not change. Figure B-11 shows these changes in environments. The throat convective film coefficient dropped 35 percent and the throat smooth wall shear stress level dropped 45 percent.

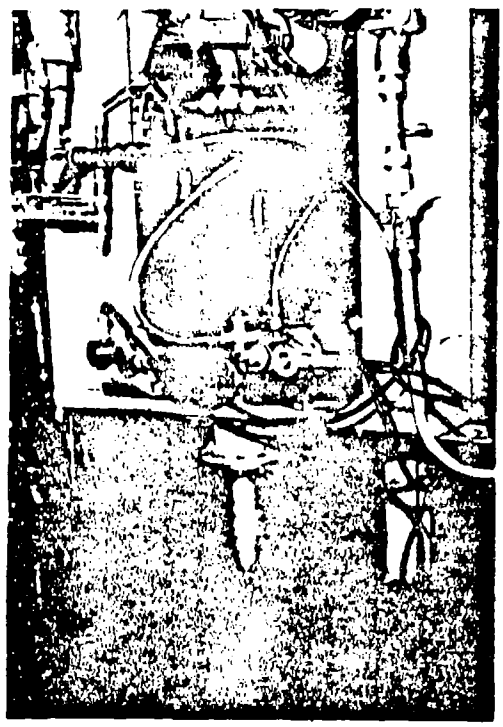

Figure B-10

Ablative Cooled 1500 lbf
Rocket Engine Mounted
in the HEPTS A1 Test Cell (U)

(U) The four best performing ablative materials were MX-2600, DC-93-104, HAVEG-41; and GE-223-50. The measured head end chamber pressure decay rates for these materials are presented in Figure B-12. The instantaneous throat erosion rates which were calculated from the measured head end chamber pressure decay rates are shown in Figure B-13. A nearly linear relationship between head end chamber pressure and instantaneous throat erosion rate was observed by comparing Figures B-12 and B-13. This indicated that the throat erosion was highly dependent upon the heat flux into the material since the convective film coefficient is dependent upon chamber pressure to the 0.8 power (see Reference 1). The thermal model which describes this ablation rate dependence upon chamber pressure, requires a knowledge of the steady-state ablation surface temperature for the materials.

Table VI. Subscale Chamber Liner Materials Evaluation Program, Ablative Liner Test Conditions and Results (U)

Test No.	Date	Material	Test Duration[1]	Head-end Chamber Press[2] Initial (psia)	Final (psia)	Total[3] Flow Rate (lb/sec)	Mixture Ratio (O/F)	Contraction[4] Ratio Initial	Final	Char Depth[4, 5] Chamber (inches)	Throat (inches)	Exit Cone (inches)	Surface Recession[4, 6] Chamber (inches)	Throat (inches)	Exit Cone (inches)
HAI-435	11/22/68	HAVEG-41	25	199	110	4.53	2.47	2.4	1.68	0.427	0.562	0.270	0.397	0.532	0.220
HAI-436	11/22/68	AVCOAT-4011	15	198	116	4.52	2.49	2.4	1.44	0.487	0.512	0.100	0.467	0.472	0.070
HAI-437	11/22/68	DC-93-104	48	204	114	4.52	2.44	2.4	1.52	0.387	0.512	0.140	0.317	0.452	0
HAI-438	11/23/68	DE-350M	51	183	109	4.57	2.45	2.4	1.38	0.207	0.542	0.190	0.197	0.532	0.140
HAI-439	11/23/68	T-500-7	53	197	111	4.53	2.43	2.4	1.50	0.267	0.522	0.170	0.257	0.512	0.160
HAI-440	11/23/68	T-500-113	15	199	109	4.53	2.43	2.4	1.55	0.247	0.482	0.110	0.237	0.472	0.100
HAI-441	11/23/68	K-742HY	5	179	105	4.50	2.43	2.4	1.33	0.207	0.572	0.190	0.197	0.562	0.180
HAI-442	11/23/68	AVCOAT-8021	5	186	112	4.56	2.42	2.4	1.39	0.147	0.482	0.150	0.147	0.482	0.150
HAI-443	11/23/68	GE-223-50	24	200	112	4.56	2.42	2.4	1.57	0.347	0.542	0.150	0.317	0.522	0.065
HAI-444	11/23/68	DE-350	13	185	113	4.54	2.43	2.4	1.49	0.237	0.502	0.070	0.217	0.487	0.040
HAI-492	2/18/69	DC-93-104H	8	194	144	4.56	2.43	2.4	-	-	-	-	-	-	-
HAI-493	2/19/69	HAVEG-41F	18	203	105	4.58	2.44	2.4	1.56	0.337	0.542	0.270	0.307	0.512	0.220
HAI-494	2/19/69	MX-2600	37	205	132	4.59	2.43	2.4	1.91	0.307	0.372	0.220	0.097	0.212	0

1. Test duration was measured from 90 percent Pch to shutdown.
2. Average of two pressure transducers.
3. Average of redundant flow meters for each propellant.
4. Measured in line with the injector full inlet.
5. Char depth is defined as the distance from the original surface to the char/virgin material interface at shutdown.
6. Surface recession is defined as the distance from the original surface to the surface of the char layer.

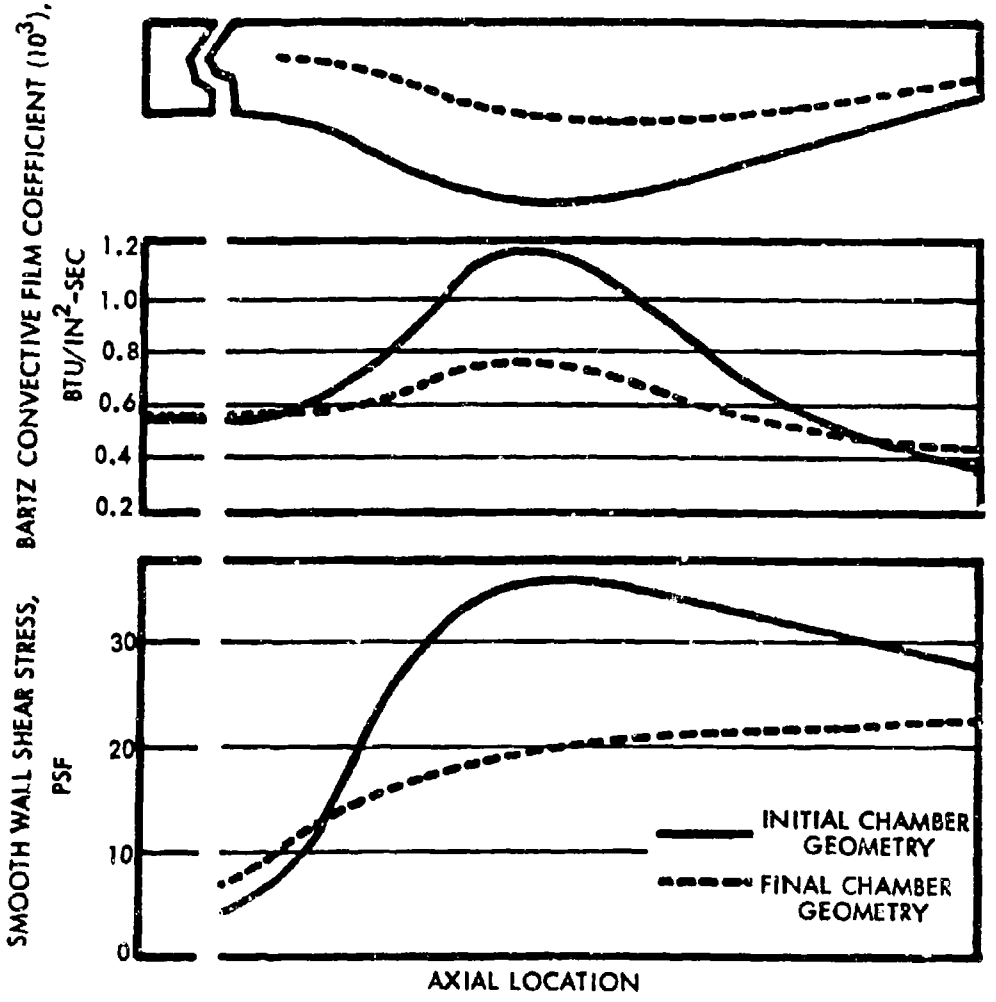

Figure B-11. Initial and Final Thermodynamic and Gas Dynamic Environments Throughout the 1500 lbf Thrust Chamber Assembly (U)

(U) Controlled chemical environment torch tests were conducted to determine the steady-state ablation surface temperature for each of the four candidate materials. Section 3.3.6 describes these tests and presents the data obtained for additional materials of interest. Table VII gives the effective heat of ablation and the steady-state ablation surface temperature as measured in the controlled chemical environment torch tests for the four candidate materials.

(U) Sections 3.3.1 through 3.3.5 discusses the results obtained during the engine testing of each material. Inspections of the photographs indicates the materials char formation characteristics. The baseline MX-2600 silica-phenolic liner maintained a thick char layer throughout the engine.

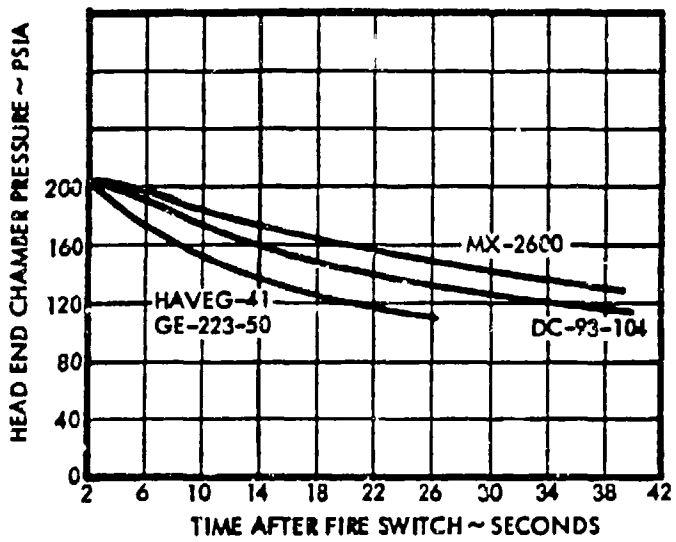

Figure B-12. Measured Head-End Chamber Pressure Decay Rates for Best Performing Ablative Materials (U)

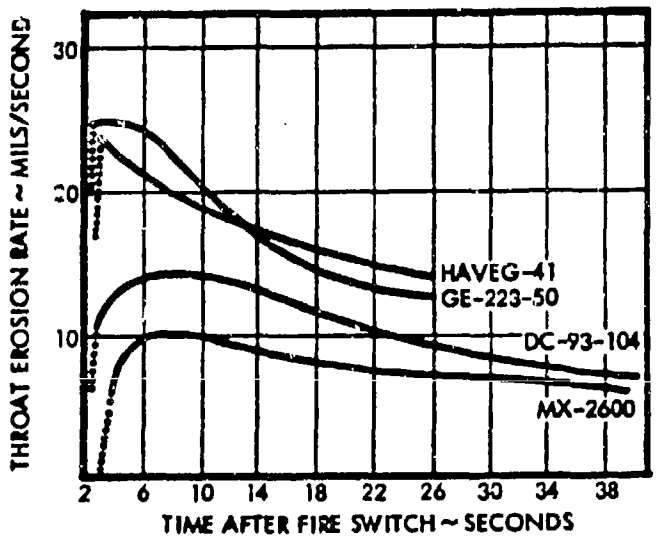

Figure B-13. Instantaneous Throat Erosion Rate for Four Best Performing Ablative Materials (U)

Table VII. Subscale Chamber Liner Materials Evaluation Program Ablative Test Results for the Candidate Materials (U)

Material	Steady State Ablation Surface Temperature (°F)	Effective Heat of Ablation (Btu/lbm)
MX-2600	3340	2400
DC-93-104	3200	1600
HAVEG-41	2880	1000
GE-223-50	3130	875

3.3.1 MX-2600 Silica-Phenolic (Fiberite Corporation)

(U) The MX-2600 silica phenolic ablative liner is shown in Figure B-14. The silica fabric was oriented 60 degrees to the center line of the chamber. The billet was cured at 320°F and a maximum pressure of 5000 psia. The internal chamber contour was machined and the billet was secondarily bonded to the steel sleeve.

(U) Figure B-15 shows the post-test condition of the MX-2600 ablative liner. The test duration was 37 seconds, during which time the measured head end chamber pressure dropped from 205 to 132 psia. The test was terminated prematurely because of possible danger to the test hardware.

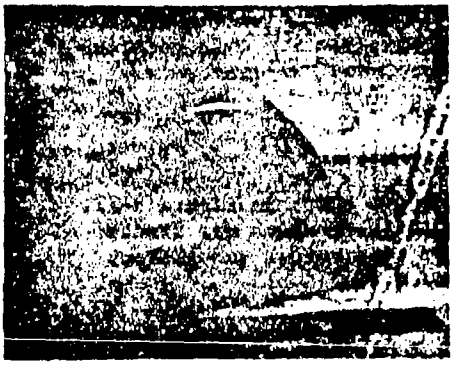

Figure B-14. MX-2600 Silica Phenolic Ablative Liner Before Testing (U)

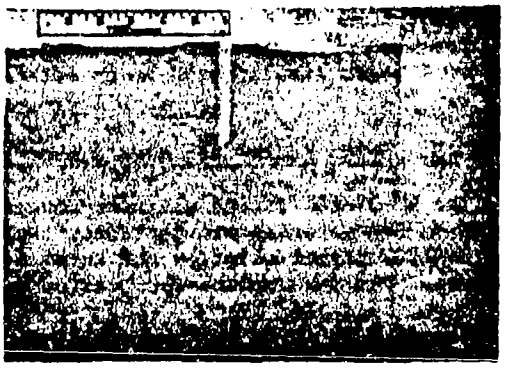

Figure B-15. MX-2600 Silica Phenolic Ablative Liner After Testing (U)

(U) Figure B-16 shows the post-test profile of the MX-2600 liner. This profile is in line with the injector fuel inlet fitting and is representative of the average ablative performance for all materials except the HAVEG-41F. Figure B-17 shows the circumferential variations in throat erosion for this liner. The surface regression rate measured from this photograph is $7.3 \pm \frac{1.3}{3.0}$ mils/second.

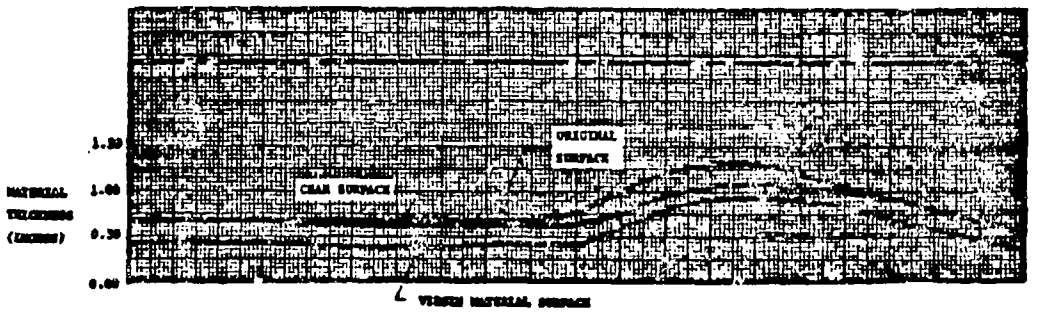

Figure B-16. Surface and Char Profiles for MX-2600 Ablative Liner Test (total on time was 37 seconds) (U)

(U) Figure B-18 shows (1) the measured head end chamber pressure decay, (2) the corrected nozzle stagnation pressure decay, (3) the calculated first derivative of the throat radius, and (4) the effective throat radius as a function of time. The effective heat of ablation for this material is 2400 Btu/lbm and is based on an ablation (surface) temperature of 3340°F.

3.3.2 DC-93-104 Filled Silicone Rubber (Dow Corning)

(U) The DC-93-104 filled silicone rubber liner is shown in Figure B-19. The DC-93-104 material was cast into the steel sleeve which was treated with DC-1200 primer solution and cured at room temperature and ambient pressure. The internal chamber contour was machined.

(U) Figure B-20 shows the post-test condition of the DC-93-104 ablative liner. The test duration was 40 seconds during which time the measured head end chamber pressure dropped from 204 to 114 psia.

(U) Figure B-21 shows the post-test profile of the DC-93-104 liner as measured in line with the injector fuel inlet. The circumferential variation in throat erosion is shown in Figure B-22. The surface regression rate measured from this photograph is $10.0 \pm \frac{4}{5}$ mils/second.

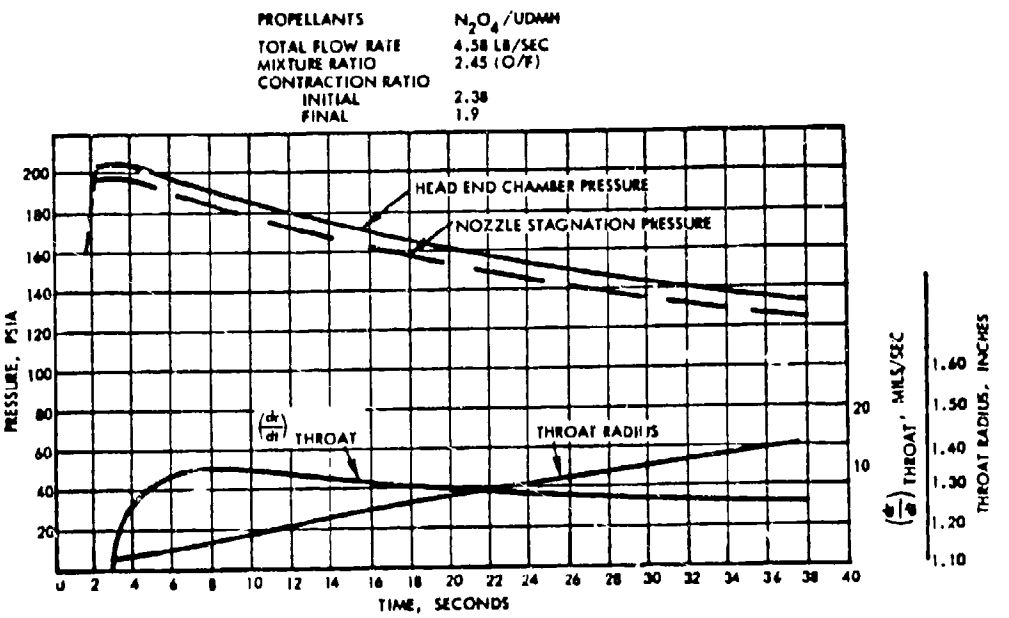

Figure B-18. MX-2600 (60° to ℄) Ablative Liner Material Evaluation Test Results (HAI-494) (U)

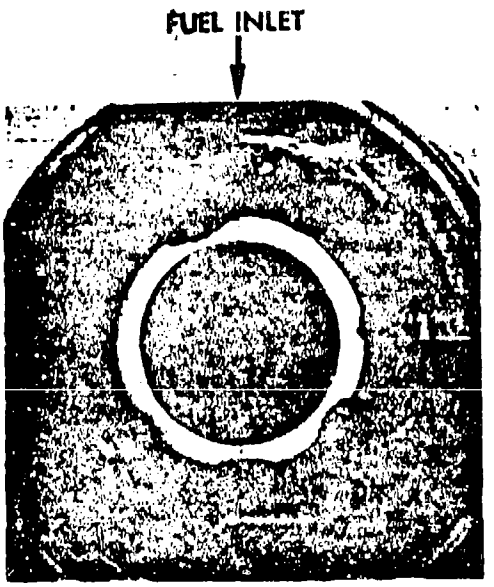

Figure B-17

MX-2600 Silica Phenolic Ablative Liner Throat Profile. Shaded area is the initial throat profile (diameter = 2.25 inches). Test duration was 37 seconds with 4.5 lb/sec total flow rate at a mixture ratio of 2.4(N_2O_4/UDMH). The average throat erosion as measured from this photograph was 7.3 mils/second. (U)

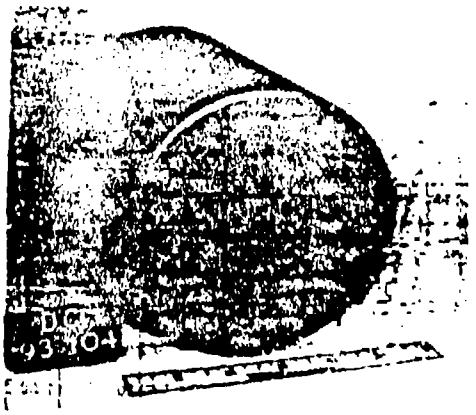

Figure B-19. DC-93-104 Filled Silicone Rubber Ablative Liner Before Testing (U)

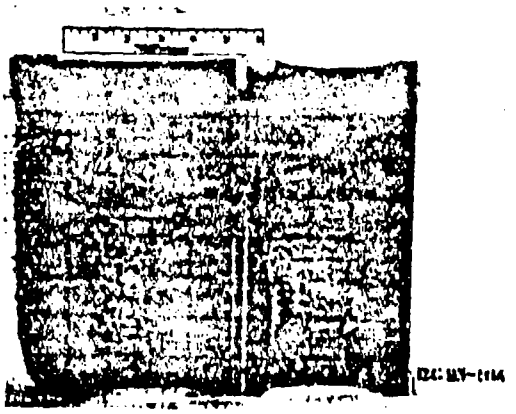

Figure B-20. DC-93-104 Filled Silicone Rubber Ablative Liner After Testing (U)

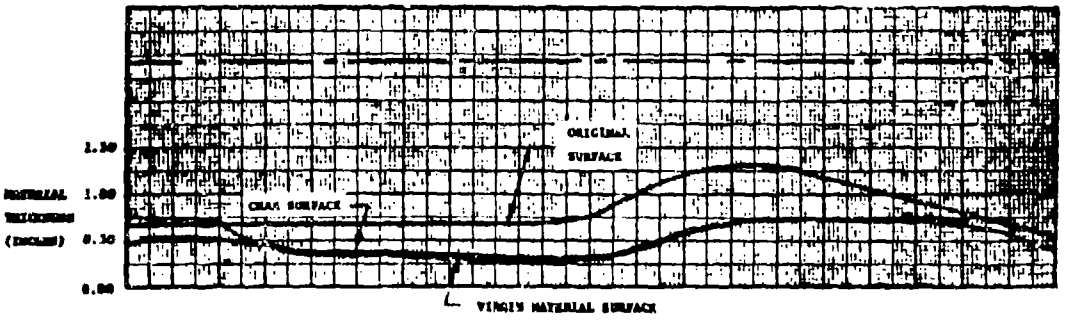

Figure B-21. Surface and Char Profiles for DC-93-104 Ablative Liner Test (total on time was 39.4 seconds) (U)

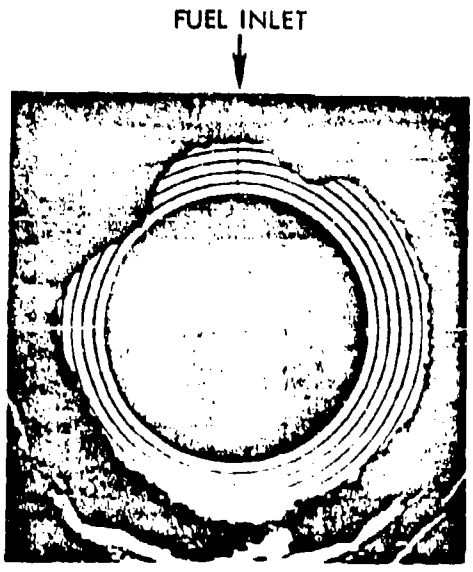

Figure B-22

DC-93-104 Filled Silicone Rubber Ablative Liner Throat Profile. Shaded area in the initial throat profile (diameter 2.25 inches). Test duration was 40 seconds with 4.5 lb/sec total flow rate at a mixture ratio of 2.4 (N_2O_4/UDMH). The average throat erosion as measured from this photograph was 10 mils/sec. (U)

(U) Figure B-23 shows (1) the measured head end chamber pressure decay, (2) the corrected nozzle stagnation pressure decay, (3) the calculated first derivative of the throat radius, and (4) the effective throat radius as a function of time. The effective heat of ablation for this material is 1600 Btu/lbm and is based on an ablation temperature of 3200°F.

3.3.3 HAVEG-41 Asbestos-Phenolic (Haveg Industries)

(U) The HAVEG-41 asbestos-phenolic ablative liner is shown in Figure B-24. The material was compression molded at 200 psi and 300°F. The internal chamber contour was machined and the billet was secondarily bonded to the steel sleeve.

(U) Figure B-25 shows the post-test condition of the HAVEG-41 ablative liner. The test duration was 25 seconds during which time the measured head end chamber pressure dropped from 199 psia to 110 psia.

(U) Figure B-26 shows the post-test profile of the HAVEG-41 liner as measured in line with the injector fuel inlet. The circumferential variation in throat erosion is shown in Figure B-27. The surface regression rate measured from this photograph is 18^{+4}_{-11} mils/second.

(U) Figure B-28 shows (1) the measured head end chamber pressure decay, (2) the corrected nozzle stagnation pressure decay, (3) the calculated first derivative of the throat radius, and (4) the effective throat radius as a function of time. The effective heat of ablation for this material is 1000 Btu/lbm and is based on an ablation temperature of 2880°F.

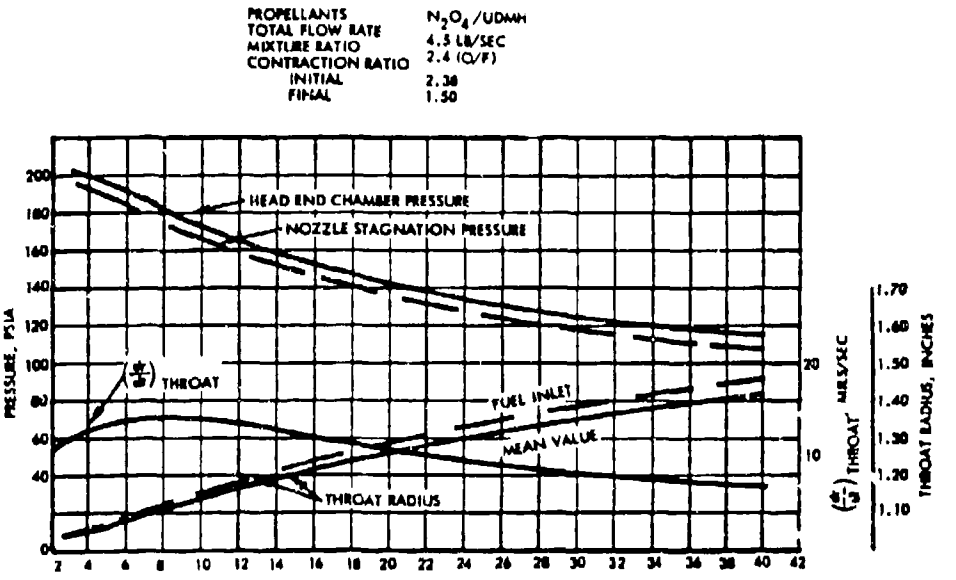

Figure B-23. DC-93-104 Filled Silicone Rubber Ablative Liner Material Evaluation Test Results (U)

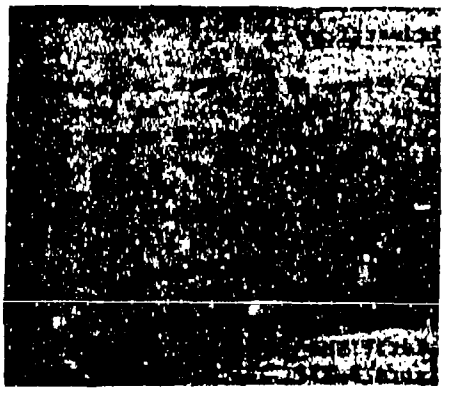

Figure B-24. HAVEG-41 Asbestos Phenolic Ablative Liner Before Testing (U)

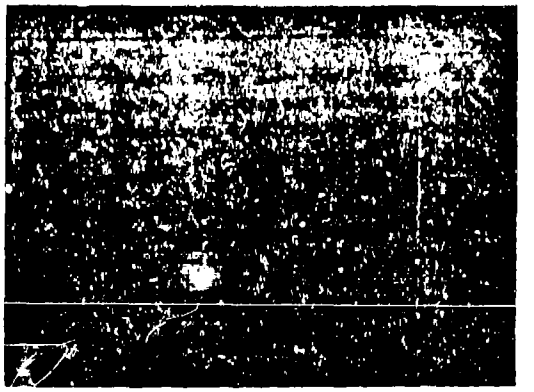

Figure B-25. HAVEG-41 Asbestos Phenolic Ablative Liner After Testing (U)

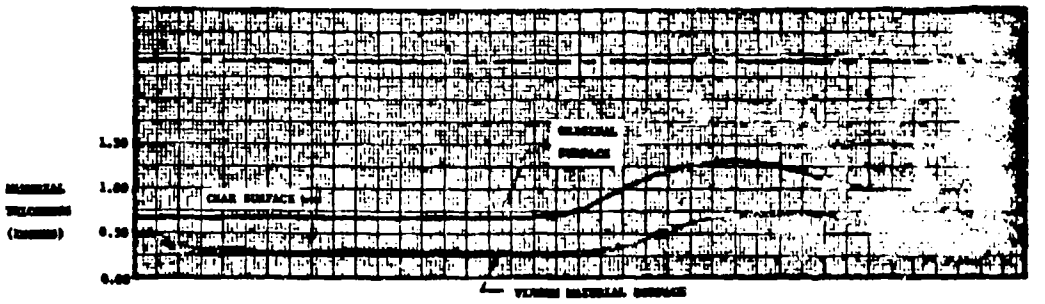

Figure B-26. Surface and Char Profiles for HAVEG-41 Ablative Liner Test (total on time was 24.9 seconds) (U)

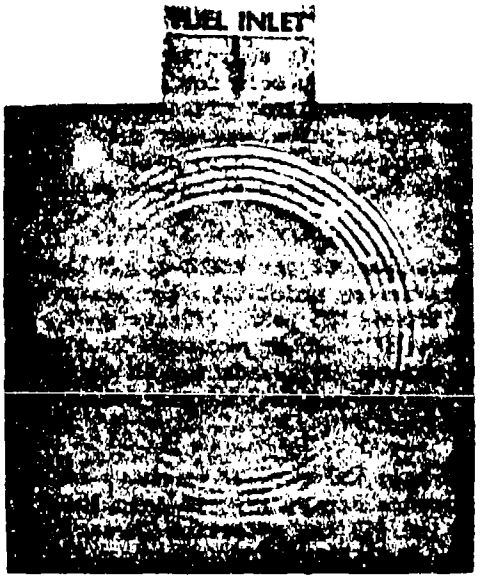

Figure B-27

HAVEG-41 Asbestos Phenolic Ablative Liner Throat Profile. Shaded area is the initial throat profile (diameter 2.25 inches). Test duration was 25 sec with 4.5 lb/sec total flow rate at a mixture ratio of 2.4 (N_2O_4/UDMH). The average throat erosion as measurdd from this photograph was 18 mils/sec. (U)

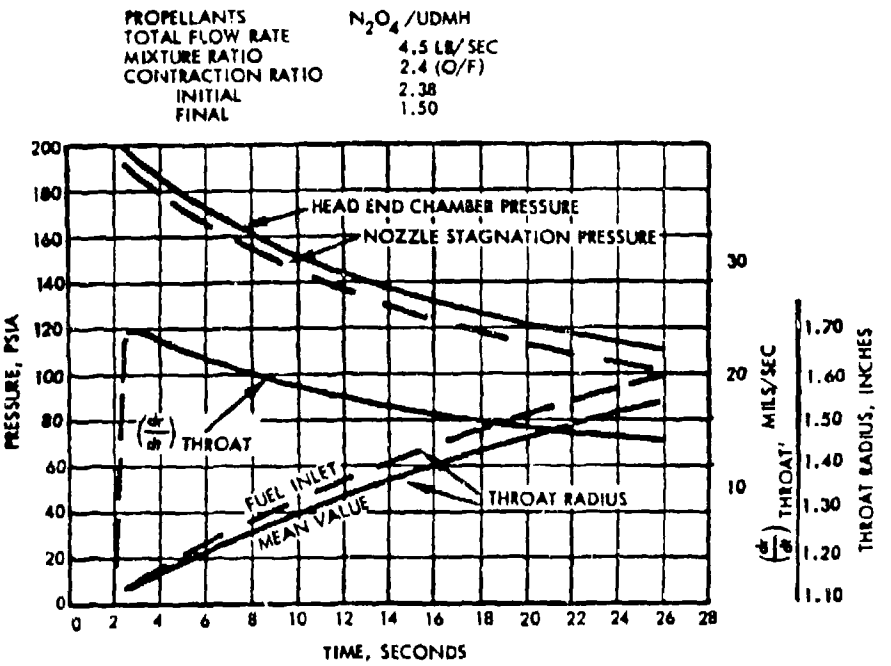

Figure B-28. HAVEG-41 Asbestos Phenolic Ablative Liner Material Evaluation Test Results (U)

3.3.4 HAVEG-41F Asbestos-Phenolic (Haveg Industries)

(U) The HAVEG-41F asbestos phenolic ablative liner is shown in Figure B-29. The steel sleeve, was sandblasted and used as an open mold for curing the HAVEG-41F material at room temperature and ambient pressure. The liner bonded to the sleeve during cure; however, the bond was weak and failed during machining of the internal contour. Isolated voids were uncovered during this machining process and were patched with the parent material.

(U) Figure B-30 shows the post-test condition of the HAVEG-41F ablative liner. The test duration was 17 seconds during which time the measured head end chamber pressure dropped from 203 to 105 psia. Figure B-31 shows the post-test profile of the HAVEG-41F liner as measured in line with the injector fuel inlet. The circumferential variation in throat erosion is shown in Figure B-32. The surface regression rate measured from this photograph is $24.5^{+3.3}_{-3.3}$ mils/second.

(U) Figure B-33 shows (1) the measured head end chamber pressure decay, (2) the corrected nozzle stagnation pressure decay, (3) the calculated first derivative of the throat radius, and (4) the effective throat radius as a function of time.

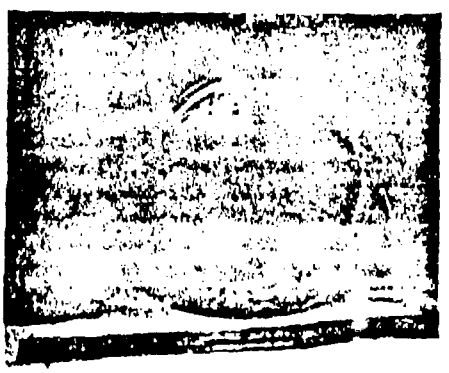

Figure B-29. HAVEG-41F Asbestos Phenolic Ablative Liner Before Testing (U)

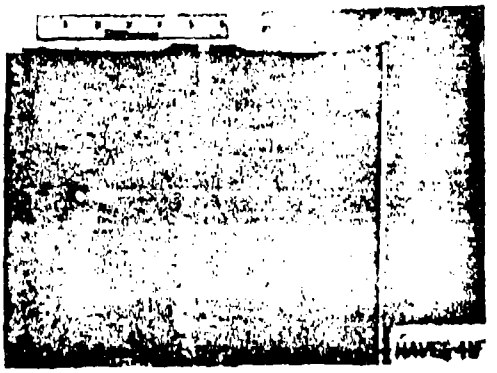

Figure B-30. HAVEG-41F Asbestos Phenolic Ablative Liner After Testing (U)

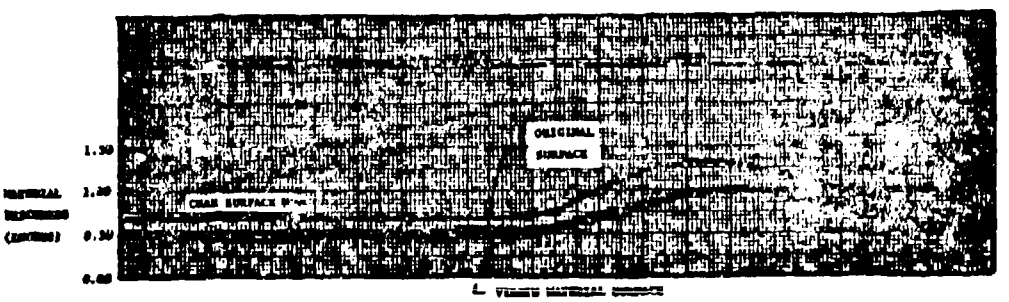

Figure B-31. Surface and Char Profiles for HAVEG-41F Ablative Liner Test (total on time was 17 seconds) (U)

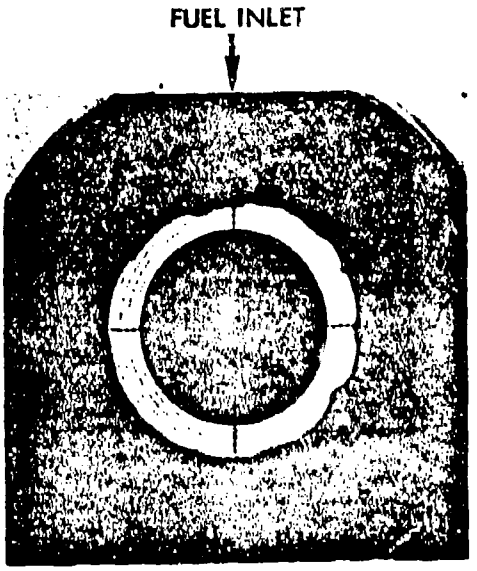

Figure B-32

HAVEG-41F Asbestos Phenolic Ablative Liner Throat Profile. Shaded area is the initial throat profile (diameter 2.25 inches). Test duration was 18 seconds with 4.5 lb/sec total flow rate at a mixture ratio of 2.4 (N_2O_4/UDMH). The average throat erosion as measured from this photograph was 24.5 mils/second. (U)

PROPELLANTS	N_2O_4/UDMH
TOTAL FLOW RATE	4.58 LB/SEC
MIXTURE RATIO	2.4 (O/F)
CONTRACTION RATIO	
INITIAL	2.33
FINAL	1.5

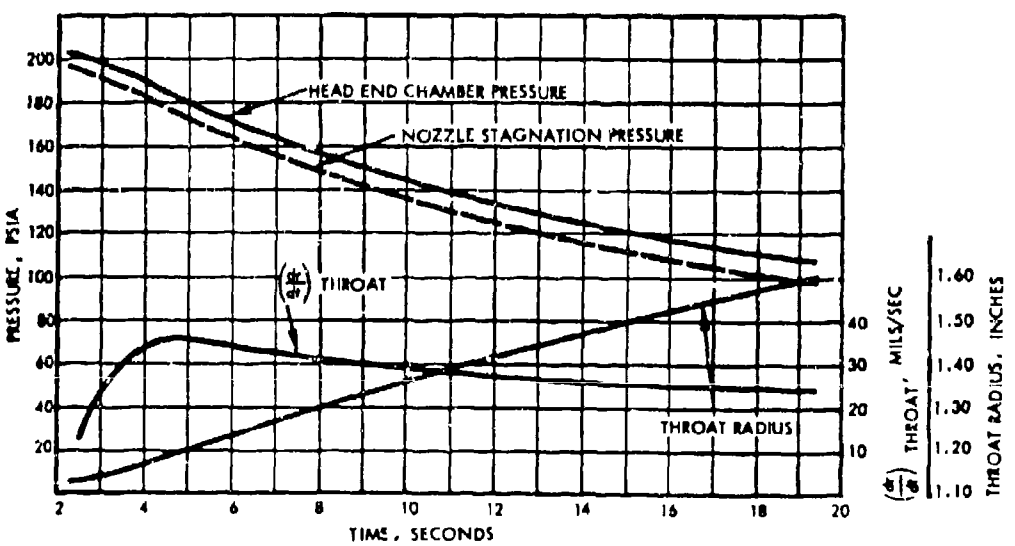

Figure B-33. HAVEG-41F Asbestos Phenolic Ablative Liner Material Evaluation Test Results (U)

3.3.5 GE-223-50 Silica Filled Epoxy Novalak (General Electric Co.)

The GE-223-50 silica epoxy Novalak ablative liner is shown in Figure B-34. The GE-223-50 material was cast into an open mold and cured at room temperature for 16 hours. The cure process was then accelerated by curing at 260°F for 12 hours. The total required cure time at room temperature is approximately 48 hours. The liner was secondarily bonded to the steel sleeve with a high temperature epoxy adhesive. The internal contour was machined which uncovered a pocket of partially cured material in the chamber section. The specimen was tested in this condition.

(U) Figure B-35 shows the post-test condition of the GE-223-50 ablative liner. The test duration was 24 seconds during which time the measured head end chamber pressure dropped from 200 to 112 psia. Figure B-36 shows the post-test profile of the GE-223-50 liner as measured in line with the injector fuel inlet. The circumferential variation in throat erosion is shown in Figure B-37. The surface regression rate measured from the photograph is 18^{+5}_{-11} mils/second.

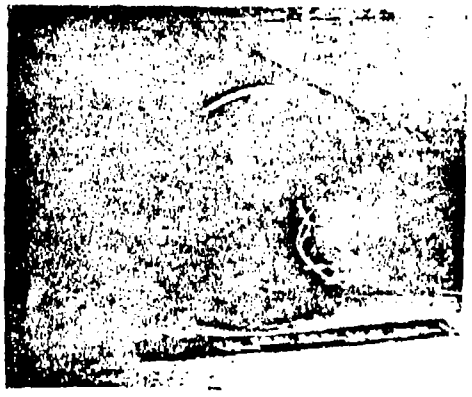

Figure B-34. GE-223-50 Silica Filled Epoxy Novalak Ablative Liner Before Testing (U)

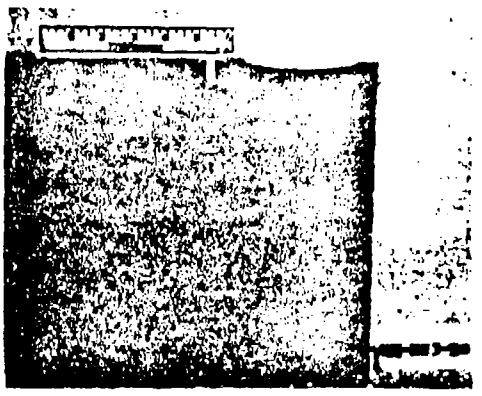

Figure B-35. GE-223-50 Silica Filled Epoxy Novalak Ablative Liner After Testing (U)

(U) Figure B-38 shows (1) the measured head end chamber pressure decay, (2) the corrected nozzle stagnation pressure decay, (3) the calculated first derivative of the throat radius, and (4) the effective throat radius as a function of time. The effective heat of ablation for this material is 875 Btu/lbm and is based on an ablation temperature of 3130°F.

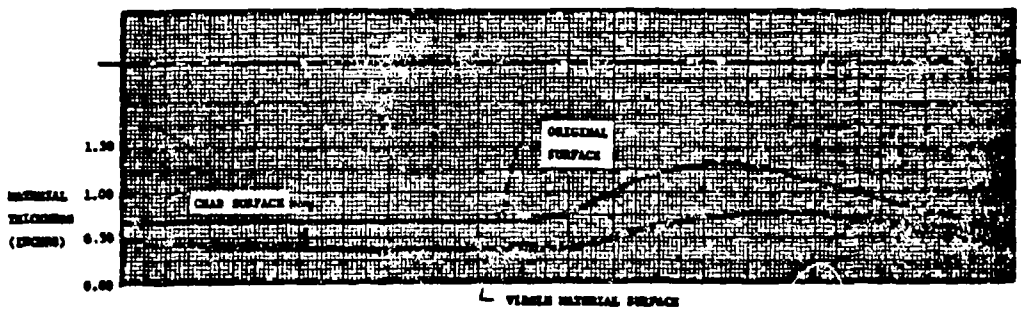

Figure B-36. Surface and Char Profiles for GE-223-50 Ablative Liner Test (total on time was 23.9 seconds) (U)

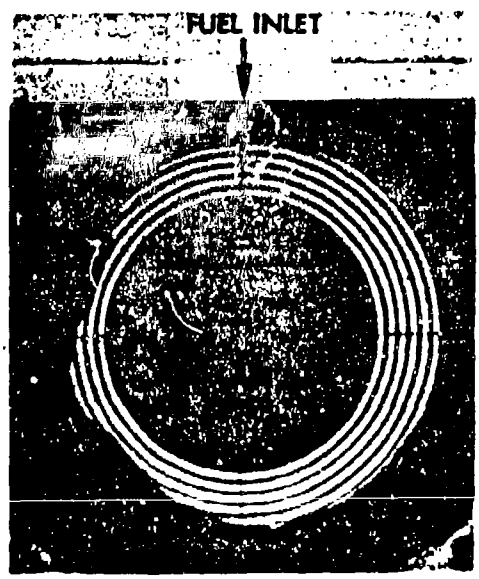

Figure B-37

GE-223-50 Silica Filled Epoxy Novalak Ablative Liner Throat Profile. Shaded area is the initial throat profile (diameter = 2.25 inches). Test duration was 24 seconds with 4.5 lb/sec. total flow rate at a mixture ratio of 2.4 (N_2O_4/UDMH). The average throat erosion as measured from this photograph was 18 mils/second. (U)

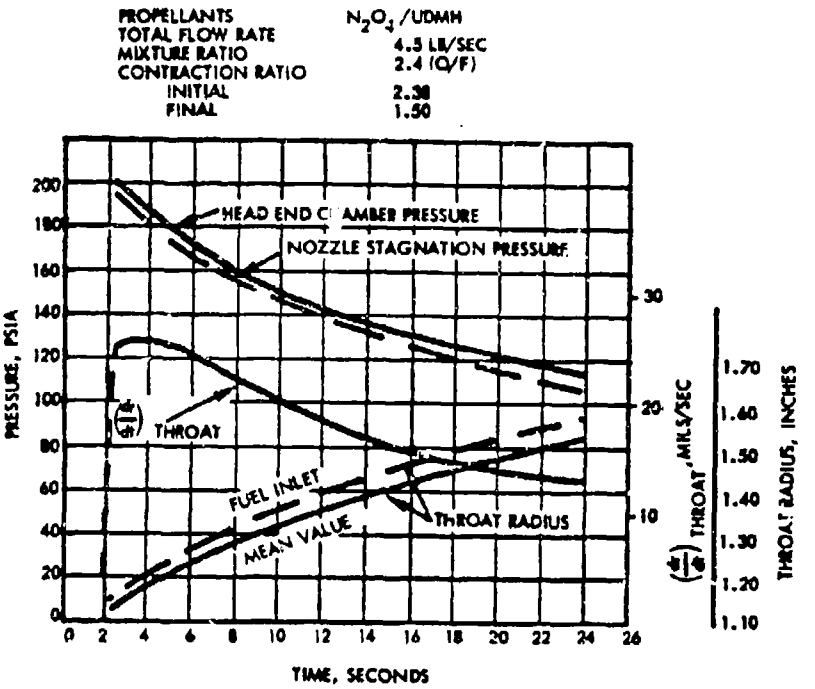

Figure B-38. GE-223-50 Silica Filled Epoxy Novalak Aolative Liner Material Evaluation Test Results (U)

3.3.6 Controlled Chemical Environment Laboratory Torch Tests

3.3.6.1 Experimental Procedure

(U) The experimental approach used was to expose candidate materials to the oxygen/methane torch and record their degradation as a function of time. These data could then be correlated with the samples' compositions to determine faborable combinations of binder and filler. Low erosion of a particular composition could lead to adoption of the material directly or possibly to development of a new product.

(U) Test specimens were machined to 1 1/2-inch diameter by 1 1/2-inch high cylinders. A 3/8-inch-diameter hole was drilled through the longitudinal axis of each sample and the torch flame directed at this hole. Typical test specimens are shown in Figure B-39. Several specimens from each material were prepared in this configuration to provide check data and tests under different conditions.

(U) Figure B-40 is a photograph of the torch testing facility. Although the torch containment vessel may be evacuated or operated with an inert atmosphere, the upper half was left off and these tests were run in an air atmosphere.

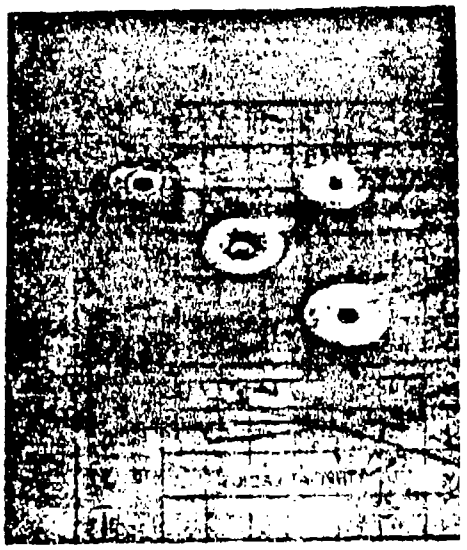

Figure B-39

Photograph of Typical Test Specimens Used for Oxygen/Methane Torch Tests. The samples are machined to cylinders and a 3/8-inch diameter hole bored through to receive the torch flame. Percent weight loss with flame exposure time is calculated, and reported as torch erosion. (U)

(U) To conduct each test, specimens were rapidly swung under the burning torch (shown in a closeup photograph in Figure B-41) which has been positioned prior to lighting the flame, and the timing started. After the required exposure of 1, 3, or 5 minutes, the sample was swung away from the flame impingement zone and allowed to cool. Any remaining flames were snuffed out with a fabric mat. During the exposure, a Pyro Instrument Company Model 95 optical pyrometer was used to measure the sample surface temperatute at the drilled hole opening. This temperature, assumed to be the highest experienced by the sample, is reported in Table VII as the equilibrium surface temperature for that sample. Determination of the heat flux was carried out by using a copper cylinder of the same specimen dimensions fitted with a thermocouple.

(U) A number of programs have been conducted to find a satisfactory low-cost chamber liner composition. Initial TRW engine tests conducted under an IR and D program found four likely candidate materials. These materials, more fully describe in Section 2 are as follows:

- MX-2600, Fiberite Corporation
- DC-93-104, Dow Corning Corporation
- HAVEG-41, Haveg Industries
- GE-223-50, General Electric Company

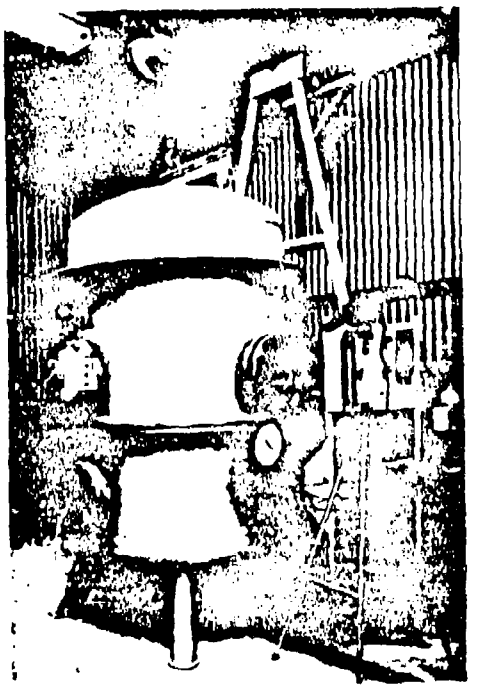

Figure B-40
Laboratory Torch Test Facility (U)

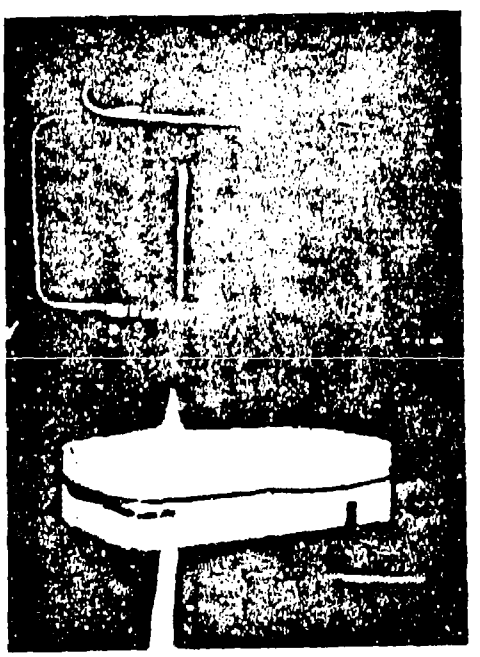

Figure B-41
Torch Test in Progress (U)

Table VIII. Erosion of Test Samples Exposed to O_2/CH_4 Torch for 1 Minute; Ranked in Order of Oxidizer-Rich Erosion Resistance (U)

	Oxidizer-Rich[a]		Fuel-Rich[b]	
Sample	Weight Loss (percent)	Surface Temperature[c] (°C)	Weight Loss (percent)	Surface[c] Temperature (°C)
DC-93-104	2.4	1730	3.0	1650
DC-93-115	2.6	1650	2.8	1580
MX-2600	4.0	1840	3.8	1740
HAVEG-41	8.1	1580	7.8	1560
MXA-150	10.3	1650	8.8	1600
GE-223	10.7	1720	10.3	1630
Ironsides	12.7	1690	13.7	1710
Plastonium	14.5	1975	14.0	1600
DE-67-22	15.5	1710	13.2	1605
ESM-1035[d]	16.8	1650	21.3	1655

[a] Flame temperature = 2670°C.

[b] Flame temperature = 2050°C.

[c] Optical pyrometer measurement.

[d] Small-sized sample.

(U) A similar program conducted by the AFRPL has shown the following materials, among others, to be attractive candidates:

- MXA-150, Fiberite Corporation
- Plastonium, Insulation Systems Incorporated
- Ironsides DP5-160, Ironsides Resins Incorporated

(U) In all, a total of 12 materials have been tested. The behavior of the above seven materials is described in the following section.

3.3.6.2 Test Results

(U) Temperatures at the flame impingement surface were measured by optical pyrometer and appear to be reproducible within ±20°C (±1 percent). This observed temperature is considered to be the maximum attained under the test conditions and is essentially the ablation mechanism reaction temperature.

(U) Additional information was obtained by weighing each specimen to the nearest milligram before and after exposure. In this way, erosion, as a result of the flame exposure, could be calculated for each specimen. Results are reported on a percent by weight basis. However, as the candidates' specific gravity values are all between 1.4 and 1.7 (with one exception, Plastonium, with a specific gravity of 0.8) these data are also reasonably comparable to percent by volume. Inherent in the erosion loss results are weight losses due to volatile products from below the char barrier. Although not actually shear-induced erosion, these losses are also a significant factor in determining the ablative and insulative properties of a material and are an appropriate component of the data.

(U) Figure B-42 shows the samples of the four candidate materials from the TRW IR&D materials evaluation program. Figure B-43 shows the samples of the three candidate materials from the AFRPL "in-house" test program.

(U) Four of the candidate materials were each tested at three flame exposures times--1, 3, and 5 minutes. Plots of erosion losses versus time gave relatively smooth curves as in Figure B-44. The curves defining this relationship are expected as the post-test specimens each had a significantly thick "wall" remaining. A sharp deflection in the erosion loss versus time curve could occur if the sample was inhomogeneous or if the wall decreased its heat sink function. Apparently neither was the case.

(U) Both oxidizer-rich and fuel-rich torch conditions were used in testing each sample. In the laboratory experiments, torch flame temperature varied from 2050°C for the fuel rich condition to 2670°C for the oxidizer rich condition. The expected flame condition in the engine is between 2000°C and 2200°C. Figure B-44 shows that generally faster erosion rates were obtained under oxidizer-rich conditions than with fuel-rich conditions. This was expected due primarily to the 620°C increase

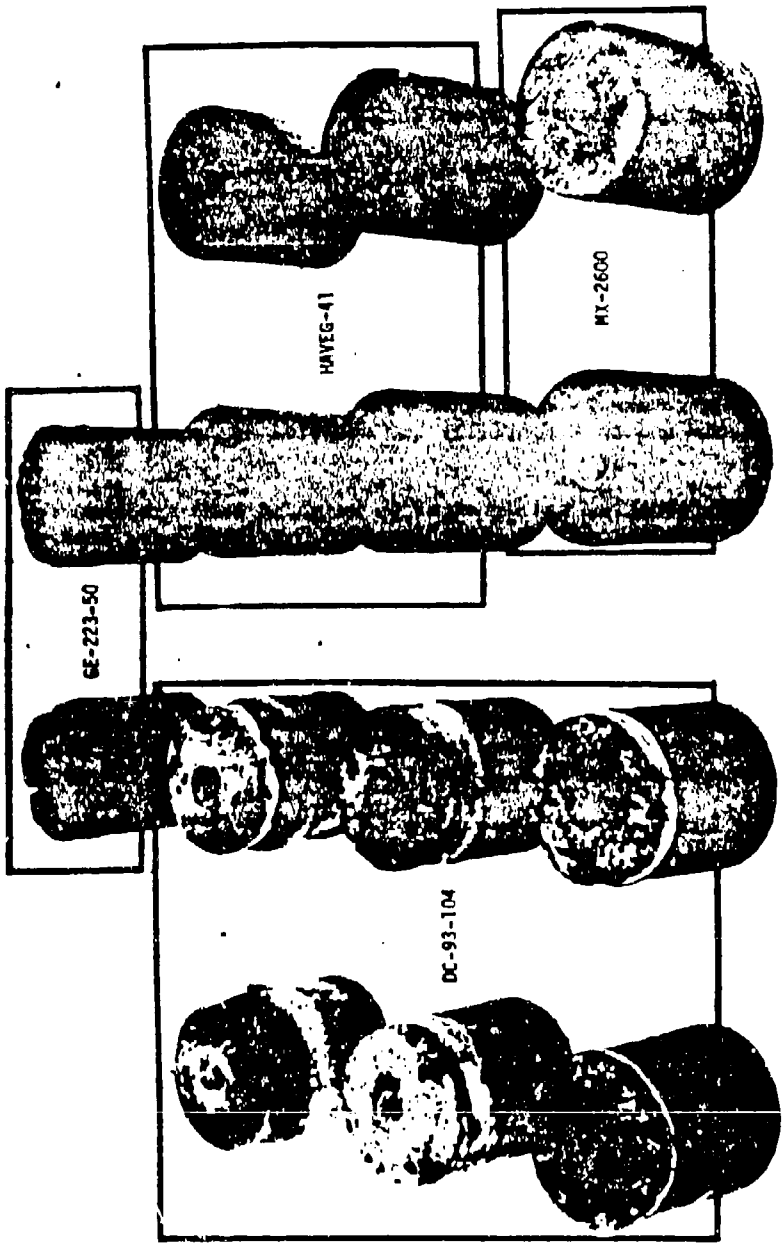

Figure B-42. Samples of Low-Cost Chamber Liner Materials Used in TRW Engine Tests (U)

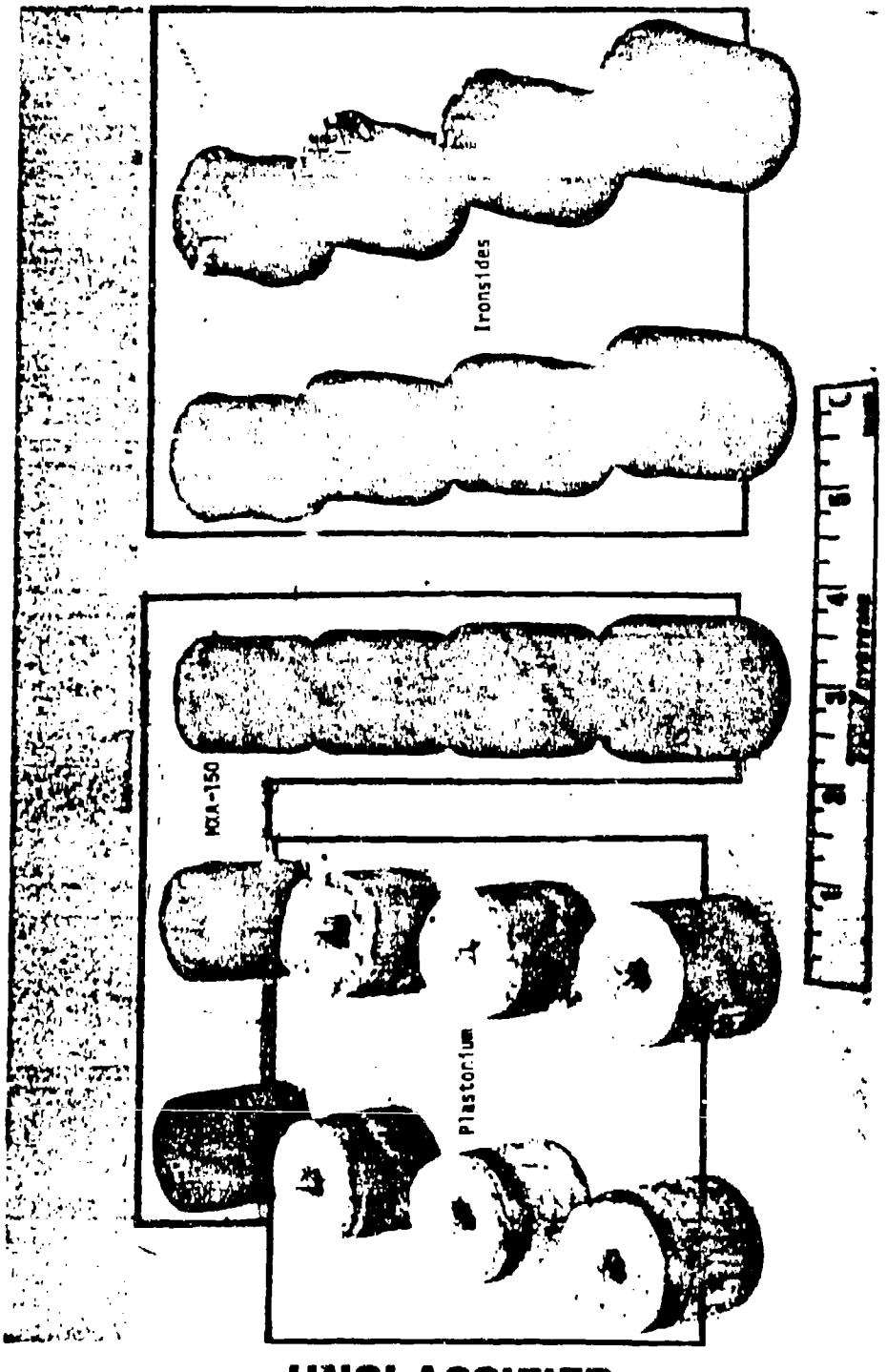

Figure B-43. Samples of Chamber Liner Materials Used in Air Force Tests at Edwards Air Force Base (U)

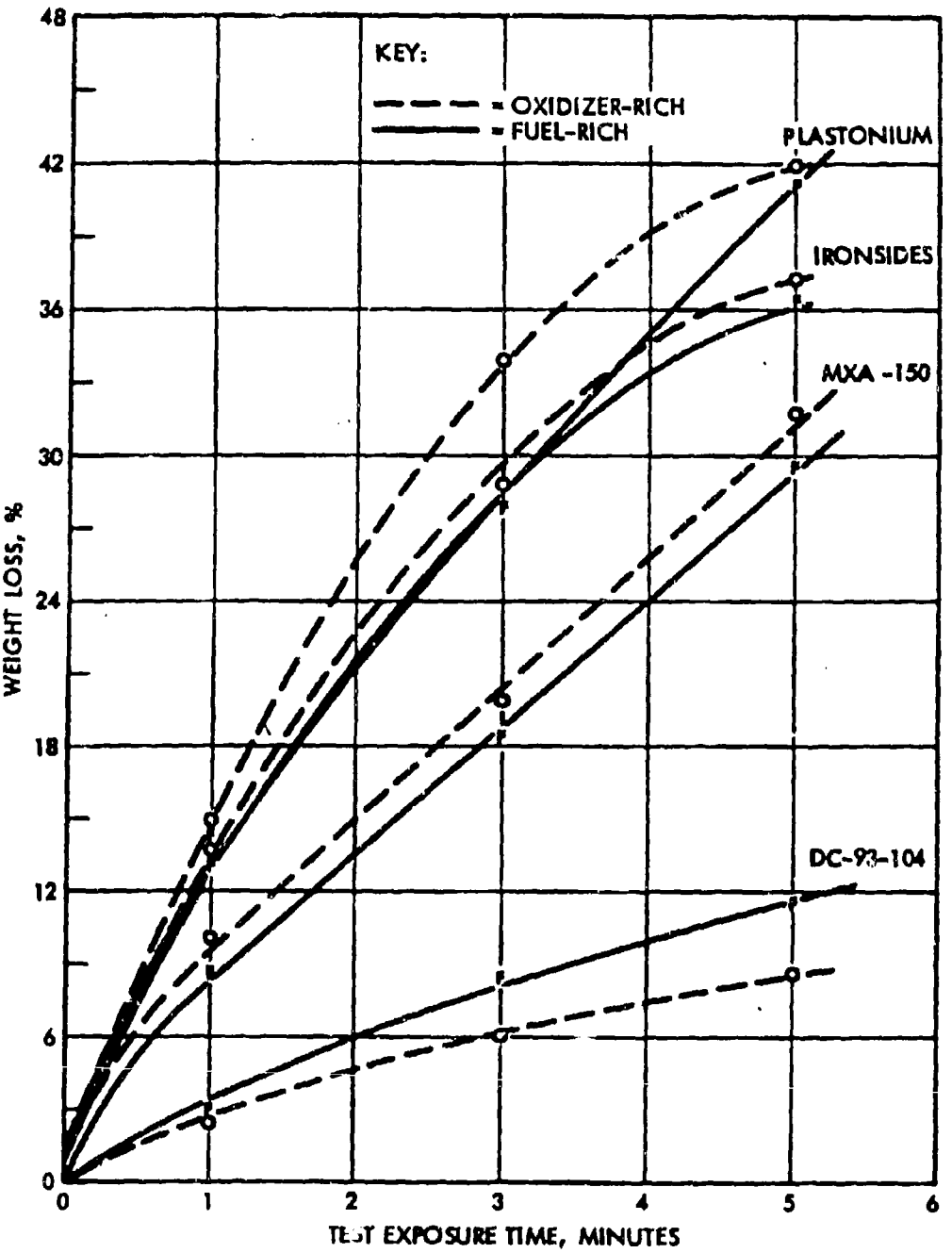

Figure B-44. O_2/CH_4 Torch Test Erosion Results (U)

(U) in flame temperature. One notable exception to this observation was found with the DC-93-104 material.

(U) The most significant result from this test series was the excellent performance of the filled silicone compounds. The weight loss for both the DC-93-104 and DC-93-115 (a low flow version of DC-93-104) was less than the weight loss for the MX-2600 silica-phenolic material.

(U) Low weight losses found for the DC-93-104/DC-93-115 samples indicate that the major products of high-temperature reactions are nonvolatile. However, the low quantities of volatiles produced serve to thermally insulate the samples' surface. Ablation temperatures of the surface exposed to the flame were similar to the other materials tested in oxidizer (1650° to 1730°C) and fuel-rich (1580° to 1650°C) environments. Because of the samples' low erosion rates and the fact that polysiloxanes retain some strength at 3900°C, the observed good results for these materials are thought to be caused by:

(1) The absence of large amounts of volatile products from endothermic filler and polymer interactions

(2) Inherent stability of the polymeric binder at the test temperature

(U) Figures B-45 through B-70 shows the post-test specimens of the seven primary material candidates. The photographs are somewhat deceiving in that the more erosion-resistant materials are most unsightly while some of the least erosion-resistant materials appear unmarked. The following observations of two of the test specimens will aid in evaluation of the photographs.

(U) The DC-93-104 samples suffered greater erosion damage on the outer surface than adjacent to the drilled hole. These samples swelled during the test which caused the hole diameter to shrink and the flame to spill around the outside of the sample. DC-93-104, a room temperature cure (RTV) material, swelled and distorted. A white coating, assumed to be SiO_2, deposited on the samples. The flame-impacted surface was fractured in an irregular pattern as if this reaction relieved internal stresses.

(U) Plastonium samples were deceptive in that very slight dimensional changes were found despite the high erosion losses. Strain cracks were few in number, but deep. Because these cracks appeared fresh and not "polished," it appears as though the cracks might have been formed during the post-test cooling period. Of the samples tested, Plastonium had the most obvious hole enlargement which conically tapered from the flame impingement surface. Compared with the other materials, Plastonium is structurally weak. The samples emerged snow white with flecks of black, indicating high volumes of filler and low volumes of carbonaceous phenolic binder were present, a condition leading to a weak material.

MX-2600 Oxidizer-Rich 60-Second Exposure (U)
Figure B-45

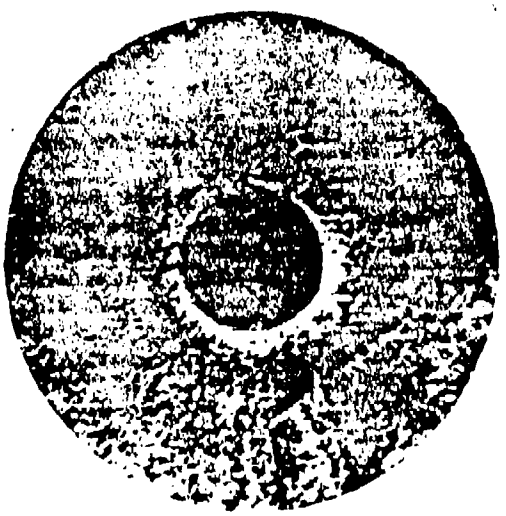

MX-2600 Fuel-Rich 60-Second Exposure (U)
Figure B-46

Haveg-41 Oxidizer-Rich 60-Second Exposure (U)
Figure B-47

Haveg-41 Fuel-Rich 60-Second Exposure (U)
Figure B-48

DC-93-104 Oxidizer-Rich 60-Second Exposure (U)

Figure B-49

DC-93-104 Fuel-Rich 60-Second Exposure (U)

Figure B-50

DC-93-104 Oxidizer-Rich 300-Second Exposure (U)

Figure B-51

DC-93-104 Fuel-Rich 300-Second Exposure (U)

Figure B-52

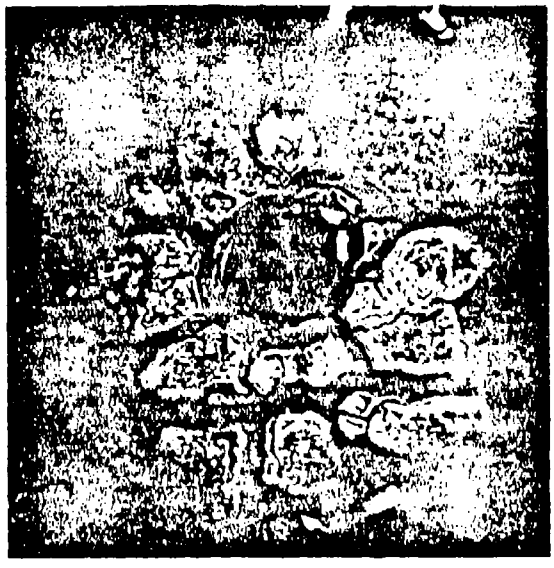

GE-223-50 Oxidizer-Rich 60-Second Exposure (U)
Figure B-53

GE-223-50 Fuel-Rich 60-Second Exposure (U)
Figure B-54

Ironsides Oxidizer-Rich 60-Second Exposure (U)

Figure B-55

Ironsides Fuel-Rich 60-Second Exposure (U)

Figure B-56

Ironsides Oxidizer-Rich 120-Second Exposure (U)

Figure B-57

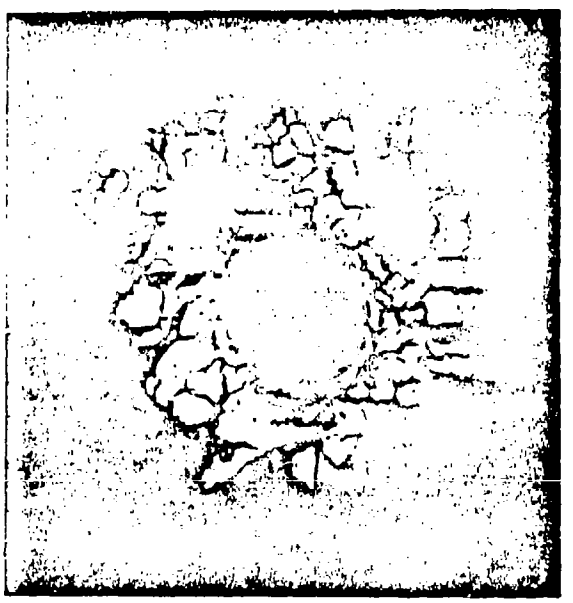

Ironsides Fuel-Rich 120-Second Exposure (U)

Figure B-58

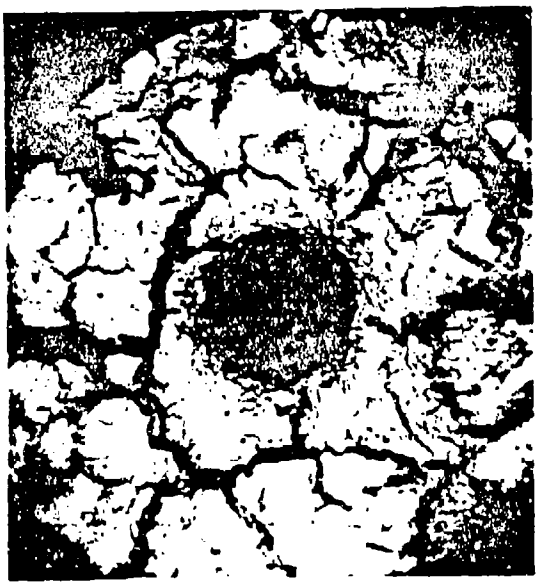

Ironsides Oxidizer-Rich 300-Second Exposure (U)

Figure B-59

Ironsides Fuel-Rich 300-Second Exposure (U)

Figure B-60

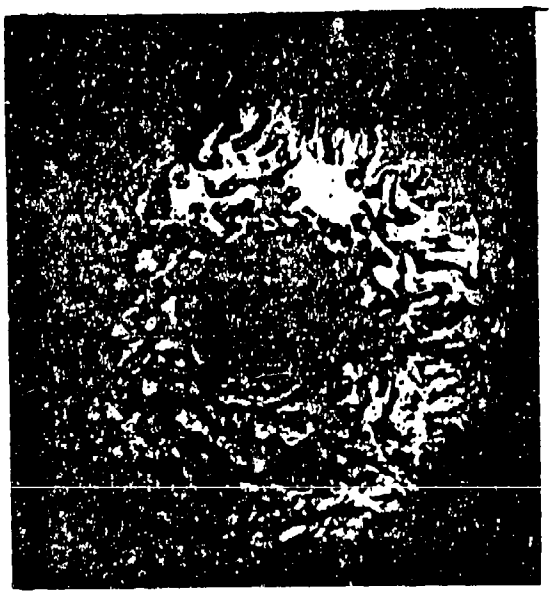

MXA-150 Oxidizer-Rich 60-Second Exposure (U)

Figure B-61

MXA-150 Fuel-Rich 60-Second Exposure (U)

Figure B-62

MXA-150 Oxidizer-Rich 180-Second Exposure (U)

Figure B-63

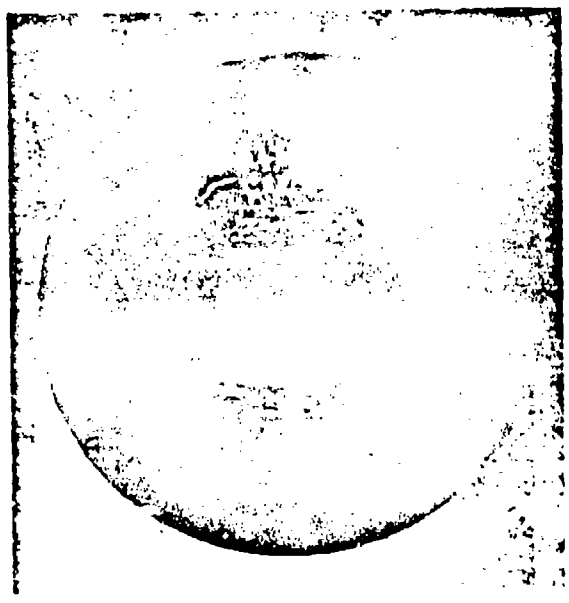

MXA-150 Fuel-Rich 180-Second Exposure (U)

Figure B-64

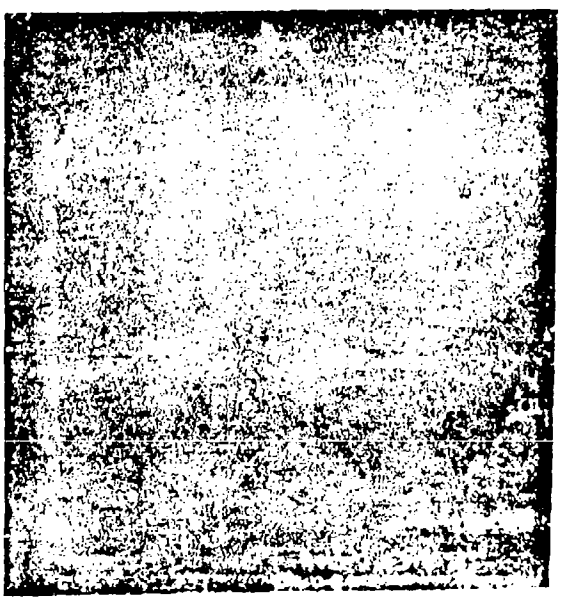

MXA-150 Oxidizer-Rich 300-Second Exposure (U)

Figure B-65

MXA-150 Fuel-Rich 300-Second Exposure (U)

Figure B-66

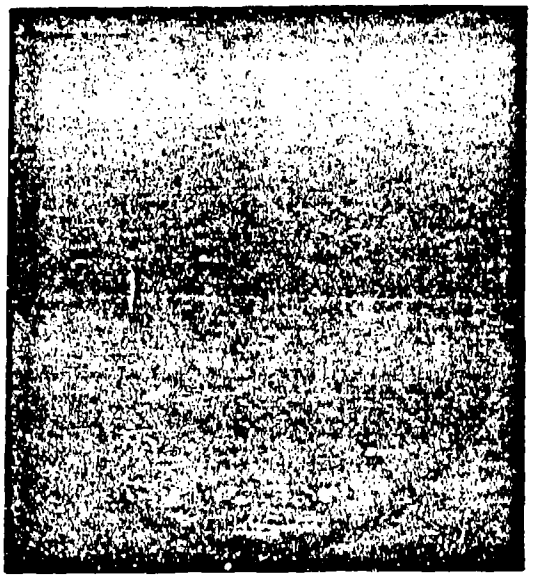

Plastonium Oxidizer-Rich 60-Second Exposure (U)

Figure B-67

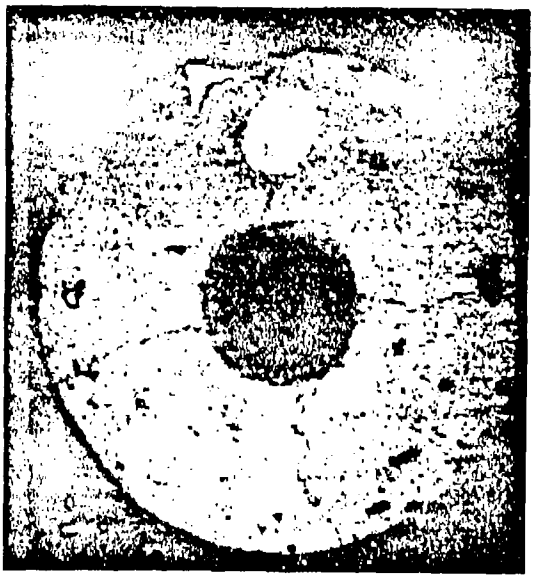

Plastonium Fuel-Rich 60-Second Exposure (U)

Figure B-68

Plastonium Oxidizer-Rich 300-Second Exposure (U)

Figure B-69

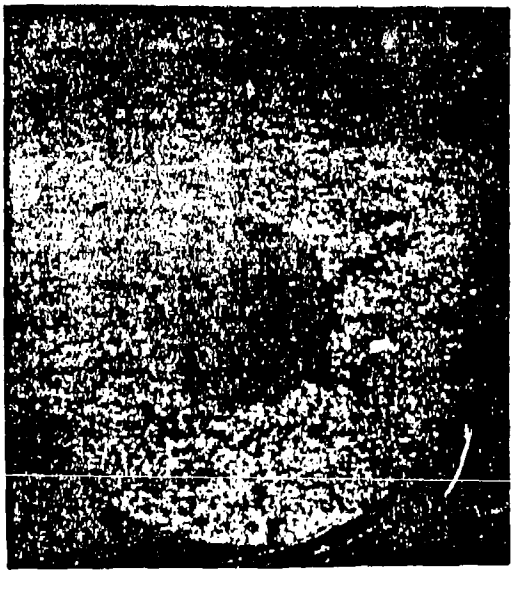

Plastonium Fuel-Rich 300-Second Exposure (U)

Figure B-70

APPENDIX C

ABLATIVE LINER SIZING

1. INTRODUCTION AND SUMMARY

(U) The three ablative liners designed and fabricated in Task II were sized according to procedures given in the following sections. The material thicknesses were determined for a 250,000 lb_f thrust (vacuum) engine operating at 300 psia with the N_2O_4/UDMH propellant combination. The basic data used in sizing the liners was developed in the TRW Systems sub-scale Materials Evaluation Program. This data was correlated using the TRW Systems Charring and Ablation Program (AB054A) which uses the model of Munson and Spindler to determine the dimensional ablation. Finally, the erosion correlations were used to size the 250,000 lb_f thrust (vacuum) ablative liners.

2. SUB-SCALE RESULTS

2.1 RECOVERY TEMPERATURE

(U) Initial sub-scale tests, which were made with a heat sink chamber, indicated that the 1500 pound thruster operated at a recovery temperature that was representative of a streaking condition. Initial data from Mammac surface thermocouples were reduced using the TRW Heat Flux Data Analysis Program (HFDAP). HFDAP computes the heat flux from the product of the thermal conductivity (k) and the temperature gradient at the wall (dT/dr) from the following equation:

$$\dot{Q}/A = -k \left[\frac{dT}{dr}\right]_{wall} \tag{1}$$

The temperature distribution through the wall as a function of time is obtained from the numerical solution of the thermal diffusion equation,

$$\rho C_p \frac{\partial T}{\partial \theta} = \frac{\partial}{\partial r}\left(k \frac{T}{r}\right) + \frac{k}{r} \frac{dT}{\partial r} \tag{2}$$

This form of the diffusion equation considers radial conduction only. The boundary conditions are the measured wall temperatures.

(U) A typical surface temperature response at the throat is shown in Figure C-1 and the corresponding heat flux is shown in Figure C-2. Data from this test indicated a throat recovery temperature of approximately 4850°F. This temperature was used in the subsequent ablation correlations to obtain the effective heats of ablation of each of the materials. In addition the surface was assumed to ablate at a temperature of approximately 3200°F. The heat transfer coefficients were determined using the simplified Bartz equation.

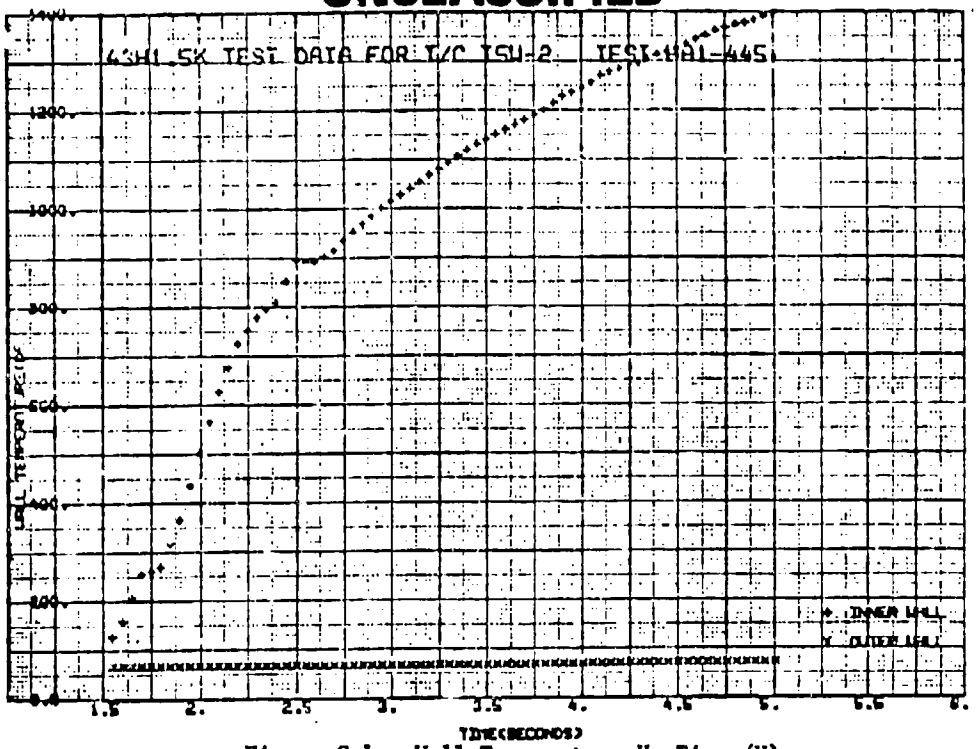

Figure C-1. Wall Temperature Vs Time (U)

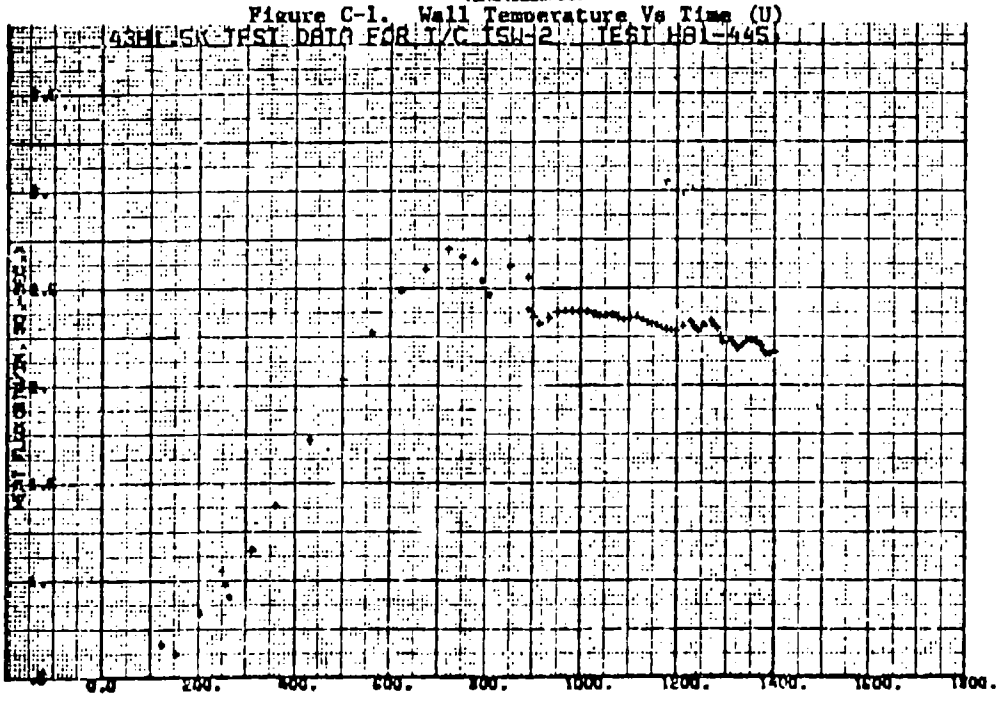

Figure C-2. Heat Flux Vs Inner Wall Temperature (°F) (U)

2.2 EROSION CORRELATION

2.2.1 Model

(U) Using the erosion and heat flux data from the sub-scale Materials Evaluation Program, correlations were made to determine the effective erosion characteristics of four candidate materials for the 250K thrust chamber. These correlations were generated using the TRW Charring and Ablation Program (AB054A) which approximates the charring phenomenon by an Arrhenius rate equation of the form

$$\frac{\partial \rho_a}{\partial \theta} = -\delta \rho_a^{\beta} e^{-\frac{\Gamma}{T}} \qquad (3)$$

where:

θ = time

ρ_a = density of the decomposable resin

T = temperature

δ, β, Γ = Arrhenius rate constants (determined experimentally)

The dimensional ablation is determined by using the erosion model of Munson and Spindler where the erosion rate can be specified by an analytical relationship, or calculated from the heat balance on the surface nodes. When the erosion rate is specified, the rate is given by

$$\dot{S} = H + UT^{V} e^{-\frac{Y}{T}} \qquad (4)$$

where:

H = heat of sublimation or reaction

T = surface temperature

U, V, Y = empirical erosion constants

In general, at the beginning of heating, the surface recession rate is given by equation 2 as a function of the surface temperature T. Upon reaching some critical temperature, such as the sublimation or melt point, the surface is then held at a constant temperature T_s as long as the heat input is sufficient to hold it at this temperature.

(U) For a thrust chamber operating at the high heat fluxes associated with chamber pressures in the order of 300 psia, the transient heat-up time for the surface temperature to reach the constant ablation temperature is relatively short. For run times in the order of 100 seconds, this transient surface temperature time is an negligible fraction of the total burn time.

(U) For the rate of heat absorbed by ablation can either be approximated by a constant surface erosion rate from equation 2) where

$$\dot{S} = H + UT_s^V e^{-\frac{Y}{T_s}} = \text{Constant at } T_s \qquad (5)$$

or the surface erosion rate can be approximated by solving the heat balance equation at the surface given by

$$-k \frac{\partial T}{\partial x} = \left[(\text{surface heat input}) - (H_{eff}\, \rho_c\, \dot{S})\right] \qquad (6)$$

where:

ρ_c = char density

H_{eff} = effective heat of ablation

The effective heat of ablation, H_{eff} essentially lumps chemical, thermal and mechanical erosion characteristics into one parameter that can be used for correlation purposes when the individual characteristics are not well known.

2.2.2 Results

(U) The experimental sub-scale tests performed during the Material Evaluation Program utilized the 1.5K thruster operated at 190 psia. The geometric size of this chamber and the 190 psia chamber pressure has been shown to yield a shear and thermal environment approximating the environments of the 250,000 lb_f thrust (vacuum) engine. Therefore, effective heats of ablation can be obtained from the experimental erosion rate and the chamber pressure decay of the candidate materials. Figures C-3 and C-4 show the head-end chamber pressure decay and the erosion rate for the candidate materials.

(U) The erosion characteristics of the candidate materials tested in the sub-scale Materials Evaluation Program were correlated using equation (6), the thermal environment from Figure C-2 (4850°), and the erosion data from Figures C-3 and C-4. These correlations are shown in Figure C-5. Subsequent to the sizing of the 250,000 lb_f thrust (vacuum) chamber liners, the surface temperatures of the candidate materials were experimentally determined. The effective heats of ablation shown in the Table of Figure C-5 are those values corresponding to the experimentally determined surface temperatures. The use of 3200°F to obtain the calculated curves in Figure C-5 introduced little or no error in the correlations since maximum surface temperature deviation represents negligible difference in heat up time.

3. LINER SIZING

(U) The primary criteria used to size the 250,000 lb_f thrust ablative liners was a limiting value of 600°F on the chamber back-wall after 120

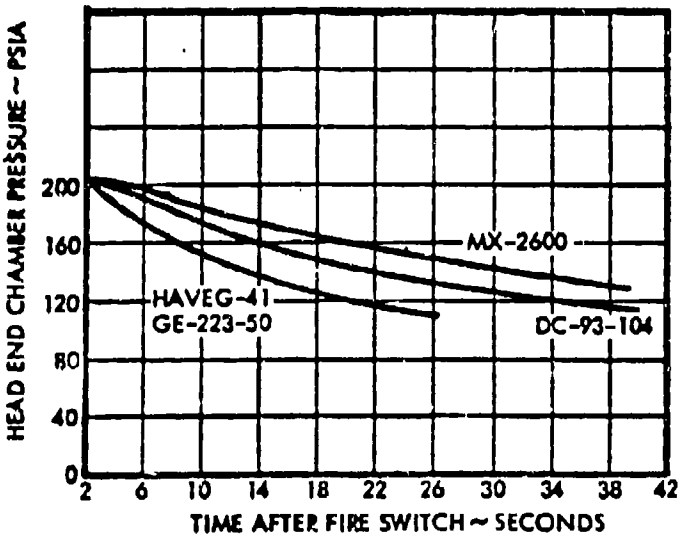

Figure C-3. Measured Head-End Chamber Pressure Decay Rates for Best Performing Ablative Materials (U)

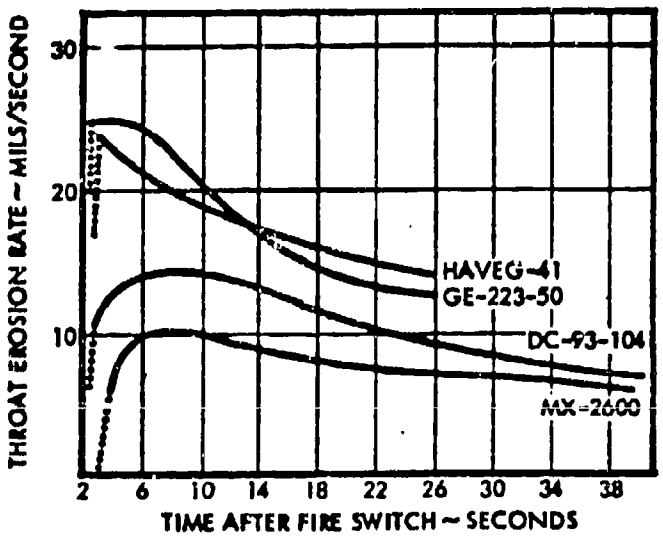

Figure C-4. Instantaneous Throat Erosion Rate for Four Best Performing Ablative Materials (U)

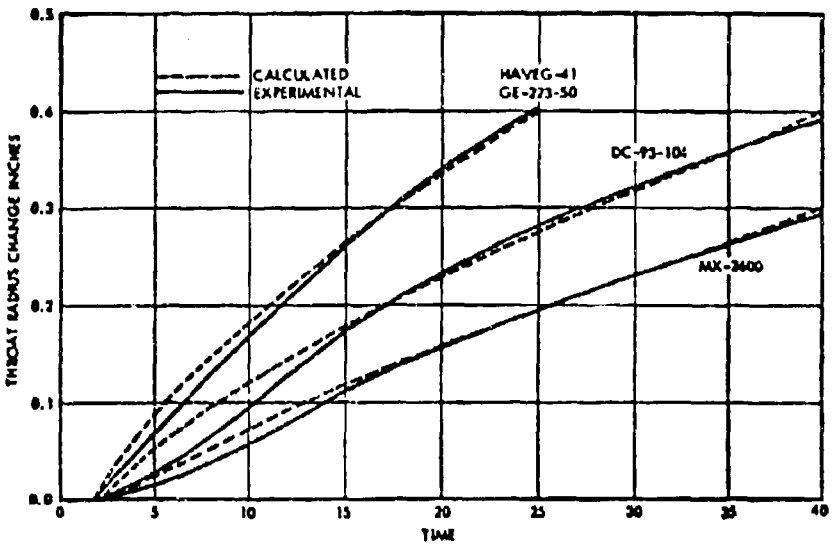

MATERIAL	EFFECTIVE HEAT OF ABLATION (BTU/LBM)	SURFACE TEMPERATURE (°F)
MX-2600	2400	3340
DC-93-104	1600	3200
HAVEG-41	1000	2980
GE-223-50	875	3130

Figure C-5. Thermal Modeling of Erosion Characteristics of Four Candidate Low-Cost Ablative Liner Materials (U)

(U) seconds firing duration. Using the Charring and Ablation Program, and input data determined in Section 2, the liner thicknesses were calculated for three materials. The required thicknesses are shown in Figure C-6 as a function of the internal radius. The dashed line shows the liner thickness required for erosion while the solid line shows the thickness required to limit the backwall temperature to 600°F.

(U) The test of the sub-scale MX-2600 material had not been completed at the time of the sizing of the ablative liners. Therefore, the required thickness was assumed to be equal to the DC93-104 material thickness. Subsequent testing of the MX-2600 sample indicated its superiority to the DC93-104 material. Figure C-5 shows the correlation obtained with the MX-2600 material. The throat inserts of the two liners employing MX-2600 were not resized and therefore have an additional margin of safety.

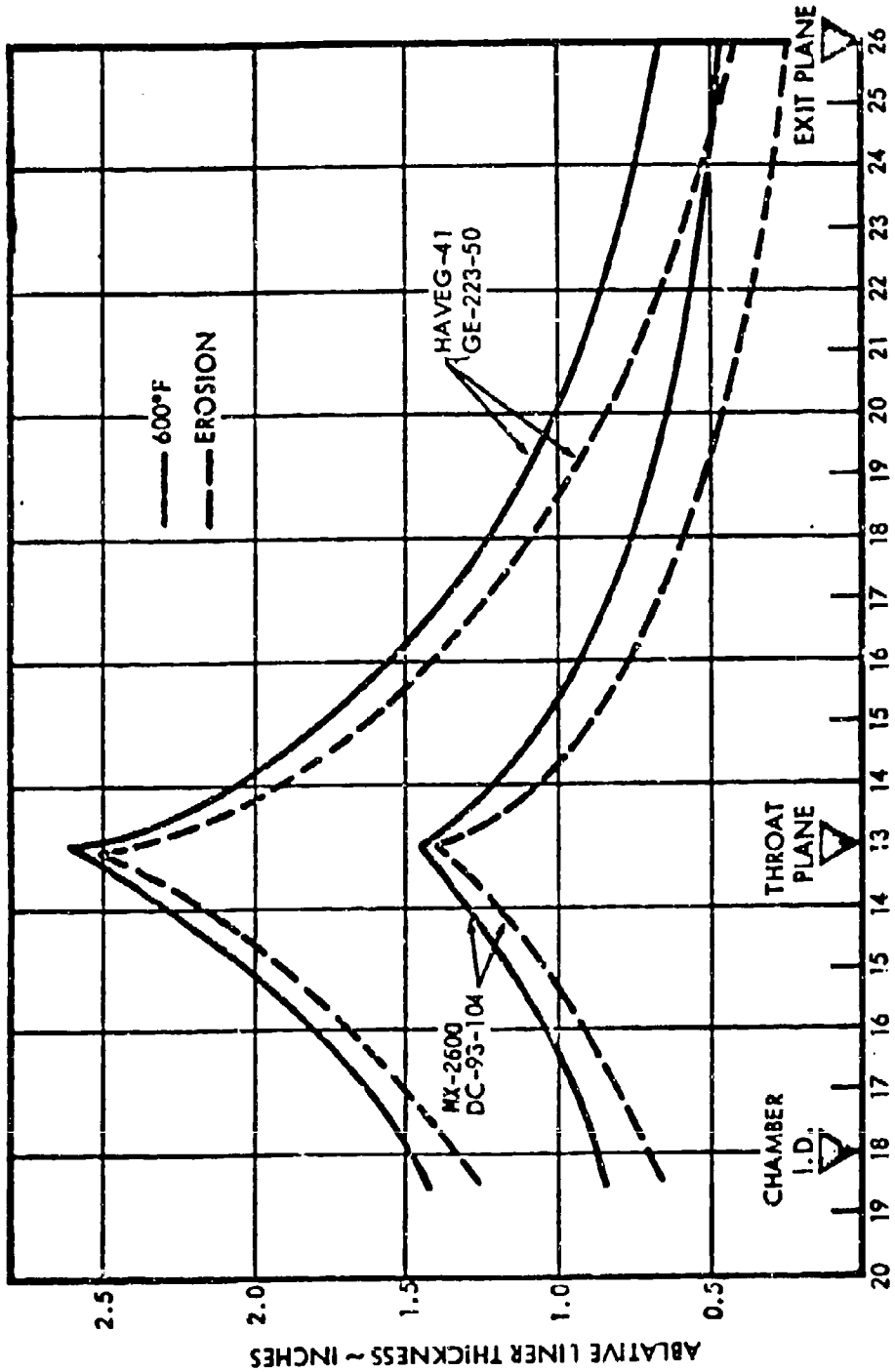

Figure C-6. 250,000 Lbf Long-Duration Thrust Chamber Ablative Liner Thickness for Single 120-Second Continuous Burn (Gas Recovery Temperature = 4850°F) (U)

APPENDIX D

COST ANALYSIS

1. ABLATIVE LINERS-PRELIMINARY DESIGNS

(U) Three ablative thrust chamber liners were designed based on the ablative performance data obtained in the TRW Systems IR&D sub-scale material evaluation program. These designs were based on the four best performing materials:

MX2600 - Silica - phenolic

DC-93-104 - Filled Silicone Rubber

Haveg 41 - Asbestos - phenolic

GE 223-50 - Silica - epoxy novalac

The three preliminary designs are summarized as follows:

1.1 CONFIGURATION NO. 1 (X404361)

(U) This configuration was designed to provide a baseline ablative liner against which the others could be compared. The throat section was MX-2600, tape-wrapped at 60° to centerline, while the exit cone was MX-2600 in a rosette pattern "lay-up." The chamber-dome section was a hand "lay-up" of MX-2600 orange-peel sections parallel to the chamber axis in the cylindrical section.

1.2 CONFIGURATION NO. 2 (X404362)

(U) This configuration was designed as an all DC-93-104 silicone rubber liner, cast-in-place and cured at room temperature and ambient pressure.

1.3 CONFIGURATION NO. 3 (X404363)

(U) The third liner was designed as a composite structure employing a tape-wrapped MX-2600 silica-phenolic throat insert, identical to that of configuration number 1, with either Haveg 41 or GE-223-50 in both chamber section and exit cone-section.

(U) Request for quotations (RFQ's) were solicited from the fabricators listed in Table I. The work statement in the RFQ's provided for alternate fabrication techniques or substitution of comparable materials which would result in lower "in-place" costs but would not reduce the quality of the ablative liner. A total of 38 quotations were received on the three configurations. These included quotes for alternate fabrication techniques, materials and various options. A majority of the alternate fabrication techniques proposed reflected the fabricators facility capability and did not result in significant cost savings.

Table I. Fabricators Solicited for Ablative Liner-Fabrication (U)

Composite Technology Inc.	Van Nuys, California
Edler Industries Inc.	Newport Beach, California
EMCCO Plastics	Palmdale, California
HITCO	Gardena, California
Haveg Industries, Inc.	Santa Fe Springs, California
General Electric Company	Philadelphia, Pennsylvania
Hadbar Division of Purolator Inc.	Alhambra, California
Thermal Systems Inc.	St. Louis, Missouri
San Rafael Plastics Company	San Rafael, California
Insulation Systems Inc.	Santa Ana, California
McDonnell Douglas Corporation	Santa Monica, California

(U) Based on the fixed-price quotes obtained on the preliminary designs and test results obtained in the AFRPL "in-house" materials evaluation program (Minimum Cost Design (MCD) Material Screening Project 305803KRD) additional quotations were solicited on the following materials.

McDormell-Douglas	- Segmented Silica-Phenolic
J-M Thermal Mix 770	- Silica-Asbestos-Phenolic
Plastonium 8	- Gypsum - Phenolic Microballoons
GE-250-50	- Silica-Epoxy Novalac
GE-227-50	- Silica-Epoxy Novalac
GE-PD-715H	- Asbestos-Epoxy Novalac
MXA-150	- Asbestos-Phenolic
DP5-161	- Silica-Phenolic

(U) A summary of the cost data obtained for all the candidate materials is presented in Table II. The costs are the result of a number of fabricators' bids on common items with the selected cost being based on the fabricator's bid and reputation for delivery of a quality part. All costs were normalized to the MXA-150/MX-2600/MXA-150 (alternate configuration three) value, since this is the most cost effective ablative chamber liner. The range of the quoted prices for the MX-2600 liner (configuration one) was $\pm$ 50 percent of the median quoted price (four quotations). The range of the quoted prices for the DC-93-104 liner was $\pm$ 30 percent of the median quoted price (four quotations). The ranking of the 12 candidate ablative liner assemblies is the same for costs with an without tooling except for items 7 and 8. Item 7 requires high pressure molding tooling while item 8 required a minimum of accountable tooling. The three most cost effective ablative chamber liner assemblies are items 6, 1, and 3, in that order.

(U) Item 6 is the composite MXA-150/MX-2600 (alternate configuration three) ablative liner. The main cost saving for this liner is in the low material

(U) costs ($2.00/lbm) of the MXA-150 molding compound, plus its relative ease of fabrication. The second most cost effective chamber liner is item 1. This is the all MX-2600 configuration one ablative liner. The material cost (~$6.00/lbm) is higher than that of MXA-150; however, less MX-2600 material is required and it was the most popular material evaluated. The contingency factor for fabricating a quality part of MX-2600 is probably less than for the remainder of materials. The third most cost effective chamber is item 3 which is the all DC-93-104 configuration two ablative liner. The raw material cost is approximately $9.00 per pound and will be reduced as the material becomes more popular throughout industry. It shows good potential of being reduced to as low as $5.00 per pound. The cost savings for this liner is in the low fabrication costs. It does not require either high temperature or pressure for curing, nor does it require secondary bonding to the pressure vessel. It is an elastomeric material with a sufficiently high elongation rate to withstand dimensional changes in the pressure shell.

Table II. Subscale Chamber Liner Materials Evaluation Program Cost Effectiveness Ranking of all Candidate Liners (U)

Item No.	Chamber Configuration	Ablative Material			Normalized Unit Costs for Quantities of Ten	
		Chamber	Throat	Exit Cone	With Tooling	Without Tooling
1	1	MX-2600	MX-2600	MX-2600	1.61	1.54
2	1	McDD	McDD	McDD	3.59	3.37
3	2	DC-93-104	DC-93-104	DC-93-104	1.64	1.62
4	3	HAVEG-41	MX-2600	HAVEG-41	1.97*	1.91*
5	3	GE-223-50	MX-2600	GE-223-50	2.39	2.12
6	3	MXA-150	MX-2600	MXA-150	1.10	1.00
7	3	TM-770	MX-2600	TM-770	1.92	1.73
8	3	PLST. 8	MX-2600	PLST. 8	1.82	1.74
9	3	GE-250-50	MX-2600	GE-250-50	2.36	2.12
10	3	GE-227-50	MX-2600	GE-227-50	2.12	1.88
11	3	GE-PD715H	MX-2600	GE-PD715H	2.57	2.32
12	3	DP5-160	MX-2600	DP5-160	No data	No data

* Estimate based on first unit costs

2. ABLATIVE LINERS - FABRICATED DESIGNS

(U) Based on the results of the TRW Systems IR&D Materials Evaluation Program, the AFRPL "in-house" materials program, and the Task I test results the preliminary designs were finalized as follows:

Table III. Task II Hardware Acquisition Costs* (U)

	Number of Units (1)	(3)	(10)
X404361 Ablative Liner (MXA-150/MX-2600/MX-2600)	14,273	14,053	13,832
X404362 Ablative Liner (DC-93-104)	14,946	14,305	13,282
X404363 Ablative Liner (DP5-161/MX-2600/MXA-150)	15,575	15,119	14,215

* The hardware acquisition costs do not include tooling costs.

Table IV. Task II Ablative Liner Tooling Costs (U)

X404361 Ablative Liner (MXA-150/MX-2600/MX-2600)	$9107
X404362 Ablative Liner (DC-93-104)	None
X404363 Ablative Liner (DP5-161/MX-2600/MXA-150)	$4485

Table V. Cost-Effectiveness Ranking of Three Ablative Liners (U)

Configuration	Ablative Material Chamber	Throat	Exit Cone	Normalized Unit Costs (10) Without Tooling	With Tooling
1	MXA-150[a]	MX-2600	MX-2600	1.04	1.73
2	DC-93-104	DC-93-104	DC-93-104	1.00	1.00
3	DP5-161	MX-2600	MXA-150[b]	1.07	1.41

Note: a. Layed-up broadgoods

b. Molded segments

Table VI. Volume and Weights of Fabricated Liners (U)

Liner Configuration	Volume, in^3	Surface, ft^2	Density, lb/in^3	Weight, lbs
X404361-1				
Chamber MXA-150	10183	36.8	.0542	551.92
Throat MX-2600	2928	12.4	.0616	180.50
Exit Cone MX-2600	4650	41.0	.0600	279.00
			Total	1011.42
X404362-1				
Chamber DC-93-104	4392	37.9	.0524	230.14
Throat DC-93-104	2928	12.4	.0524	153.41
Exit Cone DC-93-104	4650	41.0	.0524	243.66
			Total	627.21
X404363-1				
Chamber DP5-161	10183	36.8	.0499	508.13
Throat MX-2600	2928	12.4	.0627	183.50
Exit Cone MXA-150	7800	41.0	.0560	436.80
			Total	1128.43

3.1 MATERIAL COSTS

(U) The cost of the base material in the three ablative liners ranged from 47-50 percent of the total cost to 71.5 percent of the total cost. The DC-93-104 silicone rubber chamber liner had the highest material cost percentage (71.5) of the three chambers which is attributed to the limited production of the DC-93-104 material. The other three materials used in the

(U) fabrication of the three chambers were (1) MX-2600 silica-phenolic (2) MXA-150 asbestos-phenolic and (3) DP5-161 silica-phenolic. The MXA-150 asbestos-phenolic was used in both the broadgoods and molding compound forms. The cost of the molding compound being approximately 60 percent of the cost of the broadgoods. DP5-161 is an acid-catalyzed condensation product of formaldehyde (para) and a phenol (resorcinal) with a silica fiber/silica flour filler. As such it can be compared to the silica-phenolic broadgoods in the same manner that the molding compound (MXA-150) is compared to the MXA-150 broadgoods. The DP5-161 with less filler than the MX-2600 cost approximately 50 percent of the cost of the MX-2600 broadgoods.

(U) Of the four materials used in the fabrication only the DC-93-104 material offers the potential of any significant cost reduction when the material usage becomes sufficient to warrant higher production. The projected price of DC-93-104 for large-scale production (~100,000 lbs/yr) is $5.00/lb. None of the three other materials offer cost reductions approaching the reduction projected for DC-93-104.

3.2 FABRICATION COSTS

(U) For similar fabrication methods, casting of the chamber sections, the labor cost for both the DC-93-104 and DP5-161 are approximately the same; the material cost per pound differs by a factor slightly greater than 3. However, this material cost difference is nearly made up by the difference of 2.5 in the quantity of material required. Using projected prices the DC-93-104 chamber liner is more cost-effective than the DP5-161 chamber liner and approximately the same as the layed-up MXA-150 broadgoods.

(U) Evaluation of the same material (MX) fabricated from two different forms for two different liner sections was made. The amount of material used and surface area covered are approximately the same. The exit cone using the molding compound is more costly than the layed-up broadgoods chamber section even though the material cost per pound is only 60 percent that of the broadgoods. The difference in cost comes from the time consuming method of molding segments in addition to the necessity for secondarily bonding the segments into the chamber.

(U) A paradox exists in that the molded, segmented MXA-150 exit-cone is more cost effective than either the DC-93-104 or MX-2600 exit cone sections at the 250,000 lb_f thrust level size. However, using the projected price for the DC-93-104, the most cost-effective exit-cone is the silicone rubber liner. The DC-93-104 throat section is twice as cost-effective as the MX-2600 tape-wrapped throat section when the projected price of DC-93-104 is used to calculate the cost of the component.

4. ACQUISITION COSTS-PRESSURE SHELLS

(U) Three pressure shells were fabricated to contain the three ablative liners. The design was similar to the heat-sink combustion chamber (X403646) design which was used in the Task I program. Two major changes were made in the design of the pressure shell; (1) the body was split into two sections with flanges to allow insertion of the tape-wrapped MX-2600 throat and (2) the thickness of the exit cone shell was decreased to 0.25

(U) inches from 0.50 inches. In addition to these changes a stiffening ring was added to the exit cone.

(U) Three pressure shells of slightly varying configuration were fabricated from USS T-1 steel alloy. The slight variations were made to allow use of the shell as an autoclave during curing and to allow use of a thicker ablative section in the X404363 exit cone.

(U) Request for quotation (RFQ's) were solicited from the fabricators listed in Table VII. The work statement required 100 percent X-ray of all butt welds and dye penetrant inspection of all fillet welds. All welding and certification of welds was performed in accordance with the applicable ASME boiler and pressure vessel codes. Responses to the RFQ were received from four fabricators. The range of the quoted prices for three pressure shells was $\pm$ 35 percent of the median quoted price. Based on these quotations Grano Steel Co. was selected to fabricate the pressure shells.

Table VII. Fabricators Solicited for Pressure Shell Fabrication (U)

J. C. Fabricators	Gardena, California
Capital Westward, Inc.	Paramount, California
L. W. LeFort Co.	Anaheim, California
Los Angeles Boiler Works, Inc.	Los Angeles, California
SWCCO, Inc.	Los Angeles, California
American Bridge Div., USS	Los Angeles, California
Grano Steel Corporation	Los Angeles, California
Aircraft Engineering Corporation	Paramount, California

(U) Acquisition costs for the three pressure shells are shown in Table VIII. These costs include TRW Systems material handling and G&A charges, but do not include fee. There were no tooling charges for any of the pressure shells. As noted in Table VIII, the cost of the -21 pressure shell is slightly greater than the cost of either the -1 or -2 pressure shell. This results from the 48, 21/32 inch diameter drilled holes put in the stiffening ring to allow closure of the exit cone for curing the X404361 liner components. This $90 cost should be charged against the tooling costs for the X404361 ablative liner. The costs given in Table VIII represent a 90-95 percent learning curve on labor indicating that the fabrication technique is well defined and does in fact represent commercial ("low-cost") fabrication practices. Based on a dry weight of 2840 lbs and the unit price for quantities of 10 the cost per lb figure is approximately $2.00/lb.

Table VIII. Pressure Shell Acquisition Costs (U)

	Number of Units		
	(1)	(3)	(10)
X404342-1/X404342-2	$6637	$6175	$5733
X404342-21	6727	6247	5805

5. PROJECTED COSTS - 3000K ABLATIVE CHAMBER LINERS

(U) Cost estimates have been made for ablative chamber liners at the 3000K thrust level. These estimates were made on the basis of the 250,000 lb_f thrust level designs and projected material costs. All of the methods used in fabricating the 250,000 lb_f thrust chamber liners appear applicable for the larger diameter chambers. Tape-wrapping of very large components has been used in fabricating nozzles for the solid motor programs. Casting appears to be entirely feasible for the large sizes although some specialized mixing equipment will be required since mixing appears to be the limiting factor in the use of castable materials. The lay-up of broadgoods and cure insitu at low pressure using the pressure shell as the autoclave also appears to be practical.

(U) The cost estimates for the 3000K liners are based on ablative thicknesses used in the 250,000 lb_f long duration liners and as such represent a somewhat conservative design for the 120 second design firing duration. The following table gives weights and costs for two ablative lined chambers. One chamber liner is cast from DC-93-104 filled silicone rubber while the second is fabricated from MX-2600. The throat is assumed to be tape wrapped at a specific orientation to the centerline, while the chamber and exit cone are layed-up broadgoods material.

Table IX. Estimated Weights and Costs for 3000K Ablative Liners

	DC-93-104	MX-2600
Dome/Chamber, lbs	2045	2440
Throat, lbs	1695	2020
Exit Cone, lbs	4610	5500
Total Weight	8350	9960
Material Cost	$70,017	$85,305
Delivered Cost	$146,000	$171,500

The costs quoted above do not include any tooling or special handling equipment for these very large chambers.

APPENDIX E

DATA REDUCTION PROCEDURES

1. GENERAL

(U) The test results presented herein are derived from computer printout data furnished TRW Systems by the AFRPL. General performance data listings for firings 103 through 111 and 117 were reduced using standard data reduction procedures. Details of the computational procedures and of the applied corrections are given in the following sections.

2. DELIVERED SPECIFIC IMPULSE AND THRUST COEFFICIENT

(U) The measured specific impulse is defined by the following equation

$$I_{sp}\ (meas) = \frac{F\ (meas)}{\dot{W}_t} \qquad (1)$$

where:

F (meas) = F1A + F1B/2, output of dual bridge load cell, lb_f

$\dot{W}_t$ = total propellant flow rate, lb_m/sec

(U) The thrust coefficient is a measure of the nozzle performance and is given by

$$C_F\ (meas) = \frac{F\ (meas)}{P_o\ A_t} \qquad (2)$$

where:

P_o = throat stagnation pressure, psia

A_t = measured geometric throat area, in^2

(U) The throat stagnation pressure was obtained by two methods. The first method corrected the average of the two injector end pressure measurements to stagnation pressure at the throat using Figure E-1 (Ref. 1). This method assumes that the gas velocity across the injector end pressure taps is zero and, therefore, were reading head end stagnation pressure. The correction assumes no combustion in the nozzle and isentropic flow in the nozzle.

(U) The second method used the measured static pressure at the start of the nozzle convergent section which is converted to stagnation pressure at the throat by assuming no combustion in the nozzle and isentropic flow in the nozzle. The use of the second method results in higher nozzle stagnation pressures than would be computed by the first method. This result is

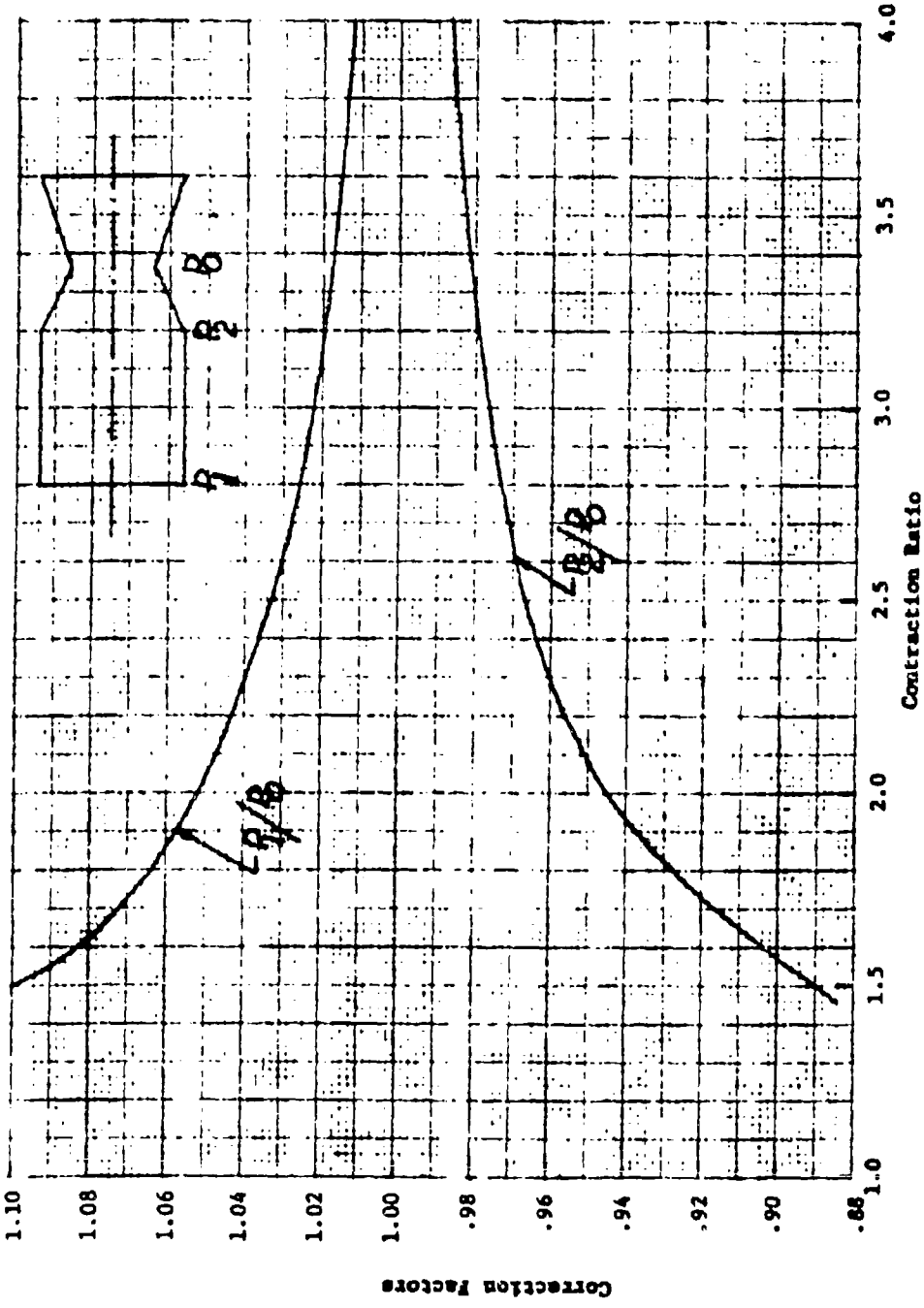

Figure E-1. Correction Factors for Chamber Pressure Measurements (U)

(U) due to a measured pressure loss between injector and nozzle entrance which is lower than that predicted using Figure E-1.

2.1 SPECIFIC IMPULSE AND NOZZLE EFFICIENCY

(U) The theoretical I_{sp} and C* (characteristic velocity) data for the pressure range of 200 psia to 300 psia and covering mixture ratios (O/F) of 1.80 to 3.20 were curve-fit and used in equation form to compute the theoretical I_{sp} and C*. The equations for the theoretical values are given by

$$I_{sp}\ (p_a = 13.2, \epsilon_n = 4.0) = 120.6491 + 379.7692\sqrt{\mu} - 124.4563\mu + 0.463773\ P_o - 0.00061575\ P_o^2 + 0.0017556\ P_o\sqrt{\mu} \quad (3)$$

$$\text{and } C^*\ (\text{theo}) = 1496.4296 + 5838.8849\sqrt{\mu} - 2072.959\mu - 0.21772\ P_o - 0.0003875\ P_o^2 + 0.379418\ P_o\sqrt{\mu} \quad (4)$$

where

$$\mu = \dot{W}_o/\dot{W}_f$$

(U) The specific impulse efficiency is computed as follows

$$\eta_{I_{sp}} = \frac{I_{sp}\ (\text{meas})}{I_{sp}(p_a = 13.2, \epsilon_n = 4.0)} \quad (5)$$

The hardware used in Task II had an expansion ratio (A_e/A_t) of 4.0 and the nominal ambient pressure at the High Thrust Facility (I-56) was 13.2 psia.

(U) The nozzle efficiency was determined using the following equation

$$\eta_{C_F} = \frac{F\ (\text{meas})}{P_o\ A_t\ C_F\ (\text{theo})} \quad (6)$$

The theoretical C_F is computed using Equations (3) and (4) as follows

$$C_F\ (\text{theo}) = \frac{I_{sp}\ (p_a = 13.2,\ \epsilon_n = 4.0)\ g}{C^*\ (\text{theo})} \quad (7)$$

2.2 EXPECTED NOZZLE EFFICIENCY

(U) The expected η_{C_F} for the 4/1 expansion ratio, 15° half-angle conical nozzle was 0.980. Theoretical calculations were made for the various losses (kinetic, divergence and friction) in the 4/1, 15° half-angle conical nozzle. These computations indicate a nozzle efficiency of 0.980 at a mixture ratio (O/F) of 2.60. Theoretical calculations for mixture ratios of 0.5 to 10.0 show less than 0.3 percent variation in the theoretical thrust coefficient.

3. MEASURED CHARACTERISTIC VELOCITY EFFICIENCY

(U) The characteristic velocity (C*) was calculated as follows:

$$C^* = \frac{P_o A_t g}{\dot{W}_t} \tag{8}$$

The characteristic velocity was computed for P_o calculated from the average of Pc-1/Pc-2 and also for P_o determined from the Pc-5 (See Figure E-2) static pressure measurement. On the ablative lined chamber firings only the injector end pressure measurements are available.

$$\eta_{C^*} = \frac{P_o A_t g}{\dot{W} C^* \text{ (theo)}} \tag{9}$$

where the theoretical C* is determined from Equation (4).

(U) The flow rates used in both the measured I_{sp} and C* equations were obtained from single turbine flowmeters using water flow calibrations. Propellant temperatures were measured in the propellant tanks, lines and at the injector. Densities for both propellants were computed from AFRPL derived equations given as Equations (10) and (11).

$$\rho_f = 51.777139 - 0.0350405\ (T_f) \tag{10}$$

$$\rho_o = 95.8447 - 0.078033\ (T_o) \tag{11}$$

4. INJECTION PARAMETERS

(U) The injector and system flow conductances were determined using the following general equation

$$K = \dot{Q}\sqrt{\frac{\rho}{\Delta P}} \tag{12}$$

where

$\dot{Q}$ = volumetric flow rate (general data testing), ft^3/sec

ρ = propellant density, lbm/ft^3

ΔP = measured pressure loss, psi

(U) The fuel injection pressure loss was measured between the entrance to the orifice (PIF-1) and the injector end chamber pressure (PC-1/PC-2) average. The oxidizer injection pressure loss was measured between PIO-1 and the injector end chamber pressure (PC-1/PC-2) average. The fuel and oxidizer orifice discharge coefficients are determined as follows:

$$C_{d_f} = 1.495 \frac{KIJCP}{A_{if}} \tag{13}$$

$$C_{d_o} = 1.495 \frac{KIJCO}{A_{io}} \tag{14}$$

5. THROAT EROSION RATE

(U) It is desired to obtain an estimate of the rate of change of the mean throat radius as a function of time, due to ablation and erosion, thermal expansion, and other thermal mechanisms. The mean throat radius is defined as r in the following equations

$$F_{(vac)} = P_o A_t C_{F(vac)} \tag{15}$$

$$A_t = \pi r^2 \tag{16}$$

where $F_{(vac)} = F_{measured} + P_{amb} A_e$ and A_e is the nozzle area.

(U) It is assumed that F (vac) and r are both time varying functions and that C_F (vac) is a time varying function which varies only a small amount from some known reference point, so that its effects may be linearized. The approach is to compute $\dot{r} = dr/dt$ as a function of the nozzle stagnation pressure, the vacuum thrust, and their derivatives.

(U) The differentiation of (15) and the back-substitution of A_t computed from (16), gives

$$\frac{\dot{P}_o}{P_o} = \frac{\dot{F}}{F} - \frac{2\dot{r}}{r} - \frac{\dot{C}_F}{C_F} \tag{17}$$

Equation (17) may then be solved for $\dot{r}$

$$\dot{r} = \frac{r}{2}\left[\frac{\dot{F}}{F} - \frac{\dot{P}_o}{P_o} - \frac{\dot{C}_F}{C_F}\right] \tag{18}$$

It is assumed that C_F (vac) is explicitly dependent on expansion ratio and nozzle stagnation pressure; then $\dot{C}_F$ is given by

$$\dot{C}_F(\epsilon_n, P_o) = \frac{\partial C_F}{\partial P_o}\dot{P}_o + \frac{\partial C_F}{\partial \epsilon_n}\dot{\epsilon}_n \tag{19}$$

and $\dot{r}$ is given by

$$\dot{r} = \frac{r}{2}\left[\frac{\dot{F}}{F} - \frac{\dot{P}_o}{P_o} - \frac{1}{C_F}\left(\frac{\partial C_F}{\partial P_o}\dot{P}_o + \frac{\partial C_F}{\partial \varepsilon_n}\dot{\varepsilon}_n\right)\right] \qquad (20)$$

(U) Equation (20) is the central equation of the computation. In order to compute and integrate $\dot{r}$, we need $P_c(t)$, $\dot{P}(t)$, $\dot{F}(t)$, $F(t)$, as well as the linearized coefficients $\partial C_F/\partial P_o$ and $\partial C_F/\partial \varepsilon_n$, and the initial throat radius, $r(o)$.

(U) Generally the first derivative of the C_F (vac) is zero since neither the nozzle stagnation pressure, P_o, or the nozzle expansion ratio, ε_n, vary significantly from the initial conditions.

Reference 1. Altman, D., et al. Liquid Propellant Rockets, Princeton University Press, 1960.

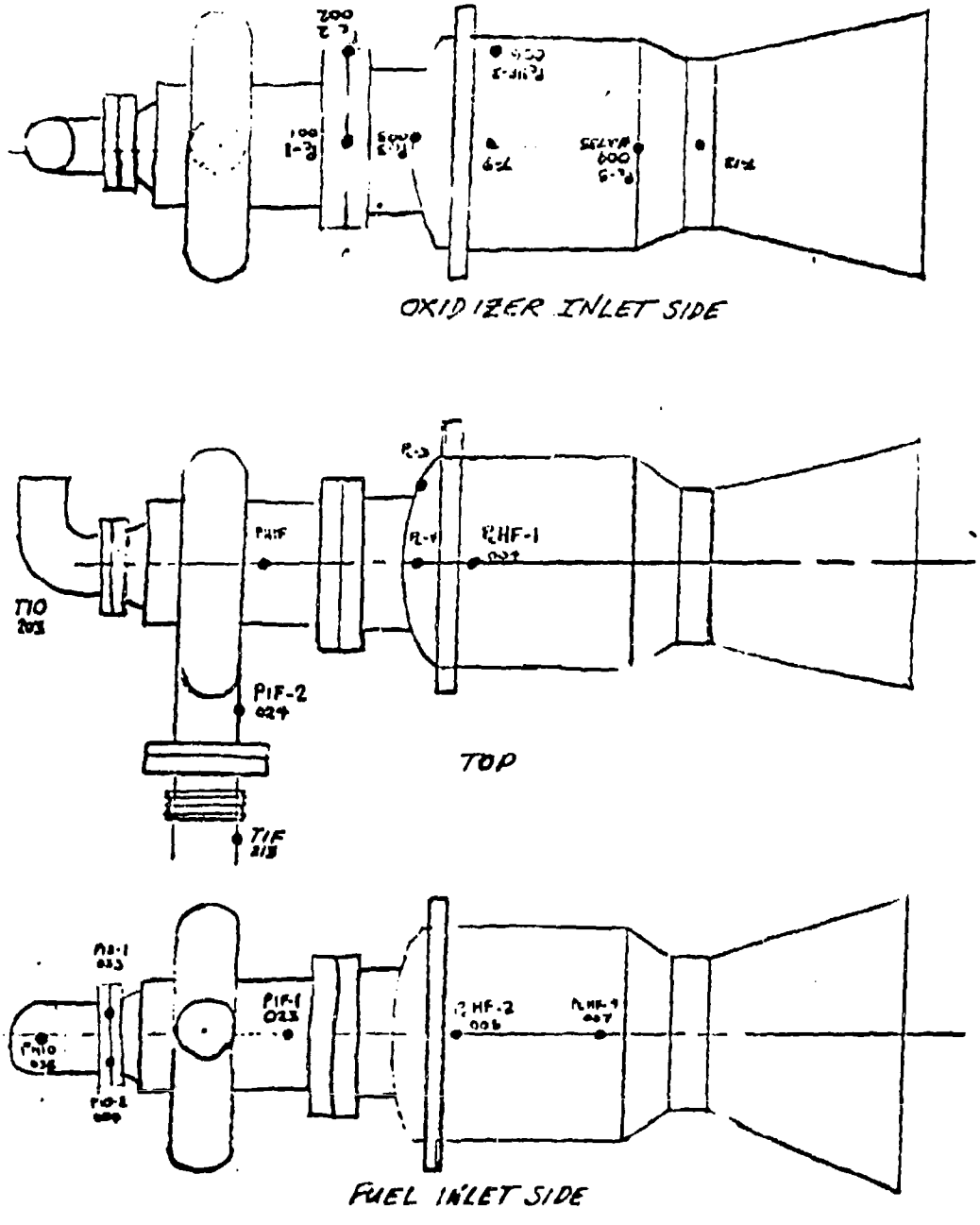

(U) Figure E-2. Instrumentation Locations (U)

Unclassified CONFIDENTIAL

Security Classification

DOCUMENT CONTROL DATA - R & D

(Security classification of title, body of abstract and indexing annotation must be entered when the overall report is classified)

1. ORIGINATING ACTIVITY (Corporate author)
TRW Systems Group
One Space Park
Redondo Beach, California

2a. REPORT SECURITY CLASSIFICATION
Confidential

2b. GROUP
Group 4

3. REPORT TITLE
Injector/Chamber Scaling Feasibility Program,
Ablative Chamber Design and Long Duration Testing
Volume II

4. DESCRIPTIVE NOTES (Type of report and inclusive dates)
Final Report, Covering Period 11 December 1968 to 5 February 1970

5. AUTHOR(S) (First name, middle initial, last name)
Voorhees, G. A., Jr.
Morton, B. G.

6. REPORT DATE	7a. TOTAL NO. OF PAGES	7b. NO. OF REFS
July 1970	165	0

8a. CONTRACT OR GRANT NO.	9a. ORIGINATOR'S REPORT NUMBER(S)
F04611-68-C-0085	Vol II - TRW 11199-6007-R8-00
b. PROJECT NO	
c.	9b. OTHER REPORT NO(S) (Any other numbers that may be assigned this report)
d.	AFRPL-TR-70-86-Vol II

10. DISTRIBUTION STATEMENT
[redacted]

11. SUPPLEMENTARY NOTES

12. SPONSORING MILITARY ACTIVITY
Air Force Rocket Propulsion Laboratory
Air Force Systems Command, USAF
Edwards CA 93523

13. ABSTRACT

The results of the Task II phase of an injector/chamber scaling feasibility program are presented. During the fourteen month program covering the period from 11 December 1968 to 5 February 1970 three ablative thrust chambers were designed, fabricated and test fired. Low-cost liner materials were used in three chamber designs; the material selection was based upon subscale test data generated by both AFRPL and TRW Systems. Low-cost fabrication techniques were employed throughout, ablative components were fabricated by tape-wrapping, hand lay-up, high pressure molding and casting. Several fabrication problems with the low-cost materials were delineated. Four ablative materials were evaluated in the test program. Two of the materials evaluated (MX-2600 silica-phenolic and Dow-Corning 93-104 filled silicone rubber) had acceptable performance for use in low-cost engines of this type and for use in multimillion pound thrust booster engines.

DD FORM 1 NOV 68 1473

CONFIDENTIAL Unclassified

Security Classification

14. KEY WORDS	LINK A		LINK B		LINK C	
	ROLE	WT	ROLE	WT	ROLE	WT
Low-Cost Injector						
Performance						
Stability						
N_2O_4/UDMH						
Scaling						
250,000 lb_f						
Low-Cost Thrust Chamber						
Ablative Liners						
Silica-Phenolic Ablatives						
Silicone Rubber Ablators						